



Casa abierta al tiempo

**UNIVERSIDAD AUTÓNOMA METROPOLITANA**  
Unidad Cuajimalpa

4 de septiembre de 2023.

**Dictamen C.I. 11/2023**

**DICTAMEN**  
**QUE PRESENTA LA COMISIÓN DE INVESTIGACIÓN DE LA DIVISIÓN DE CIENCIAS DE LA COMUNICACIÓN Y DISEÑO**

**ANTECEDENTES**

- I. El Consejo Divisional de Ciencias de la Comunicación y Diseño, en la sesión 08.23, celebrada el 2 de mayo de 2023, integró esta Comisión en los términos señalados en el artículo 55 de Reglamento Interno de los Órganos Colegiados Académicos.
  
- II. El Consejo Divisional designó para esta Comisión a los siguientes integrantes:
  - a) Órganos personales:
    - ✓ Dra. Margarita Espinosa Meneses, Jefa del Departamento de Ciencias de la Comunicación;
    - ✓ Dra. Erika Cecilia Castañeda Arredondo, Jefa del Departamento de Teoría y Procesos del Diseño;
    - ✓ Dr. Carlos Roberto Jaimez González, Jefe del Departamento de Tecnologías de la Información.
  
  - b) Representantes propietarios:
    - Personal académico:
      - ✓ Dr. Diego Carlos Méndez Granados, Departamento de Ciencias de la Comunicación;
      - ✓ Dr. Manuel Rodríguez Viqueira, Departamento de Teoría y Procesos del Diseño;
      - ✓ Mtra. Betzabet García Mendoza, Departamento de Tecnologías de la Información.

**CONSIDERACIONES**

- I. La Comisión recibió, para análisis y discusión, el segundo reporte parcial de resultados del proyecto de investigación denominado **“El diseño ante el cambio climático: divulgación, normatividad e información climatológico”** presentado por el Dr. Christopher Heard Wade, aprobado en la Sesión 14.21 celebrada el 11 de junio de 2021, mediante el Acuerdo DCCD.CD.16.14.21.



**División de Ciencias  
de la Comunicación  
y Diseño**

**Unidad Cuajimalpa**

DCCD | División de Ciencias de la Comunicación y Diseño  
**Oficina Técnica del Consejo Divisional**  
Torre III, 5to. piso. Av. Vasco de Quiroga 4871,  
Colonia Santa Fe Cuajimalpa. Alcaldía Cuajimalpa de Morelos.  
C.P. 05348, Ciudad de México.  
Tel.: (+52) 55.5814.3505  
<http://dccc.cua.uam.mx>



Casa abierta al tiempo

**UNIVERSIDAD AUTÓNOMA METROPOLITANA**  
Unidad Cuajimalpa

- II. El Consejo Divisional en la Sesión 19.21 celebrada el 16 de diciembre de 2021, mediante Acuerdo DCCD.CD.11.19.21, aprobó una recalendarización de dicho proyecto por un periodo del 14 de junio de 2021 al 13 de junio de 2024.
- III. El Consejo Divisional en la Sesión 22.22 celebrada el 19 de octubre de 2022, mediante Acuerdo DCCD.CD.04.22.22, aprobó el primer reporte parcial de resultados del proyecto de investigación.
- IV. La Comisión de Investigación sesionó el 4 de septiembre de 2023, fecha en la que concluyó su trabajo de análisis y evaluación del reporte parcial de resultados, con el presente Dictamen.
- V. La Comisión tomó en consideración los siguientes elementos:
  - *"Lineamientos para la creación de grupos de investigación y la presentación, seguimiento y evaluación de proyectos de investigación"* aprobados en la Sesión 06.16 del Consejo Divisional de Ciencias de la Comunicación y Diseño, celebrada el 6 de junio de 2016, mediante al acuerdo DCCD.CD.15.06.16.
  - Protocolo de investigación.
  - Relevancia para el Departamento.
  - Objetivos planteados.
  - Resultados obtenidos.

#### VI. **Objetivo general:**

Desarrollar información, modelos y formas de presentación significativa y accesible para facilitar el diseño de artefactos y sistemas que toman en cuenta las necesidades ocasionadas por el cambio climático. El objetivo concuerda con "Desarrollar investigación enfocada en la sustentabilidad" como prioridad definida por la planeación institucional.

#### VII. **Objetivos particulares:**

- Actualizar y desarrollar bases de datos meteorológicos aptos para uso en el diseño de edificios y vivienda representativos con efectos de cambio climático para los principales centros urbanos de la República Mexicana.
- Desarrollar estudios puntuales del impacto posible del cambio climático sobre lugares y regiones de la República Mexicana con respecto a temperaturas, precipitación y eventos meteorológicos extremos con énfasis en la resiliencia de los diseños significativos.



División de Ciencias  
de la Comunicación  
y Diseño

#### Unidad Cuajimalpa

DCCD | División de Ciencias de la Comunicación y Diseño  
Oficina Técnica del Consejo Divisional  
Torre III, 5to. piso. Av. Vasco de Quiroga 4871,  
Colonia Santa Fe Cuajimalpa. Alcaldía Cuajimalpa de Morelos.  
C.P. 05348, Ciudad de México.  
Tel.: (+52) 55.5814.3505  
<http://dccc.cua.uam.mx>



Casa abierta al tiempo

**UNIVERSIDAD AUTÓNOMA METROPOLITANA**  
Unidad Cuajimalpa

- Diseñar un sistema de divulgación de la ciencia usando modelos de arquitectura de información para el cambio climático, de semiótica para propiciar diseño significativo, duradero y ambientalmente responsable.
- Desarrollo de tecnología para el uso de agua no-tratada, gris o del mar como fuente o sumidero del calor sin el uso de aditivos químicos perjudicial al medio ambiente.
- Desarrollo y diseño de objetos y artefactos enfocados a la sustentabilidad empleando modelos semióticos para su representación abstracta.

#### VIII. Actividades realizadas del 14 de junio de 2022 al 14 de junio de 2023:

- ✓ Desarrollo de archivos de datos meteorológicos de años típicos futuros basado en los resultados de simulaciones de cambio climático regional CMIP6 y los datos horarios de la base de datos de sesenta sitios de la República Mexicana con control de calidad mejorada.
- ✓ Desarrollo de un sistema para revisión de los datos horarios de cada sitio para reducir el impacto de datos con errores de registro original y mejorar la fidelidad de los años típicos basados en los datos históricos.
- ✓ Generar una base de datos de años típicos históricos mejorado para uso como referencia o punto de partida para generación de años típicos estimados para años futuros. Estos archivos serán libres de las restricciones del licenciamiento de los archivos con los cuales se cuentan actualmente tanto los del ASHRAE como los del proyecto CONACyT/SENER Fondo de Sustentabilidad.

Adicionalmente se realizaron simulaciones del comportamiento térmico de una casa típica con la última versión del ESP-r, programa de simulación térmica de edificaciones con datos históricos para analizar tendencias en el confort térmico modelado para una selección de ciudades de la República Mexicana (Cancún, Huajuapán de León, Bahías de Huatulco, Mérida, Oaxaca, Puerto Ángel, Progreso, Valladolid, Xococotlán) y comparación de comportamiento entre construcción típica y construcción de madera maciza.

En relación a la actividad de: Obtención de información y desarrollo de modelos relacionados con el intercambio de calor en lechos fluidizados líquido/sólido con geometrías novedosas orientados a lograr dispositivos más compactos, de operación más sencillo y confiable que la tecnología actual, se elaboró un artículo con análisis de datos de la literatura conjuntamente con datos experimentales obtenidos



**División de Ciencias  
de la Comunicación  
y Diseño**

**Unidad Cuajimalpa**

DCCD | División de Ciencias de la Comunicación y Diseño  
**Oficina Técnica del Consejo Divisional**  
Torre III, 5to. piso. Av. Vasco de Quiroga 4871,  
Colonia Santa Fe Cuajimalpa. Alcaldía Cuajimalpa de Morelos.  
C.P. 05348, Ciudad de México.  
Tel.: (+52) 55.5814.3505  
<http://dccd.cua.uam.mx>



Casa abierta al tiempo

**UNIVERSIDAD AUTÓNOMA METROPOLITANA**

**Unidad Cuajimalpa**

con un proyecto de investigación anterior de la Universidad en el contexto del programa doctoral de la División de Ciencias Naturales e Ingeniería. Se publicó un artículo: "Heat Transfer and Pressure Drops in a Helical Flow Channel Liquid/Solid Fluidized Bed" en Energies el 6 de diciembre de 2022, <https://doi.org/10.3390/en15239239>

### DICTAMEN

#### ÚNICO:

Tras evaluar el segundo reporte parcial de resultados del proyecto de investigación denominado "El diseño ante el cambio climático: divulgación, normatividad e información climatológico" presentado por el Dr. Christopher Heard Wade, la Comisión de Investigación recomienda al Consejo Divisional de Ciencias de la Comunicación y Diseño aceptarlo.

#### VOTOS:

Integrantes	Sentido de los votos
Dra. Margarita Espinosa Meneses	A favor
Dra. Erika Cecilia Castañeda Arredondo	A favor
Dr. Carlos Roberto Jaimez González	A favor
Dr. Diego Carlos Méndez Granados	----
Dr. Manuel Rodríguez Viqueira	A favor
Mtra. Betzabet García Mendoza	A favor
<b>Total de los votos</b>	<b>5 votos a favor</b>

Coordinadora



Mtra. ~~Gabriela~~ ~~García~~ ~~Martínez~~

Secretaria del Consejo Divisional de Ciencias de la Comunicación y Diseño



**División de Ciencias  
de la Comunicación  
y Diseño**

**Unidad Cuajimalpa**

DCCD | División de Ciencias de la Comunicación y Diseño  
Oficina Técnica del Consejo Divisional  
Torre III, 5to. piso. Av. Vasco de Quiroga 4871,  
Colonia Santa Fe Cuajimalpa. Alcaldía Cuajimalpa de Morelos.  
C.P. 05348, Ciudad de México.  
Tel.: (+52) 55.5814.3505  
<http://dccd.cua.uam.mx>



Casa abierta al tiempo

UNIVERSIDAD AUTÓNOMA METROPOLITANA  
Unidad Cuajimalpa

Ciudad de México 31 de agosto 2023

DTPD.091.23

**Asunto:**

Reporte parcial de resultados: "El diseño  
ante el cambio climático: divulgación,  
normatividad e información climatológico"

**Dra. Gloria Angélica Martínez de la Peña**

Presidenta del Consejo Divisional

División de Ciencias de la Comunicación y Diseño

Universidad Autónoma Metropolitana

Unidad Cuajimalpa

Presente

Por este medio hago de su conocimiento el reporte parcial de resultados del proyecto de investigación "El diseño ante el cambio climático: divulgación, normatividad e información climatológico", cuyo responsable es el Dr. Christopher Lionel Heard Wade, para su dictamen y aprobación.

El proyecto de investigación "El diseño ante el cambio climático: divulgación, normatividad e información climatológico" fue aprobado por el Consejo Divisional de la DCCD en la Sesión 14.21 del Consejo Divisional, mediante el acuerdo DCCD.CD.16.14.21 del 11 de junio de 2021, por un período de un año (del 14 de junio de 2021 al 13 de junio de 2022) y una recalendarización aprobada a tres años en sesión 19.21, acuerdo dccd.cd.11.19.21 del 16-dic-21 (del 14 de junio de 2021 al 13 de junio de 2024).

Para su análisis y dictaminación, **se anexan el siguiente documento:**



- **Reporte parcial de resultados de la Investigación.**

División de Ciencias  
de la Comunicación  
y Diseño

Unidad Cuajimalpa  
DCCD | División de Ciencias de la Comunicación y Diseño  
Jefatura del Departamento de Teoría y Procesos del Diseño



Casa abierta al tiempo

**UNIVERSIDAD AUTÓNOMA METROPOLITANA**  
Unidad Cuajimalpa

De igual forma, se anexa con la intención de contextualizar el proyecto:

- Aprobación en el Consejo Divisional de CCD.

Sin más por el momento, quedo a sus órdenes para cualquier duda o aclaración y le envío un cordial saludo.

**Atentamente**

Casa abierta al tiempo



**Dra. Erika Cecilia Castañeda Arredondo**

Jefa del Departamento de Teoría y procesos del Diseño

\*ccp. Archivo



División de Ciencias  
de la Comunicación  
y Diseño

Unidad Cuajimalpa  
DCCD | División de Ciencias de la Comunicación y Diseño  
Jefatura del Departamento de Teoría y Procesos del Diseño



Casa abierta al tiempo

**UNIVERSIDAD AUTÓNOMA METROPOLITANA**  
Unidad Cuajimalpa

Dra. Erika Cecilia Castañeda Arredondo  
Jefa del Departamento de Teoría y Procesos del Diseño.  
División de Ciencias de la Comunicación y Diseño.  
Universidad Autónoma Metropolitana. Unidad Cuajimalpa

25 de agosto de 2023

Por medio del presente solicito que se canaliza el informe de avance anual del proyecto "El diseño ante el cambio climático: Divulgación, normatividad e información climatológico" que cubre actividades del periodo 14 de junio de 2022 al 14 de junio de 2023 a la Comisión de Investigación del Consejo Divisional para su análisis, dictaminación y registro.

Atentamente

Dr. Christopher Heard

Informe de avance anual del proyecto "El diseño ante el cambio climático: Divulgación, normatividad e información climatológico".

Agosto 2023

Autores:

Dr. Christopher Lionel Heard Wade  
Dr. Sazcha Marcelo Olivera Villarroel  
Dra. Esperanza García López  
Dra. Lucero Fabiola García Franco

## Introducción

El proyecto fue aprobado en la sesión 14.21 celebrada el 11 de junio de 2021 mediante el acuerdo DCCD.CD.15.14.21 bajo el nombre de "El diseño ante el cambio climático: Divulgación, normatividad e información climatológico", iniciando el 14 de junio de 2021. Se notó un error en la propuesta original donde en el cronograma no se indicó que los periodos de tiempo eran trimestres y por lo tanto el proyecto fue aprobado con duración de un año. Actualmente se ha aprobado la recalendarización para tener una duración de tres años.

## Actividades del periodo 14 de junio de 2022 al 14 de junio de 2023.

Las actividades principales durante periodo fueron:

- 6.1 Desarrollo de archivos de datos meteorológicos de años típicos futuros basado en los resultados de simulaciones de cambio climático regional CMIP6 y los datos horarios de la base de datos de sesenta sitios de la República Mexicana con control de calidad mejorada.
  - 6.1.1 Se desarrollará un sistema para revisión de los datos horarios de cada sitio para reducir el impacto de datos con errores de registro original y mejorar la fidelidad de los años típicos basados en los datos históricos.
  - 6.1.2 Se generará un base de datos de años típicos históricos mejorado para uso como referencia o punto de partida para generación de años típicos estimados para años futuros. Estos archivos serán libres de las restricciones del licenciamiento de los archivos con los cuales se cuentan actualmente tanto los del ASHRAE como los del proyecto CONACyT/SENER Fondo de Sustentabilidad.



Adicionalmente se realizaron simulaciones del comportamiento térmico de una casa típica con la última versión del ESP-r, programa de simulación térmica de edificaciones con datos históricos para analizar tendencias en el confort térmico modelado para una selección de ciudades de la República Mexicana (Cancún, Huajuapán de León, Bahías de Huatulco, Mérida, Oaxaca, Puerto Ángel, Progreso, Valladolid, Xococotlán) y comparación de comportamiento entre construcción típica y construcción de madera maciza.

En relación a la actividad de: Obtención de información y desarrollo de modelos relacionados con el intercambio de calor en lechos fluidizados líquido/sólido con geometrías novedosas orientados a lograr dispositivos más compactos, de operación más sencillo y confiable que la tecnología actual, se elaboró un artículo con análisis de datos de la literatura conjuntamente con datos experimentales obtenidos con un proyecto de investigación anterior de la Universidad en el contexto del programa doctoral de la División de Ciencias Naturales e Ingeniería. Se publicó un artículo: "Heat Transfer and Pressure Drops in a Helical Flow Channel Liquid/Solid Fluidized Bed" en *Energies* el 6 de diciembre de 2022, <https://doi.org/10.3390/en15239239> .

## Revisión de datos horarios de cada sitio

Debido a que estos años típicos son derivados de los archivos originales de años suministrados por Whitebox Technologies, ya no son sujetos a derechos de esta compañía. Sin embargo los datos más recientes en esta base de datos son del año 2014.

## Desarrollo de una base de datos de años típicos históricos mejorado

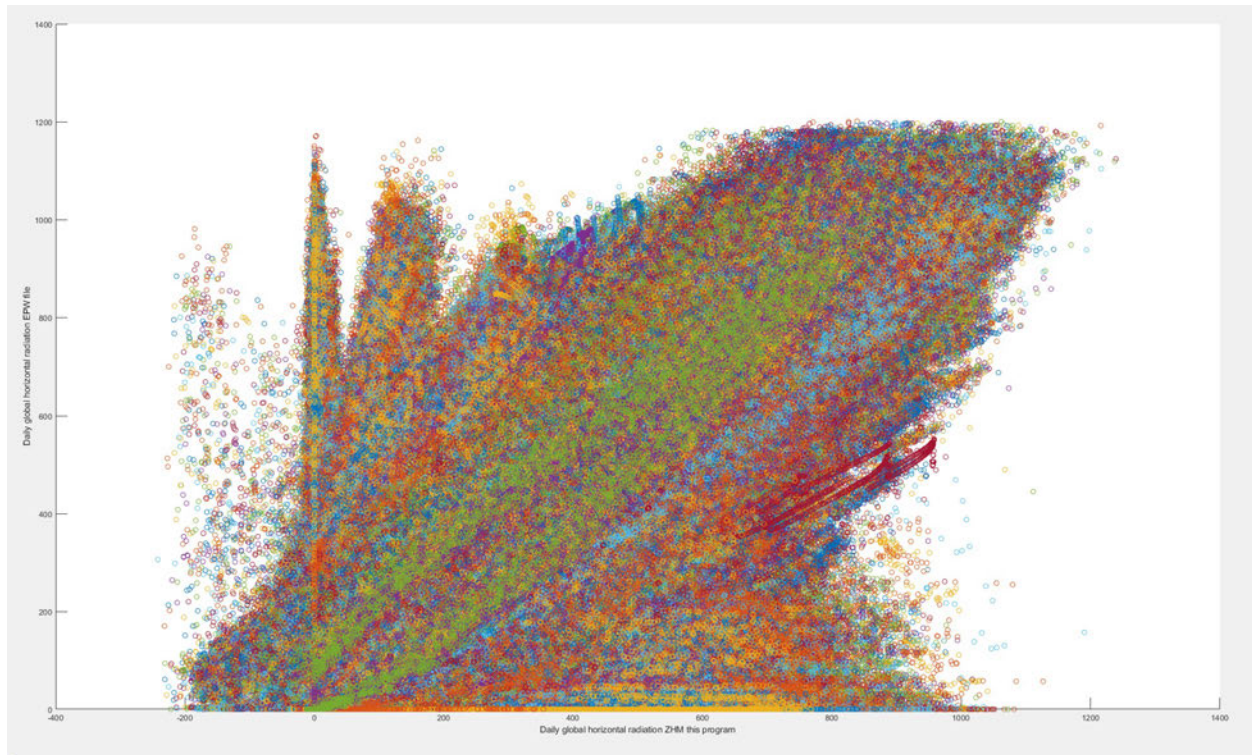
Con el fin de actualizar los datos meteorológicos disponibles para la construcción de años típicos mejorados se inició el desarrollo de código de Matlab para procesar los datos en bruto obtenidos del Integrated Surface Dataset (Global), National Centers for Environmental Information de la NOAA de Estados Unidos<sup>1</sup>.

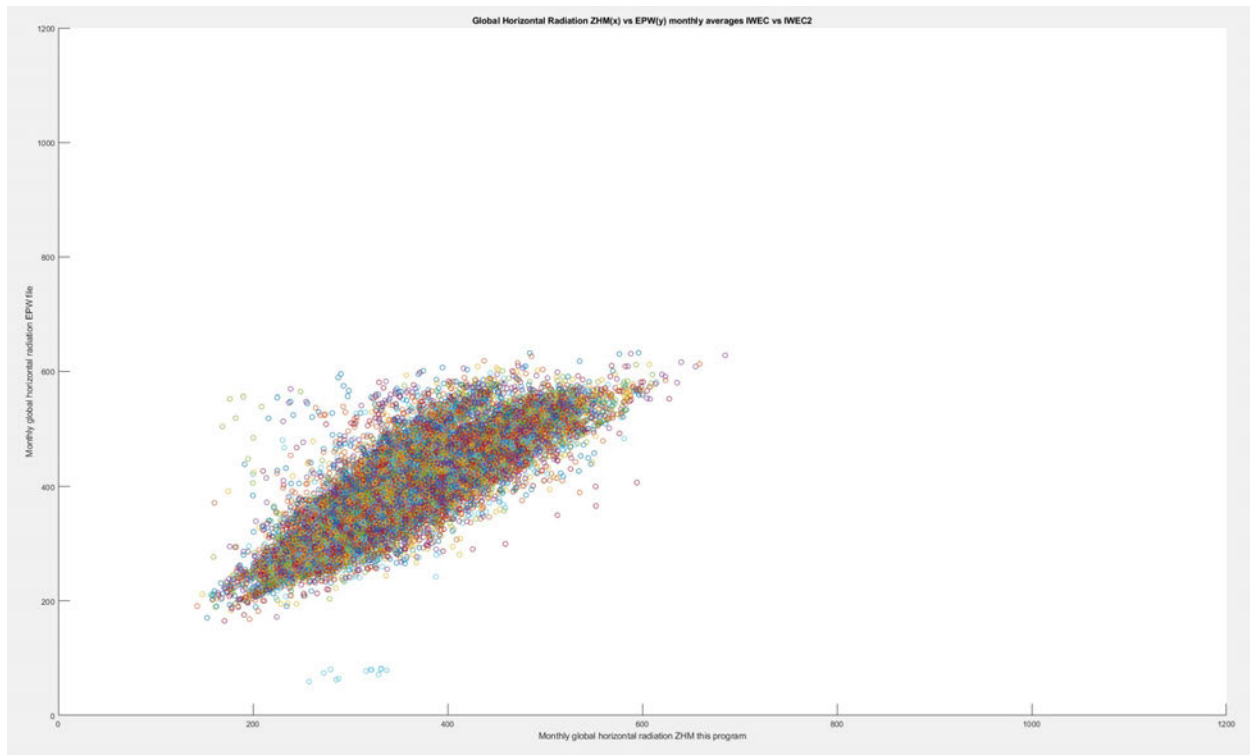
El procesamiento de los datos requiere el uso de sistemas de interpolación para normalizar el horario de los datos, reposición de datos faltantes y estimación de radiación solar a partir de datos alternos (Cobertura de nubes, temperatura del aire y la humedad relativa).

Se desarrolló código para extraer los datos y normalizarlos sobre la hora exacta en la forma necesaria para archivos EPW. Se avanzó 85% en codificar y probar simular radiación solar horario directa y difusa siguiendo la metodología publicada en "Development of 3012 IWEC2Weather Files for International Locations (RP-1477)"<sup>2</sup>

El código de Matlab se encuentra en el Apéndice 1.

Se compararon los resultados con los de los archivos de EPW proveniente de WhiteBox Technologies (Los cuales utilizaron una versión anterior de sistema de estimación de radiación solar) y se encontró una correspondencia buena para los promedios mensuales pero existen algunas discrepancias que necesitan resolución en los datos horarios, probablemente derivados de diferencias en las ecuaciones de tiempo en los dos sistemas de modelado (Figuras x y y).





## Actualización de simulaciones de una casa típica de la Ciudad de México

Se realizaron simulaciones del comportamiento térmico de una casa típica con la última versión del ESP-r, programa de simulación térmica de edificaciones con datos históricos para analizar tendencias en el confort térmico modelado para una selección de ciudades de la República Mexicana (Cancún, Huajuapán de León, Bahías de Huatulco, Mérida, Oaxaca, Puerto Ángel, Progreso, Valladolid, Xococotlán) y comparación de comportamiento entre construcción típica y construcción de madera maciza.

El reporte del trabajo se encuentra en el Apéndice 2.

## Obtención de información y desarrollo de modelos relacionados con el intercambio de calor en lechos fluidizados líquido/sólido

Se publicó un artículo: "Heat Transfer and Pressure Drops in a Helical Flow Channel

Liquid/Solid Fluidized Bed” en Energies el 6 de diciembre de 2022, <https://doi.org/10.3390/en15239239> .

El artículo se encuentra en el Apéndice 3.

## The social assimilation of a new architectural proposal for comfort

Se publicó un artículo en la revista “Sustainability”: “Social Acceptance of a Thermal Architectural Implementation Proposal, <https://doi.org/10.3390/su15054121> .

El artículo se encuentra en el Apéndice 4.

## Orthodox or Sustainable Economic Recovery

Se publicó un capítulo en el libro “SDGs in the Americas and Caribbean Region, Implementing the UN Sustainable Development Goals – Regional Perspectives”, [https://doi.org/10.1007/978-3-030-91188-1\\_12-1](https://doi.org/10.1007/978-3-030-91188-1_12-1) .

El artículo se encuentra en el Apéndice 5.

## Referencias

1. <https://www.ncei.noaa.gov/access/search/data-search/global-hourly?dataset=DS3505&countryabbv=&georegionabbv=&resolution=40> Consultado 25 Noviembre 2021.
2. Joe, Yu, et al. "Development of 3012 IWEC2 weather files for international locations (RP-1477)." Ashrae Transactions 120.1 (2014).

Apéndice 1: Código para el procesamiento de datos meteorológicos con implementación del modelo (85%) de radiación solar horario directa y difusa siguiendo la metodología publicada en “Development of 3012 IWECC2Weather Files for International Locations (RP-1477)”<sup>1</sup> y su comparación con los datos de WhiteBox Technologies.

```
% Author: Christopher Heard
% Created: 2023-03-17
```

```
% Reads in EPW file and uses the cloudcover etc. to apply the methods of
% "Development of 3012 IWECC2Weather Files for International Locations
% (RP-1477)"
% by Huang et al
%
```

```
% This script is to read in an epw file
% It extracts data from the header to find the latitude and longitude for interpolation of data
% from CMIP5 model results
% from a historical file and a future file.
% The year for each month's data in the TMY epw file (Typical Meteorological Year - made up of
% real months)
%
% EPW data field descriptions taken from:
% https://bigladdersoftware.com/epx/docs/8-3/auxiliary-programs/energyplus-weather-file-epw-data-dictionary.html
```

#### %Data Field Descriptions

```
%Descriptions of the fields are taken from the IWECC manual - as descriptive of what should be
% contained in the data fields.
```

```
%Field:1 Year
```

```
%This is the Year of the data. Not really used in EnergyPlus. Used in the Weather Converter
% program for display in audit file.
```

```
%Field:2 Month
```

```
%This is the month (1-12) for the data. Cannot be missing.
```

```
%Field:3 Day
```

```
%This is the day (dependent on month) for the data. Cannot be missing.
```

```
%Field:4 Hour
```

```
%This is the hour of the data. (1 - 24). Hour 1 is 00:01 to 01:00. Cannot be missing.
```

```
%Field:5 Minute
```

```
%This is the minute field. (1..60)
```

```
%Field:6 Data Source and Uncertainty Flags
```

```
%The data source and uncertainty flags from various formats (usually shown with each field) are
% consolidated in the E/E+ EPW format. More is shown about Data Source and Uncertainty in Data
% Sources/Uncertainty section later in this document.
```

```
%Field:7 Dry Bulb Temperature
```

```
%This is the dry bulb temperature in C at the time indicated. Note that this is a full numeric
% field (i.e. 23.6) and not an integer representation with tenths. Valid values range from -70 C to
% 70 C. Missing value for this field is 99.9.
```

```
%Field:8 Dew Point Temperature
```

```
%This is the dew point temperature in C at the time indicated. Note that this is a full numeric
% field (i.e. 23.6) and not an integer representation with tenths. Valid values range from -70 C to
% 70 C. Missing value for this field is 99.9.
```

```
%Field:9 Relative Humidity
```

```
%This is the Relative Humidity in percent at the time indicated. Valid values range from 0% to
% 110%. Missing value for this field is 999.
```

```
%Field:10 Atmospheric Station Pressure
```

```
%This is the station pressure in Pa at the time indicated. Valid values range from 31,000 to
% 120,000. (These values were chosen from the "standard barometric pressure" for all elevations of
% the World). Missing value for this field is 999999.
```

```
%Field:11 Extraterrestrial Horizontal Radiation
```

```
%This is the Extraterrestrial Horizontal Radiation in Wh/m2. It is not currently used in
% EnergyPlus calculations. It should have a minimum value of 0; missing value for this field is
```

9999.

%Field:12 Extraterrestrial Direct Normal Radiation

%This is the Extraterrestrial Direct Normal Radiation in Wh/m2. (Amount of solar radiation in Wh/m2 received on a surface normal to the rays of the sun at the top of the atmosphere during the number of minutes preceding the time indicated). It is not currently used in EnergyPlus calculations. It should have a minimum value of 0; missing value for this field is 9999.

%Field:13 Horizontal Infrared Radiation Intensity

%This is the Horizontal Infrared Radiation Intensity in Wh/m2. If it is missing, it is calculated from the Opaque Sky Cover field as shown in the following explanation. It should have a minimum value of 0; missing value for this field is 9999.

%Field:14 Global Horizontal Radiation

%This is the Global Horizontal Radiation in Wh/m2. (Total amount of direct and diffuse solar radiation in Wh/m2 received on a horizontal surface during the number of minutes preceding the time indicated.) It is not currently used in EnergyPlus calculations. It should have a minimum value of 0; missing value for this field is 9999.

%Field:15 Direct Normal Radiation

%This is the Direct Normal Radiation in Wh/m2. (Amount of solar radiation in Wh/m2 received directly from the solar disk on a surface perpendicular to the sun's rays, during the number of minutes preceding the time indicated.) If the field is "missing ( 9999)" or invalid (<0), it is set to 0. Counts of such missing values are totaled and presented at the end of the runperiod.

%Field:16 Diffuse Horizontal Radiation

%This is the Diffuse Horizontal Radiation in Wh/m2. (Amount of solar radiation in Wh/m2 received from the sky (excluding the solar disk) on a horizontal surface during the number of minutes preceding the time indicated.) If the field is "missing ( 9999)" or invalid (<0), it is set to 0. Counts of such missing values are totaled and presented at the end of the runperiod.

%Field:17 Global Horizontal Illuminance

%This is the Global Horizontal Illuminance in lux. (Average total amount of direct and diffuse illuminance in hundreds of lux received on a horizontal surface during the number of minutes preceding the time indicated.) It is not currently used in EnergyPlus calculations. It should have a minimum value of 0; missing value for this field is 999999 and will be considered missing of >= 999900.

%Field:18 Direct Normal Illuminance

%This is the Direct Normal Illuminance in lux. (Average amount of illuminance in hundreds of lux received directly from the solar disk on a surface perpendicular to the sun's rays, during the number of minutes preceding the time indicated.) It is not currently used in EnergyPlus calculations. It should have a minimum value of 0; missing value for this field is 999999 and will be considered missing of >= 999900.

%Field:19 Diffuse Horizontal Illuminance

%This is the Diffuse Horizontal Illuminance in lux. (Average amount of illuminance in hundreds of lux received from the sky (excluding the solar disk) on a horizontal surface during the number of minutes preceding the time indicated.) It is not currently used in EnergyPlus calculations. It should have a minimum value of 0; missing value for this field is 999999 and will be considered missing of >= 999900.

%Field:20 Zenith Luminance

%This is the Zenith Illuminance in Cd/m2. (Average amount of luminance at the sky's zenith in tens of Cd/m2 during the number of minutes preceding the time indicated.) It is not currently used in EnergyPlus calculations. It should have a minimum value of 0; missing value for this field is 9999.

%Field:21 Wind Direction

%This is the Wind Direction in degrees where the convention is that North=0.0, East=90.0, South=180.0, West=270.0. (Wind direction in degrees at the time indicated. If calm, direction equals zero.) Values can range from 0 to 360. Missing value is 999.

%Field:22 Wind Speed

%This is the wind speed in m/sec. (Wind speed at time indicated.) Values can range from 0 to 40. Missing value is 999.

%Field:23 Total Sky Cover

%This is the value for total sky cover (tenths of coverage). (i.e. 1 is 1/10 covered. 10 is total coverage). (Amount of sky dome in tenths covered by clouds or obscuring phenomena at the hour indicated at the time indicated.) Minimum value is 0; maximum value is 10; missing value is 99.

%Field:24 Opaque Sky Cover

%This is the value for opaque sky cover (tenths of coverage). (i.e. 1 is 1/10 covered. 10 is total coverage). (Amount of sky dome in tenths covered by clouds or obscuring phenomena that prevent observing the sky or higher cloud layers at the time indicated.) This is not used unless the field for Horizontal Infrared Radiation Intensity is missing and then it is used to calculate

Horizontal Infrared Radiation Intensity. Minimum value is 0; maximum value is 10; missing value is 99.

%Field:25 Visibility

%This is the value for visibility in km. (Horizontal visibility at the time indicated.) It is not currently used in EnergyPlus calculations. Missing value is 9999.

%Field:26 Ceiling Height

%This is the value for ceiling height in m. (77777 is unlimited ceiling height. 88888 is cirroform ceiling.) It is not currently used in EnergyPlus calculations. Missing value is 99999.

%Field:27 Present Weather Observation

%If the value of the field is 0, then the observed weather codes are taken from the following field. If the value of the field is 9, then "missing" weather is assumed. Since the primary use of these fields (Present Weather Observation and Present Weather Codes) is for rain/wet surfaces, a missing observation field or a missing weather code implies "no rain".

%TMY 2 data fields

% Field 1 Year (2 digits)

% Field 2 Month

% Field 3 Day

% Field 4 Hour - Note TMY hour is that of local standard time - in EPW the time zone is indicated

% Field 5 Extraterrestrial Horizontal Radiation: (11 EPW 5 in WF\_data) - Amount of solar radiation in Wh/m<sup>2</sup> received on a horizontal surface at the top of the atmosphere during the 60 minutes preceding the hour indicated

% Field 6 Extraterrestrial Direct Normal Radiation: (12 EPW 6 in WF\_data) - Amount of solar radiation in Wh/m<sup>2</sup> received on a surface normal to the sun at the top of the atmosphere during the 60 minutes preceding the hour indicated

% Field 7 Global Horizontal Radiation: (14 EPW 8 in WR\_data) - Total amount of direct and diffuse solar radiation in Wh/m<sup>2</sup> received on a horizontal surface during the 60 minutes preceding the hour indicated

% Field 8 Direct Normal Radiation: (15 EPW 9 in WR\_data) - Amount of solar radiation in Wh/m<sup>2</sup> received within a 5.7° field of view centered on the sun during the 60 minutes preceding the hour indicated

% Field 9 Diffuse Horizontal Radiation: (16 EPW 10 in WR\_data) - Amount of solar radiation in Wh/m<sup>2</sup> received from the sky (excluding the solar disk) on a horizontal surface during the 60 minutes preceding the hour indicated

% Field 10 Global Horiz. Illuminance: (17 EPW 11 in WR\_data) - Average total amount of direct and diffuse illuminance in hundreds of lux received on a horizontal surface during the 60 minutes preceding the hour indicated

% Field 11 Direct Normal Illuminance: (18 EPW 12 in WR\_data) - Average amount of direct normal illuminance in hundreds of lux received within a 5.7° field of view centered on the sun during the 60 minutes preceding the hour indicated.

% Field 12 Diffuse Horiz. Illuminance: (19 EPW 13 in WR\_data) - Average amount of illuminance in hundreds of lux received from the sky (excluding the solar disk) on a horizontal surface during the 60 minutes preceding the hour indicated.

% Field 13 Zenith Luminance: (20 EPW 14 in WR\_data) - Average amount of luminance at the sky's zenith in tens of Cd/m<sup>2</sup> during the 60 minutes preceding the hour indicated.

% Field 14 Total Sky Cover: (23 EPW 17 in WR\_data) - Amount of sky dome in tenths covered by clouds or obscuring phenomena at the hour indicated

% Field 15 Opaque Sky Cover: (24 EPW 18 in WR\_data) - Amount of sky dome in tenths covered by clouds or obscuring phenomena that prevent observing the sky or higher cloud layers at the hour indicated

% Field 16 Dry Bulb Temperature: (7 EPW in C, 1 in WR\_data) - Dry bulb temperature in tenths of oC at the hour indicated -500 to 500 = -50.0 to 50.0oC

% Field 17 Dew Point Temperature: (8 EPW in C, 2 in WR\_data) - Dew point temperature in tenths of oC at the hour indicated -600 to 300 = -60.0 to 30.0oC

% Field 18 Relative Humidity: (9 EPW 3 in WR\_data) - Relative humidity in percent at the hour indicated

% Field 19 Atmospheric Pressure: (10 EPW in Pa, 4 in WR\_data) - Atmospheric pressure at station in millibars at the hour indicated (Pa / 100)

% Field 20 Wind Direction: (21 EPW 15 in WR\_data) - Wind direction in degrees at the hour indicated. ( N = 0 or 360, E = 90, S = 180,W = 270 ). For calm winds, wind direction equals zero.

% Field 21 Wind Speed: (22 EPW in m/s, 16 in WR\_data) - Wind speed in tenths of meters per second

```

at the hour indicated.
% Field 22 Visibility: (25 EPW in km, 17 in WR_data) - Horizontal visibility in tenths of
kilometers at the hour indicated.
% Field 23 Ceiling Height: (26 EPW 18 in WR_data) - Ceiling height in meters at the hour
indicated.
% Field 24 Present Weather: (27 EPW 19 in WR_data) - Present weather conditions denoted by a
10-digit number.

% For Cumulative distribution functions and Weighting values for FS statistics: TMY3 weightings
and parameters
% Daily max dry bulb temperature 1/20
% Daily min dry bulb temperature 1/20
% Daily mean dry bulb temperature 2/20
% Daily max dewpoint temperature 1/20
% Daily min dewpoint temperature 1/20
% Daily mean dewpoint temperatue 2/20
% Daily max wind velocity 1/20
% Daily mean wind velocity 1/20
% Daily global radiation 5/20
% Daily direct radiation 5/20

%Day number for first day of each month except leap years
Daynumber = [1,32,60,91,121,152,182,213,244,274,305,335];

WS_data_resampled.EstimHourlySol = zeros(8760,1);
WS_data_resampled.RelativeHumidity = zeros(8760,1);
WS_data_resampled.SolAltAngle = zeros(8760,1);
WS_data_resampled.HourAngle = zeros(8760,1);
WS_data_resampled.SolarTime = zeros(8760,1);
WS_data_resampled.Declination = zeros(8760,1);
WS_data_resampled.Precipit = zeros(8760,1);
WS_data_resampled.DayOfYear = zeros(8760,1);
WS_data_resampled.Second = zeros(8760,1);
WS_data_resampled.Minute = zeros(8760,1);
WS_data_resampled.Hour = zeros(8760,1);
WS_data_resampled.DayOfMonth = zeros(8760,1);
WS_data_resampled.Month = zeros(8760,1);
WS_data_resampled.Year = zeros(8760,1);
WS_data_resampled.CloudCover = zeros(8760,1);
WS_data_resampled.WindSpeed = zeros(8760,1);
WS_data_resampled.WindDir = zeros(8760,1);
WS_data_resampled.DewPoint = zeros(8760,1);
WS_data_resampled.DryBulb = zeros(8760,1);
WS_data_resampled.Pressure = zeros(8760,1);

% Set up classes for Koppen-Gieger classification of sites for coefficients
% for solar radiation estimation from JOE, Yu, et al. Development of 3012
% IWEC2 Weather Files for International Locations (RP-1477).
% Ashrae Transactions, 2014, vol. 120, no 1.
% Source KoppenGeiger.m : Beck, H., Zimmermann, N., McVicar, T. et al.
% Present and future Köppen-Geiger climate classification maps at 1-km resolution.
% Sci Data 5, 180214 (2018). https://doi.org/10.1038/sdata.2018.214

classes = {...
    1,1,'Af','Tropical, rainforest',[0 0 255];...
    2,1,'Am','Tropical, monsoon',[0 120 255];...
    3,1,'Aw','Tropical, savannah',[70 170 250];... % also As - same coefficients for solar
estimation
    4,2,'BWh','Arid, desert, hot',[255 0 0];...
    5,2,'BWk','Arid, desert, cold',[255 150 150];...
    6,2,'BSh','Arid, steppe, hot',[245 165 0];...
    7,2,'BSk','Arid, steppe, cold',[255 220 100];...

```



```

8,3,'Csa','Temperate, dry summer, hot summer',[255 255 0];...
9,3,'Csb','Temperate, dry summer, warm summer',[200 200 0];...
10,3,'Csc','Temperate, dry summer, cold summer',[150 150 0];...
11,3,'Cwa','Temperate, dry winter, hot summer',[150 255 150];...
12,3,'Cwb','Temperate, dry winter, warm summer',[100 200 100];...
13,3,'Cwc','Temperate, dry winter, cold summer',[50 150 50];...
14,3,'Cfa','Temperate, no dry season, hot summer',[200 255 80];...
15,3,'Cfb','Temperate, no dry season, warm summer',[100 255 80];...
16,3,'Cfc','Temperate, no dry season, cold summer',[50 200 0];...
17,4,'Dsa','Cold, dry summer, hot summer',[255 0 255];...
18,4,'Dsb','Cold, dry summer, warm summer',[200 0 200];...
19,4,'Dsc','Cold, dry summer, cold summer',[150 50 150];...
20,4,'Dsd','Cold, dry summer, very cold winter',[150 100 150];...
21,4,'Dwa','Cold, dry winter, hot summer',[170 175 255];...
22,4,'Dwb','Cold, dry winter, warm summer',[90 120 220];...
23,4,'Dwc','Cold, dry winter, cold summer',[75 80 180];...
24,4,'Dwd','Cold, dry winter, very cold winter',[50 0 135];...
25,4,'Dfa','Cold, no dry season, hot summer',[0 255 255];...
26,4,'Dfb','Cold, no dry season, warm summer',[55 200 255];...
27,4,'Dfc','Cold, no dry season, cold summer',[0 125 125];...
28,4,'Dfd','Cold, no dry season, very cold winter',[0 70 95];...
29,5,'ET','Polar, tundra',[178 178 178];...
30,5,'EF','Polar, frost',[102 102 102];...
};
KoppenClass = {...
'MEX_ACAPULCO_768050','Aw','-6';...
'MEX_ACAPULCO-G-ALVAREZ_768056','Aw','-6';...
'MEX_AGUASCALIENTES_765710','BSh','-6';...
'MEX_ALTAR-SON_761130','BSh','-7';...
'MEX_ARRIAGA_768400','Aw','-6';...
'MEX_BAHIAS-DE-HUATULCO_768485','Aw','-6';...
'MEX_CABO-SAN-LUCAS_767503','BWh','-7';...
'MEX_CAMPECHE-IGNACIO_766950','Aw','-6';...
'MEX_CAMPECHE-IGNACIO_766961','Aw','-6';...
'MEX_CANCUN_765950','Aw','-6';...
'MEX_CANCUN-IAP_765905','Aw','-6';...
'MEX_CHETUMAL_767500','Aw','-6';...
'MEX_CHICHEN-ITZA_767501','Aw','-6';...
'MEX_CHIHUAHUA-G-FIERRO_762253','BSh','-6';...
'MEX_CHIHUAHUA-IAP_762252','BSh','-6';...
'MEX_CHIHUAHUA-UNIVERSIT_762250','BSh','-6';...
'MEX_CHILPANCINGO_767620','Aw','-6';...
'MEX_CHOIX_763110','Csa','-7';...
'MEX_CIUADAD-CONSTITUCION_764020','BWh','-7';...
'MEX_CIUADAD-DEL-CARMEN-I_767493','Aw','-6';...
'MEX_CIUADAD-GUZMAN_766560','Csb','-6';...
'MEX_CIUADAD-JUAREZ_760751','BWh','-6';...
'MEX_CIUADAD-OBREGON-SON_762580','BWh','-7';...
'MEX_CIUADAD-VICTORIA_764910','Cfa','-6';...
'MEX_COATZACOALCOS_767410','Am','-6';...
'MEX_COLIMA_766580','Aw','-6';...
'MEX_COLONIA-JUAN-CARRAS_764580','Aw','-7';...
'MEX_COLOTLAN_765190','Csa','-6';...
'MEX_COMITAN_768480','Cwb','-6';...
'MEX_COZUMEL-AP_766480','Aw','-6';...
'MEX_COZUMEL-IAP_766493','Aw','-6';...
'MEX_C-P-A-CARLOS-ROVIRO_767433','Af','-6';...
'MEX_CUERNAVACA_767260','Aw','-6';...
'MEX_CULIACAN(CITY)_764120','BSh','-7';...
'MEX_DE-GUANAJUATO-IAP_765773','BSh','-6';...
'MEX_DON-MIGUEL-Y-HIDALG_766133','Csa','-6';...
'MEX_DURANGO(CITY)_764230','BSk','-6';...
'MEX_DURANGO-IAP_764235','BSk','-6';...
'MEX_EJIDO-NUEVO-LEON-BC_760400','BWh','-7';...

```

'MEX\_EMPALME\_762560', 'BWh', '-7';...  
 'MEX\_FELIPE-CARRILLO-PUE\_766980', 'Aw', '-6';...  
 'MEX\_FES-CUAUTITLAN\_766700', 'Cwb', '-6';...  
 'MEX\_GEOGRAFIA-UNAM\_766810', 'Cwb', '-6';...  
 'MEX\_GUADALAJARA\_766120', 'Csa', '-6';...  
 'MEX\_GUADALAJARA-IAP\_766131', 'Csa', '-6';...  
 'MEX\_GUANAJUATO\_765770', 'Csa', '-6';...  
 'MEX\_GUAYMAS-G-YANEZ-AP\_762555', 'BWh', '-7';...  
 'MEX\_HACIENDA-YLANG-YLAN\_766920', 'Aw', '-6';...  
 'MEX\_HERMOSILLO-IAP\_761600', 'BWh', '-7';...  
 'MEX\_HUAJUAPAN-DE-LEON\_767730', 'Cwb', '-6';...  
 'MEX\_ISLA-GUADALUPE\_761510', 'BSh', '-7';...  
 'MEX\_ISLA-SOCORRO\_767230', 'BWh', '-7';...  
 'MEX\_IXTAPA-ZIHUATANEJO\_767584', 'Aw', '-6';...  
 'MEX\_IXTEPEC\_767502', 'Aw', '-6';...  
 'MEX\_JALAPA\_766870', 'Cfa', '-6';...  
 'MEX\_JUAREZ-G-GONZALEZ\_760753', 'BWh', '-6';...  
 'MEX\_LAGOS-DE-MORENO\_765730', 'Csa', '-6';...  
 'MEX\_LA-PAZ(CITY)\_764050', 'BWh', '-7';...  
 'MEX\_LA-PAZ-G-MARQUEZ-AP\_764055', 'BWh', '-7';...  
 'MEX\_LEON-SAN-CARLOS\_765752', 'BSh', '-6';...  
 'MEX\_LICENCIADO-GUSTAVO\_766013', 'Aw', '-6';...  
 'MEX\_LICENCIADO-Y-GEN-IG\_766546', 'Cwb', '-6';...  
 'MEX\_LORETO\_763050', 'BWh', '-7';...  
 'MEX\_LOS-CABOS-IAP\_764056', 'BWh', '-7';...  
 'MEX\_MANZANILLO\_766540', 'Aw', '-6';...  
 'MEX\_MATAMOROS-G-CANALES\_763993', 'Cfa', '-6';...  
 'MEX\_MATAMOROS-IAP\_763991', 'Cfa', '-6';...  
 'MEX\_MATLAPA\_765850', 'Aw', '-6';...  
 'MEX\_MAZATLAN-G-BUELNA-I\_764591', 'Aw', '-7';...  
 'MEX\_MAZATLAN-G-BUELNA-II\_764593', 'Aw', '-7';...  
 'MEX\_MERIDA-IAP\_766440', 'Aw', '-6';...  
 'MEX\_MEXICALI\_760051', 'BWh', '-7';...  
 'MEX\_MEXICALI-G-SANCHEZ\_760053', 'BWh', '-7';...  
 'MEX\_MEXICO-CITY\_766800', 'Cwb', '-6';...  
 'MEX\_MEXICO-CITY-B-JUAREZ\_766793', 'Cwb', '-6';...  
 'MEX\_MEXICO-CITY-IAP\_766790', 'Cwb', '-6';...  
 'MEX\_MINATITLAN\_767383', 'Am', '-6';...  
 'MEX\_MONCLOVA\_763420', 'BSh', '-6';...  
 'MEX\_MONTERREY(CITY)\_763930', 'BSh', '-6';...  
 'MEX\_MONTERREY-G-ESCOBEDO\_763943', 'BSh', '-6';...  
 'MEX\_MONTERREY-IAP\_763940', 'BSh', '-6';...  
 'MEX\_MORELIA\_766650', 'Cwb', '-6';...  
 'MEX\_MORELIA-G-MUJICA-AP\_766655', 'Cwb', '-6';...  
 'MEX\_NUEVA-CASAS-GRANDES\_761220', 'BSk', '-6';...  
 'MEX\_NUEVO-LAREDO\_762861', 'BSh', '-6';...  
 'MEX\_OAXACA\_767750', 'Cwa', '-6';...  
 'MEX\_ORIZABA-VER\_767370', 'Cwb', '-6';...  
 'MEX\_PACHUCA\_766320', 'BSk', '-6';...  
 'MEX\_PARRAL\_763230', 'BSk', '-6';...  
 'MEX\_PIEDRAS-NEGRAS\_762430', 'Cfa', '-6';...  
 'MEX\_PILARES-DE-NACOZARI\_761180', 'BSh', '-7';...  
 'MEX\_PLAYA-DE-ORO-IAP\_766534', 'Aw', '-6';...  
 'MEX\_PROGRESO\_765930', 'BSh', '-6';...  
 'MEX\_PUEBLA\_766850', 'Cwb', '-6';...  
 'MEX\_PUERTO-ANGEL\_768550', 'Am', '-6';...  
 'MEX\_PUERTO-ESCONDIDO\_768556', 'Aw', '-6';...  
 'MEX\_PUERTO-PENASCO\_760610', 'BWh', '-7';...  
 'MEX\_QUERETARO\_766250', 'BSk', '-6';...  
 'MEX\_QUETZALCOATL-IAP\_762863', 'BSh', '-6';...  
 'MEX\_REYNOSA-G-BLANCO-AP\_763503', 'BSh', '-6';...  
 'MEX\_REYNOSA-IAP\_763501\_75', 'BSh', '-6';...  
 'MEX\_RIO-VERDE\_765810', 'Cfa', '-6';...  
 'MEX\_SALINA-CRUZ\_768330', 'Aw', '-6';...

```
'MEX_SALTILLO_763900', 'BSh', '-6';...
'MEX_SAN-FELIPE_760550', 'BWh', '-7';...
'MEX_SAN-LUIS-POTOSI_765390', 'BSk', '-6';...
'MEX_SANTA-ROSALIA_762530', 'BSh', '-7';...
'MEX_SN-CRISTOBAL-LAS-C_768450', 'Cwb', '-6';...
'MEX_SOMBRERETE_764710', 'BSk', '-6';...
'MEX_SOTO-LA-MARINA_764990', 'BSh', '-6';...
'MEX_TAJIN_766127', 'Af', '-6';...
'MEX_TAMPICO_765480', 'BSh', '-6';...
'MEX_TAMPICO-GEN-FJ-MINA_765491', 'BSh', '-6';...
'MEX_TAMPICO-G-MINA-AP_765493', 'BSh', '-6';...
'MEX_TAMUIN-SLP_765430_02', 'Aw', '-6';...
'MEX_TAPACHULA-CITY_769030', 'Aw', '-6';...
'MEX_TAPACHULA-IAP_769043', 'Aw', '-6';...
'MEX_TEMOSACHIC_762200', 'BSk', '-7';...
'MEX_TEPEHUANES_763730', 'Csb', '-6';...
'MEX_TEPIC_765560', 'Cwa', '-6';...
'MEX_TIJUANA-G-RODRIGUE_760013', 'BSh', '-7';...
'MEX_TLAXCALA_766830', 'Cwb', '-6';...
'MEX_TOLUCA_766750', 'Cwb', '-6';...
'MEX_TOLUCA-LA-LOPEZ-AP_766753', 'Cwb', '-6';...
'MEX_TORREON-AP_763820', 'BWh', '-6';...
'MEX_TULANCINGO_766340', 'Cfb', '-6';...
'MEX_TUXPAN-VER_766400', 'Am', '-6';...
'MEX_TUXTLA-GUTIERREZ_760754', 'Aw', '-6';...
'MEX_TUXTLA-GUTIERREZ-A_768430', 'Aw', '-6';...
'MEX_VALLADOLID_766470', 'Aw', '-6';...
'MEX_VALLE-DEL-FUERTE-IN_763615', 'BWh', '-7';...
'MEX_VERACRUZ-GEN-JARA_766910', 'Aw', '-6';...
'MEX_VERACRUZ-G-JARA-AP_766913', 'Aw', '-6';...
'MEX_VILLAHERMOSA_767441_75', 'Am', '-6';...
'MEX_VILLAHERMOSA-TAB_767430', 'Am', '-6';...
'MEX_XOXOCOTLAN-IAP_767755', 'Cwb', '-6';...
'MEX_ZACATECAS(CITY)_765250', 'Cwb', '-6';...
'MEX_ZACATECAS-G-RUIZ-AP_765255', 'Cwb', '-6';...
'MEX_ZAMORA_766620', 'Csa', '-6';
```

```
% Tau d and b for ASHRAE clear sky models from chapter 14 2021 fundamentals
% handbook database
```

```
taud =
[2.556000000000000,2.539000000000000,2.491000000000000,2.462000000000000,2.428000000000000,2.423000000000000,2.428000000000000,
0,2.441000000000000,2.513000000000000,2.512000000000000,2.496000000000000];
taub =
[0.310000000000000,0.321000000000000,0.333000000000000,0.344000000000000,0.363000000000000,0.366000000000000,0.394000000000000,
0.395000000000000,0.420000000000000,0.485000000000000,0.584000000000000,0.616000000000000,
0.482000000000000,0.490000000000000,0.479000000000000,0.474000000000000,0.434000000000000,0.41
200000000000000,0.396000000000000,0.379000000000000,0.384000000000000,0.384000000000000,0.428000000
000000,0.447000000000000,0.475000000000000,0.489000000000000,0.447000000000000,0.420000000000000,
0.408000000000000,0.392000000000000,0.387000000000000,0.380000000000000,0.399000000000000,0.42100
0000000000,0.485000000000000,0.498000000000000,0.453000000000000,0.469000000000000,0.4460000000000
00,0.428000000000000,0.404000000000000,0.390000000000000,0.389000000000000];
LatDecim = [32.5410000000000,32.6310000000000,29.7840000000000,35.0030000000000,30.2000000000000,28.5140000000000,31.82
LongDecim = [-116.970000000000,-115.242000000000,-119.310000000000,-105.339000000000,-107.161000000000,-101.239000000000];
LatLong = zeros(49,2);
LatLong(:,1) = LatDecim;
LatLong(:,2) = LongDecim;
```

```
Hournumber = [0,744,1416,2160,2880,3624,4344,5088,5832,6552,7296,8016,8760];
```

```
% Load epw file
% Provide location of files
%file_location =
'C:\Users\usuario\Documents\Christopher\RawYearlyData\BAJA-CALIF-NORTE\MEXICALI-G-SANCHEZ_760053\
```

```

';
%file_location = 'C:\Wthr\MEX_RIO-VERDE_765810_80.epw';
%file_location = 'C:\Wthr\MEX_MEXICO-CITY-B-JUAREZ_766793_14.epw';
%file_location = 'C:\Wthr\MEX_MERIDA-IAP_766440_08.epw';

file_location = 'C:\Wthr\';
file_list = dir([file_location, '*.epw']);
n_files = size(file_list,1);
%run through all of the files
for ifile = 1:n_files
    if ifile < 1
        clear (WF_date);
    end
    %ifile=1;
    WF_file = [file_location,file_list(ifile).name];
    WF_data = importdata(WF_file, ',', 8);

    %WF_file = [file_location];

    %extract the information from the header

    header = WF_data.textdata(1:8,1);
    flag_end = size(WF_data.textdata,1);

    %remove 29th of February for leap year
    if flag_end == 8792
        WF_datec(1:1416,1:5) = WF_data.textdata(9:1424,1:5);
        WF_datec(1417:8760,1:5) = WF_data.textdata(1449:8792,1:5);
        WS_data(1:1416,:) = WF_data.data(1:1416,:);
        WS_data(1417:8760,:) = WF_data.data(1441:8784,:);
    else
        WF_datec(1:8760,1:5) = WF_data.textdata(9:flag_end,1:5); %if matlab
        WS_data = WF_data.data; % If Matlab
    end

    %WF_date = [WF_data.data(1:8760,1:5)]; %, WF_data.textdata(9:flag_end,:));
    %once extracted the data is all that is left to get.
    %WS_data = WF_data.data; % If Matlab

    %WF_data = WF_data.data(:,7:end);

    % Assign climate classification from file name and classification list
    % KoppenClass

    FilePlace =
extractBefore(string(file_list(ifile).name),strlength(string(file_list(ifile).name))-7);
    KoppenStr = KoppenClass(:,1);
    KoppClass = KoppenClass(contains(KoppenStr,FilePlace),2);
    UTCdiff = KoppenClass(contains(KoppenStr,FilePlace),3);
    UTCdiffd = str2double(cell2mat(UTCdiff)); % Time zone difference from UTC (GMT)
    %extract the important information - this can be edited accordingly - Need to deal with
Typical/Extreme periods and ground temperatures
    C = strsplit(header{1,1}, ',', 'CollapseDelimiters', false);
    Lat = str2double(C{7});
    Lon = str2double(C{8});
    Altitude = str2double(C{10});
    RelativeToUTC = UTCdiffd; %str2double(C{9});
    Year = str2num(cell2mat(WF_datec(1,1)));
    Leap = ~mod(Year,4);
    if Leap

```

```

    Daynumber = [1,32,61,92,122,153,183,214,245,275,306,336];
end

Latitude = Lat;
Longitude = Lon;

WF_date = str2double(WF_datec);
WS_data_resampled.DayOfYear = 1:1:8760;
WS_data_resampled.DayOfYear = reshape(WS_data_resampled.DayOfYear,8760,1);
WS_data_resampled.Second = zeros(8760,1); %Not in EPW therefore zero
WS_data_resampled.Minute = WF_date(:,5);
WS_data_resampled.Hour = WF_date(:,4);
WS_data_resampled.DayOfMonth = WF_date(:,3);
WS_data_resampled.Month = WF_date(:,2);
WS_data_resampled.Year = WF_date(:,1);

WS_data_resampled.RelativeHumidity = WS_data(:,3);
WS_data_resampled.Precipit = zeros(8760,1);
WS_data_resampled.CloudCover = WS_data(:,17);
WS_data_resampled.WindSpeed = WS_data(:,16);
WS_data_resampled.WindDir = WS_data(:,15);
WS_data_resampled.DewPoint = WS_data(:,2);
WS_data_resampled.DryBulb = WS_data(:,1);
WS_data_resampled.Pressure = WS_data(:,4);

% Solar calculations https://www.ncbi.nlm.nih.gov/pmc/articles/PMC7085731/

% Declination angle

WS_data_resampled.Declination = -0.40927971*sin(2*pi*(WS_data_resampled.DayOfYear+284)/365); %
in radians ASHRAE fundamentals 2021 SI equation 10 from Chpt. 14 page 14.10 %

23.45 degrees = 0.40927971 radians
% Local time - in Mexico there are two time zones which cover most of the
% country UTC -6 Baja California UTC -8 The state of Baja California Sur, Sonora and
% Chihuahua uses UTC -7. Quintana Roo uses UTC -5.

%ASHRAE fundamentals 2021 SI equations 5 & 6 from Chpt. 14 page 14.9
%Equation of time

B = (WS_data_resampled.DayOfYear-1)*2*pi/365; % B is in radians - Equation 6 Chpt 14 page 14.9
2021
E = 2.2918*(0.0075+0.1868*cos(B) - 3.2077*sin(B) - 1.4615*cos(2*B) - 4.089*sin(2*B)); % E is in
minutes - Equation 5 Chpt 14 page 14.9 2021

% ASHRAE handbook 2019 HVAC Applications Chapter 36 Equation 5
%  $ET = 9.87 \sin 2B - 7.53 \cos B - 1.5 \sin B$  (5)
% where  $B = 0.989(N - 81)$  &  $N =$  day of year, with January 1 = 1
%  $B = 0.989*(WS\_data\_resampled.DayOfYear - 81)*2*pi/365$ ; % B is in radians
%  $E = 9.87*\sin(2*B) - 7.53*\cos(B) - 1.5*\sin(B)$ ;

Lst = RelativeToUTC*15; % 0 degrees because the raw data files are in UTC - but resampled is
in local time zone civil
% time as are EPW files
Loc = Longitude; % in degrees

WS_data_resampled.SolarTime = mod(WS_data_resampled.Hour + (4*(Lst-Loc)-E)/60,24); % In hours
% According to ASHRAE Applications 2019 Chpt. 36 Equation 4 - needs equation of time.
% AST = LST + ET + (4 min) (LST meridian - Local longitude)

```

```

WS_data_resampled.HourAngle = (WS_data_resampled.SolarTime-12)*pi/12; % In radians
% Solar altitude angle - equation 12 Chpt 14 page 14.10 2021
% WS_data_resampled.SolAltAngle =
asin(sin(WS_data_resampled.Declination)*sin(Latitude*pi*2/360)...
%
+cos(WS_data_resampled.Declination).*cos(Latitude*pi*2/360).*cos(WS_data_resampled.HourAngle));

% Solar altitude angle from SolarAzEl Programed by Darin C. Koblick
% 2/17/2009 and Darin C. Koblick 4/16/2013 Vectorized for Speed

DateVector = zeros (8760,6);
DateVector(1:8760,1) = WS_data_resampled.Year;
DateVector(1:8760,2) = WS_data_resampled.Month;
DateVector(1:8760,3) = WS_data_resampled.DayOfMonth;
DateVector(1:8760,4) = WS_data_resampled.Hour;
DateVector(1:8760,5) = WS_data_resampled.Minute;
DateVector(1:8760,6) = WS_data_resampled.Second;
t1 = datetime(DateVector,'TimeZone','America/Mexico_City'); %
datetime(DateVector,'TimeZone','America/Mexico_City'); EPW time is local timezone
t1.TimeZone = 'UTC';
%jd = juliandate(t1);
Latvector(1:8760,1) = Latitude;
Longvector(1:8760,1) = Longitude;
Altvector(1:8760,1) = Altitude/1000;
[Az,E1] = SolarAzEl(t1,Latvector,Longvector,Altvector);
WS_data_resampled.SolAltAngle = deg2rad(E1);
%Check declination, solar angle etc. by plotting them over the year -
%looks alright for Tijuana

% Relative humidity

% For relative humidity saturated partial pressure (pws) and dew point partial pressure (pw) is
needed
% The saturation pressure over ice for the temperature range of -100 to 0°C is given by
% ln pws = C1/T + C2 + C3T + C4T^2 + C5T^3 + C6T^4 + C7 ln T
% where
C1 = -5.6745359e+3;
C2 = 6.3925247e00;
C3 = -9.6778430e-3;
C4 = 6.2215701e-7;
C5 = 2.0747825e-9;
C6 = -9.4840240e-13;
C7 = 4.1635019e00;
%
% The saturation pressure over liquid water for the temperature range of 0 to 200°C is given by
% ln pws = C8/T + C9 + C10T + C11T^2 + C12^T 3 + C13 ln T
% where
%
C8 = -5.8002206e+03;
C9 = 1.3914993e+00;
C10 = -4.8640239e-02;
C11 = 4.1764768e-05;
C12 = -1.4452093e-08;
C13 = 6.5459673E+00;
%
% In both Equations (5) and (6),
% pws = saturation pressure, Pa
% T = absolute temperature, K = °C + 273.15
%
T = WS_data_resampled.DryBulb+273.15;
% Then equation 6
pws = exp(C8./T + C9 + C10.*T + C11*T.^2 + C12*T.^3 + C13*log(T))/1e3;
INDEX = (WS_data_resampled.DryBulb < 0);
% Then equation 5

```

```

pws(INDEX) = exp(C1./T(INDEX) + C2 + C3*T(INDEX) + C4*T(INDEX).^2 + C5*T(INDEX).^3 +
C6*T(INDEX).^4 + C7*log(T(INDEX)))/1e3;

    T = WS_data_resampled.DewPoint+273.15;
% Then equation 6
pw = exp(C8./T + C9 + C10.*T + C11*T.^2 + C12*T.^3 + C13*log(T))/1e3;
INDEX = (WS_data_resampled.DewPoint < 0);
% Then equation 5
pw(INDEX) = exp(C1./T(INDEX) + C2 + C3*T(INDEX) + C4*T(INDEX).^2 + C5*T(INDEX).^3 +
C6*T(INDEX).^4 + C7*log(T(INDEX)))/1e3;

WS_data_resampled.RelativeHumidity = (pw./pws)*100;

WS_data_resampled.EstimHourlySol = zeros(8760,1);
WS_data_resampled.EstimDaylySol = zeros(365,24,1);
WS_data_resampled.Taub = zeros(365,1);
WS_data_resampled.Taud = zeros(365,1);

% Day light hours index
INDEX = (WS_data_resampled.SolAltAngle > 0); %Don't estimate solar radiation at night

% Use correlations from Development of 3012 IWEC2Weather Files
% for International Locations (RP-1477) Huang et al ASHRAE Transactions
% Volume 120 part 1 pp 340 - 355 - Table 2
% Change the following to make using the coefficients easier

ConstsSol(1,1:7) = [0.97136,0.24936,-0.32165,0.03768,-0.0076,0.00794,-2.23175]; % Af
ConstsSol(2,1:7) = [0.71868,-0.11359,-0.07259,0.01038,-0.00285,0.00866,-8.42023]; % Am
%ConstsSol.As = [0.8089,0.07355,-0.40101,-0.00424,-0.00242,0.00342,-8.395]; % As has the same
criteria as Aw and same the regression coefficients
ConstsSol(3,1:7) = [0.8089,0.07355,-0.40101,-0.00424,-0.00242,0.00342,-8.395]; % Aw
ConstsSol(6,1:7) = [0.68149,-0.04697,-0.2842,0.01726,-0.00081,0.00453,-8.91306]; % BSh
ConstsSol(7,1:7) = [0.57692,-0.08062,-0.24399,0.0261,0.00054,0.00277,-1.21103]; % BSk
ConstsSol(4,1:7) = [0.51315,0.1554,-0.42157,0.01427,-0.00035,0.00469,-9.55426]; % BWh
ConstsSol(5,1:7) = [0.6997,-0.03001,-0.27693,0.01529,-0.00169,0.0051,-9.23071]; % BWk
ConstsSol(14,1:7) = [0.67839,0.03646,-0.39075,0.01359,-0.00148,0.0073,-8.71373]; % Cfa
ConstsSol(12,1:7) = [0.7437,-0.02988,-0.26353,0.02606,-0.00323,-8E-05,-1.97366]; % Cfb
ConstsSol(16,1:7) = [0.7437,-0.02988,-0.26353,0.02606,-0.00323,-8E-05,-1.97366]; % Cfc
ConstsSol(8,1:7) = [0.54698,0.21871,-0.42476,0.0233,-0.00038,0.00183,-9.83335]; % Csa
ConstsSol(9,1:7) = [0.6425,0.06685,-0.35491,0.01935,-0.00111,1E-05,-5.40989]; % Csb
ConstsSol(11,1:7) = [0.68175,0.15988,-0.43455,0.01972,-0.00303,0.00201,-6.67731]; % Cwa
ConstsSol(12,1:7) = [0.65533,-0.00683,-0.13621,0.0324,-0.00252,-0.0032,0.17022]; % Cwb
ConstsSol(25,1:7) = [0.73067,0.04956,-0.32687,0.01269,-0.00298,0.00581,0.30725]; % Dfa
ConstsSol(26,1:7) = [0.69491,-0.10822,-0.22999,0.01232,-0.00091,0.0039,-3.46883]; % Dfb
ConstsSol(27,1:7) = [0.73447,-0.03502,-0.18087,0.01923,-0.00225,-0.00443,-3.61457]; % Dfc
ConstsSol(17,1:7) = [0.73447,-0.03502,-0.18087,0.01923,-0.00225,-0.00443,-3.61457]; % Dsa
ConstsSol(18,1:7) = [0.73447,-0.03502,-0.18087,0.01923,-0.00225,-0.00443,-3.61457]; % Dsb
ConstsSol(19,1:7) = [0.73447,-0.03502,-0.18087,0.01923,-0.00225,-0.00443,-3.61457]; % Dsc
ConstsSol(21,1:7) = [0.66459,0.59148,-0.80274,0.03374,-0.00376,0.01662,-21.1779]; % Dwa
ConstsSol(22,1:7) = [0.73447,-0.03502,-0.18087,0.01923,-0.00225,-0.00443,-3.61457]; % Dwb
ConstsSol(23,1:7) = [0.73447,-0.03502,-0.18087,0.01923,-0.00225,-0.00443,-3.61457]; % Dwc
ConstsSol(24,1:7) = [0.73447,-0.03502,-0.18087,0.01923,-0.00225,-0.00443,-3.61457]; % Dwd
ConstsSol(29,1:7) = [0.77029,0.00687,-0.35561,0.01849,-0.00149,-0.00278,-6.41702]; % ET
ConstsSol(30,1:7) = [0.77029,0.00687,-0.35561,0.01849,-0.00149,-0.00278,-6.41702]; % EF

for i = 1:12
    Tmonth(1,1,i) = mean(WS_data_resampled.DryBulb(Hournumber(i)+1:Hournumber(i+1),1));
    P(1,1,i) = sum(WS_data_resampled.Precipit(Hournumber(i)+1:Hournumber(i+1),1));
end

%[Class, BroadClass] = KoppenGeiger(Tmonth,P,classes);
%Sc0 = 0.5598;
%Sc1 = 0.4982;
%Sc2 = -0.6762;

```

```

%Sc3 = 0.02842;
%Sc4 = -0.00317;
%Sc5 = 0.014;
%Sd = -17.853;
%Sk = 0.843;

Class = cell2mat(classes(contains(classes(:,3),KoppClass),1));
%BroadClass = 3;

% This is a bodge to not rewrite regression equation code below

Sc0 = ConstsSol(Class,1);
Sc1 = ConstsSol(Class,2);
Sc2 = ConstsSol(Class,3);
Sc3 = ConstsSol(Class,4);
Sc4 = ConstsSol(Class,5);
Sc5 = ConstsSol(Class,6);
Sd = ConstsSol(Class,7);
%Sk = 0.843; %- This is not used in the Huang et al ASHRAE version of the
%equation and looks to just have been a factor in the Qingyuan
%paper - the coefficients can just be divided through by Sk

IO = 1367.7; %W/m^2 from
% Use T to hold dry bulb at hour n-3 - use a wrap around on the data at
% the beginning of the year just to make logical consistency although
% these hours will always be nighttime with a negative solar altitude
% angle and so the data will not be used.
T(1:3) = WS_data_resampled.DryBulb(8758:8760);
T(4:8760) = WS_data_resampled.DryBulb(1:8757);

WS_data_resampled.EstimHourlySol = zeros(8760,1);
%WS_data_resampled.EstimHourlySol(INDEX)=
(IO*sin(WS_data_resampled.SolAltAngle(INDEX)).*(Sc0+Sc1.*WS_data_resampled.CloudCover(INDEX)./10
...
%
+Sc2.*((WS_data_resampled.CloudCover(INDEX)./10).^2)+Sc3.*(WS_data_resampled.DryBulb(INDEX)-T(INDEX))...
% +Sc4.*WS_data_resampled.RelativeHumidity(INDEX)+Sc5.*WS_data_resampled.WindSpeed(INDEX))...
% +Sd); %./Sk;

WS_data_resampled.EstimHourlySol=
(IO*sin(WS_data_resampled.SolAltAngle).*(Sc0+Sc1.*WS_data_resampled.CloudCover./10 ...
+Sc2.*((WS_data_resampled.CloudCover./10).^2)+Sc3.*(WS_data_resampled.DryBulb - T)...
+Sc4.*WS_data_resampled.RelativeHumidity+Sc5.*WS_data_resampled.WindSpeed)...
+Sd);
% Limits based on extraterrestrial radiation (IO*sin(SolAltAngle)
clear INDEX;
INDEX = (WS_data_resampled.EstimHourlySol(:,1) <
0.1*IO*sin(WS_data_resampled.SolAltAngle(:,1)));
WS_data_resampled.EstimHourlySol(INDEX,1) = 0.1*IO*sin(WS_data_resampled.SolAltAngle(INDEX,1));

INDEX = (WS_data_resampled.EstimHourlySol(:,1) >
0.9*IO*sin(WS_data_resampled.SolAltAngle(:,1)));
WS_data_resampled.EstimHourlySol(INDEX,1) = 0.9*IO*sin(WS_data_resampled.SolAltAngle(INDEX,1));

INDEX = (WS_data_resampled.EstimHourlySol(:,1) < 0);
WS_data_resampled.EstimHourlySol(INDEX,1) = 0;

% Need to detect clear days and use ASHRAE clear sky model to smooth out
% direct/total radiation over the day as per Gueymard & Thevenard
% Source for tau b & d (beam and diffuse pseudo optical depths) values
% from ASHRAE data for Mexican sites (40) and interpolated for the sites
% that are not in the ASHRAE data set.

```



```

%"To improve the hourly solar profiles in the IWECC
%weather files, the ASHRAE 2009 Clear Sky Model (Gueymard
%and Thevenard 2013), or ACSM09 for brevity, is used to
%recalculate the hourly distribution of global horizontal radiation
%while leaving the total daily solar radiation computed by
%the ZHM unchanged. For clear days, defined as those where
%the aggregate cloud cover during daylight hours is no more
%than 10 and the cloud cover during any daylight hour is no
%more than 1, the hourly solar profile from ACSM09 is scaled
%to the daily total and substituted for the hourly profile from the
%ZHM." Development of 3012 IWECCWeather Files for International Locations (RP-1477)
% Huang et al. Ashrae Transactions, 2014, vol. 120, no 1, 340-355.

% Direct Normal Solar Radiation from model by Zhang et al (2004): sigmoidal
% Gompertz function.

% Reshape estimated hourly solar energy data into daily sets of 24 hours by 365 days
% Reshape all the weather data

%Temp8 = zeros(8760,1);
%Temp8(1:8761+RelativeToUTC,1) = WS_data_resampled.EstimHourlySol(-RelativeToUTC:8760,1);
%Temp8(8762+RelativeToUTC:8760,1) = WS_data_resampled.EstimHourlySol(1:-RelativeToUTC-1,1);
%WS_data_resampled.EstimDaylySol = reshape(Temp8,[24,365]);
WS_data_resampled.EstimDaylySol = reshape(WS_data_resampled.EstimHourlySol,[24,365]);

%Temp8 = zeros(8760,1);
%Temp8(1:8761+RelativeToUTC,1) = WS_data_resampled.SolarTime(-RelativeToUTC:8760,1);
%Temp8(8762+RelativeToUTC:8760,1) = WS_data_resampled.SolarTime(1:-RelativeToUTC-1,1);
%WS_data_resampled.SolarTimeDayly = reshape(Temp8,[24,365]);
WS_data_resampled.SolarTimeDayly = reshape(WS_data_resampled.SolarTime,[24,365]);

%Temp8 = zeros(8760,1);
%Temp8(1:8761+RelativeToUTC,1) = WS_data_resampled.Pressure(-RelativeToUTC:8760,1);
%Temp8(8762+RelativeToUTC:8760,1) = WS_data_resampled.Pressure(1:-RelativeToUTC-1,1);
%WS_data_resampled.PressureDayly = reshape(Temp8,[24,365]);
WS_data_resampled.PressureDayly = reshape(WS_data_resampled.Pressure,[24,365]);

%Temp8 = zeros(8760,1);
%Temp8(1:8761+RelativeToUTC,1) = WS_data_resampled.DryBulb(-RelativeToUTC:8760,1);
%Temp8(8762+RelativeToUTC:8760,1) = WS_data_resampled.DryBulb(1:-RelativeToUTC-1,1);
%WS_data_resampled.DryBulbDayly = reshape(Temp8,[24,365]);
WS_data_resampled.DryBulbDayly = reshape(WS_data_resampled.DryBulb,[24,365]);

%Temp8 = zeros(8760,1);
%Temp8(1:8761+RelativeToUTC,1) = WS_data_resampled.DewPoint(-RelativeToUTC:8760,1);
%Temp8(8762+RelativeToUTC:8760,1) = WS_data_resampled.DewPoint(1:-RelativeToUTC-1,1);
%WS_data_resampled.DewPointDayly = reshape(Temp8,[24,365]);
WS_data_resampled.DewPointDayly = reshape(WS_data_resampled.DewPoint,[24,365]);

%Temp8 = zeros(8760,1);
%Temp8(1:8761+RelativeToUTC,1) = WS_data_resampled.WindDir(-RelativeToUTC:8760,1);
%Temp8(8762+RelativeToUTC:8760,1) = WS_data_resampled.WindDir(1:-RelativeToUTC-1,1);
%WS_data_resampled.WindDirDayly = reshape(Temp8,[24,365]);
WS_data_resampled.WindDirDayly = reshape(WS_data_resampled.WindDir,[24,365]);

%Temp8 = zeros(8760,1);
%Temp8(1:8761+RelativeToUTC,1) = WS_data_resampled.WindSpeed(-RelativeToUTC:8760,1);
%Temp8(8762+RelativeToUTC:8760,1) = WS_data_resampled.WindSpeed(1:-RelativeToUTC-1,1);
%WS_data_resampled.WindSpeedDayly = reshape(Temp8,[24,365]);
WS_data_resampled.WindSpeedDayly = reshape(WS_data_resampled.WindSpeed,[24,365]);

```

```

%Temp8 = zeros(8760,1);
%Temp8(1:8761+RelativeToUTC,1) = WS_data_resampled.CloudCover(-RelativeToUTC:8760,1);
%Temp8(8762+RelativeToUTC:8760,1) = WS_data_resampled.CloudCover(1:-RelativeToUTC-1,1);
%WS_data_resampled.CloudCoverDayly = reshape(Temp8,[24,365]);
WS_data_resampled.CloudCoverDayly = reshape(WS_data_resampled.CloudCover,[24,365]);

%Temp8 = zeros(8760,1);
%Temp8(1:8761+RelativeToUTC,1) = WS_data_resampled.Precipit(-RelativeToUTC:8760,1);
%Temp8(8762+RelativeToUTC:8760,1) = WS_data_resampled.Precipit(1:-RelativeToUTC-1,1);
%WS_data_resampled.PrecipitDayly = reshape(Temp8,[24,365]);
WS_data_resampled.PrecipitDayly = reshape(WS_data_resampled.Precipit,[24,365]);

%Temp8 = zeros(8760,1);
%Temp8(1:8761+RelativeToUTC,1) = WS_data_resampled.Declination(-RelativeToUTC:8760,1);
%Temp8(8762+RelativeToUTC:8760,1) = WS_data_resampled.Declination(1:-RelativeToUTC-1,1);
%WS_data_resampled.DeclinationDayly = reshape(Temp8,[24,365]);
WS_data_resampled.DeclinationDayly = reshape(WS_data_resampled.Declination,[24,365]);

%Temp8 = zeros(8760,1);
%Temp8(1:8761+RelativeToUTC,1) = WS_data_resampled.SolAltAngle(-RelativeToUTC:8760,1);
%Temp8(8762+RelativeToUTC:8760,1) = WS_data_resampled.SolAltAngle(1:-RelativeToUTC-1,1);
%WS_data_resampled.SolAltAngleDayly = reshape(Temp8,[24,365]);
WS_data_resampled.SolAltAngleDayly = reshape(WS_data_resampled.SolAltAngle,[24,365]);

%Temp8 = zeros(8760,1);
%Temp8(1:8761+RelativeToUTC,1) = WS_data_resampled.HourAngle(-RelativeToUTC:8760,1);
%Temp8(8762+RelativeToUTC:8760,1) = WS_data_resampled.HourAngle(1:-RelativeToUTC-1,1);
%WS_data_resampled.HourAngleDayly = reshape(Temp8,[24,365]);
WS_data_resampled.HourAngleDayly = reshape(WS_data_resampled.HourAngle,[24,365]);

% Day light hours index
INDEXDAYTIME = (WS_data_resampled.SolAltAngleDayly > 0); %Don't estimate solar radiation at
night
INDEXDAYTIME7 = (WS_data_resampled.SolAltAngleDayly > 0.3); %Cutoff at 17 degrees solar angle -
for direct/diffuse split below this angle considered 100% diffuse.
%Direct/diffuse split for cos solar
angle >0.3
WS_data_resampled.DayAverageCldCvr = zeros(24,365);
WS_data_resampled.DaylightCloudCover(1:24,1:365) = nan;
WS_data_resampled.DaylightCloudCover(INDEXDAYTIME) =
WS_data_resampled.CloudCoverDayly(INDEXDAYTIME);
WS_data_resampled.DayAverageCldCvr(1,1:365) =
sum(WS_data_resampled.DaylightCloudCover,'omitnan'); %Total cloud cover during daylight hours in
column 1
WS_data_resampled.DayAverageCldCvr(2,1:365) = max(WS_data_resampled.DaylightCloudCover);
%Maximum cloud cover at any point of daylight hours for a given day in column 2.
INDEXCLEARDAY = (WS_data_resampled.DayAverageCldCvr(1,:) < 10 &
WS_data_resampled.DayAverageCldCvr(2,:) <= 1);
WS_data_resampled.DayAverageCldCvr(3,1:365) = sum(WS_data_resampled.EstimDaylySol); %Total daily
solar energy estimated from ZHM model in column 3.

% Interpolate values for Taub and Taud for ASHRAE clear sky model using
% the 'nearest' parameter - it is likely there are very small difference in
% latitude and longitude between the values for the sites from the raw
% data source and the ASHRAE data table - for the 49 sites which ASHRAE
% provides data, it is likely that there is a one to one correspondance
% with raw data sites. For any other site the values of the nearest
% available site is used.

taub12 = zeros(12,1);
taud12 = zeros(12,1);
taub365 = zeros(365,1);

```

```

taud365 = zeros(365,1);
taub397 = zeros(397,1);
taud397 = zeros(397,1);

QLatLong = [Latitude,Longitude];

k = dsearchn(LatLong,QLatLong); %Nearest point search k = dsearchn(X,XI) performs the search
without using a triangulation. %With large X and small XI, this approach is faster and
uses much less memory.
taub12 = taub(k,:);
taud12 = taud(k,:);
taub14(1) = taub12(12);
taub14(2:13) = taub12;
taub14(14) = taub12(1);
taud14(1) = taud12(12);
taud14(2:13) = taud12;
taud14(14) = taud12(1);
tau14x = [1,32,63,91,122,152,183,213,244,275,315,336,366,397];

DaysOfTheYear = (1:397);
taub397 = interp1(tau14x,taub14,DaysOfTheYear,'linear');
taud397 = interp1(tau14x,taud14,DaysOfTheYear,'linear');
taub365 = taub397(12:376);
taud365 = taud397(12:376);

% Air mass from equation 16 Chpt. 14 ASHRAE Fundamentals Handbook 2021 SI

WS_data_resampled.Airmass(1:24,1:365) = zeros(24,365);
WS_data_resampled.Airmass(1:24,1:365) = nan;
WS_data_resampled.Airmass(INDEXDAYTIME) =
1.0./(sin(WS_data_resampled.SolAltAngleDayly(INDEXDAYTIME))...
+0.50572.*((6.07995+WS_data_resampled.SolAltAngleDayly(INDEXDAYTIME).*360./(2.*pi)).^(-1.6364)));

% Clear sky solar radiation: equations 19, 20, 17 & 18 Chpt. 14 ASHRAE Fundamentals Handbook
2021 SI
% Equation 19 & 20 Air mass exponents ab and ad are correlated to taub and taud through
% the following empirical relationships:

ab = zeros(24,365);
ad = zeros(24,365);
E0 = zeros(24,365);
taub24365 = zeros(24,365);
taud24365 = zeros(24,365);
WS_data_resampled.DailyEb = zeros(24,365);
WS_data_resampled.DailyEd = zeros(24,365);
WS_data_resampled.DailyEbh = zeros(24,365);
WS_data_resampled.DailyASHRAEHORIZ = zeros(24,365);
WS_data_resampled.DailyZHMmntAvg = zeros(24,12); % Averages for each hour of the day for each
month

for Idaytau = 1:365
for Ihourtau = 1:24
ab(Ihourtau,Idaytau) = 1.454 -0.406*taub365(Idaytau) - 0.268*taud365(Idaytau) +
0.021*taub365(Idaytau)*taub365(Idaytau);
ad(Ihourtau,Idaytau) = 0.507 -0.205*taub365(Idaytau) - 0.080*taud365(Idaytau) +
0.190*taub365(Idaytau)*taub365(Idaytau);
% Extraterrestrial Solar Radiation Equation 4 Chpt. 14 ASHRAE
% Fundamentals Handbook 2021 SI in W/m^2
E0(Ihourtau,Idaytau) = 1367*(1+0.033*cos(2*pi*(Idaytau-3)/365));
taub24365(Ihourtau,Idaytau) = taub365(Idaytau);
taud24365(Ihourtau,Idaytau) = taud365(Idaytau);
end
end

```

```

end
CLEARDAYINDEX = reshape(INDEXCLEARDAY,[365,1]);

ab(~INDEXDAYTIME)= nan;
EO(~INDEXDAYTIME)= nan;
taub24365(~INDEXDAYTIME)= nan;
taud24365(~INDEXDAYTIME)= nan;
WS_data_resampled.DailyEb(~INDEXDAYTIME)= nan;
WS_data_resampled.DailyEd(~INDEXDAYTIME)= nan;
WS_data_resampled.DailyEbh(~INDEXDAYTIME)= nan;
WS_data_resampled.DailyASHRAEHoriz(~INDEXDAYTIME)= nan;

WS_data_resampled.DailyEb(INDEXDAYTIME) =
EO(INDEXDAYTIME).*exp(-taub24365(INDEXDAYTIME).*WS_data_resampled.Airmass(INDEXDAYTIME).^ (ab(INDE
XDAYTIME))); %Beam
WS_data_resampled.DailyEd(INDEXDAYTIME) =
EO(INDEXDAYTIME).*exp(-taud24365(INDEXDAYTIME).*WS_data_resampled.Airmass(INDEXDAYTIME).^ (ad(INDE
XDAYTIME))); %Diffuse on horizontal surface

% Beam on horizontal surface

WS_data_resampled.DailyEbh(INDEXDAYTIME)=
WS_data_resampled.DailyEb(INDEXDAYTIME).*cos(pi/2-WS_data_resampled.SolAltAngleDayly(INDEXDAYTIME
));

WS_data_resampled.DailyASHRAEHoriz(INDEXDAYTIME)=
WS_data_resampled.DailyEbh(INDEXDAYTIME)+WS_data_resampled.DailyEd(INDEXDAYTIME);

WS_data_resampled.DayAverageCldCvr(4,1:365) = sum(WS_data_resampled.DailyASHRAEHoriz,'omitnan');
%Total daily beam solar energy from ASHRAE clear sky model on horizontal surface in column 4.
WS_data_resampled.DayAverageCldCvr(5,1:365) = sum(WS_data_resampled.DailyEd,'omitnan'); %Total
daily diffuse solar energy on horizontal surface from ASHRAE clear sky model in column 5.
WS_data_resampled.DayAverageCldCvr(6,1:365) = sum(WS_data_resampled.EstimDaylySol); %ZHM daily
totals in column 6.
WS_data_resampled.DayAverageCldCvr(7,1:365) =
WS_data_resampled.DayAverageCldCvr(6,1:365)./WS_data_resampled.DayAverageCldCvr(4,1:365); % ZHM
daily total/ASHRAE clear sky daily total
WS_data_resampled.DayAverageCldCvr(8,1:365) =
WS_data_resampled.DayAverageCldCvr(4,1:365)+WS_data_resampled.DayAverageCldCvr(5,1:365); % ASHRAE
clear sky daily total on horizontal surface in column 8

%Clear days hourly ASHRAE scaled to ZHM daily totals
WS_data_resampled.DailyClearScaledToZHM = nan(24,365);
WS_data_resampled.DailyClearScaledToZHM(1:24,CLEARDAYINDEX) =
WS_data_resampled.DailyASHRAEHoriz(1:24,CLEARDAYINDEX).*WS_data_resampled.DayAverageCldCvr(7,INDE
XCLEARDAY);

% Cloudy days - needs ZHM monthly average profile (hour by hour) - then
% scale the ASHRAE clear sky to the monthly average. Hourly difference
% between that result and hourly monthly

% Set month days' indecies

INDEXJANDAYS = false(365,1);
INDEXJANDAYS (1:31) = true;
%INDEXmonthDAYS (1,1:31) = true;
INDEXFEBDAYS = false(365,1);
INDEXFEBDAYS (32:59) = true;
%INDEXmonthDAYS (2,32:59) = true;
INDEXMARDAYS = false(365,1);
INDEXMARDAYS (60:90) = true;
%INDEXmonthDAYS(3,60:90) = true;
INDEXAPRDAYS = false(365,1);
INDEXAPRDAYS (91:120) = true;

```

```

%INDEXmonthDAYS (4,91:120) = true;
INDEXMAYDAYS = false(365,1);
INDEXMAYDAYS (121:151) = true;
%INDEXmonthDAYS (5,121:151) = true;
INDEXJUNDAYS = false(365,1);
INDEXJUNDAYS (152:181) = true;
%INDEXmonthDAYS (6,152:181) = true;
INDEXJULDAYS = false(365,1);
INDEXJULDAYS (182:212) = true;
%INDEXmonthDAYS (7,182:212) = true;
INDEXAUGDAYS = false(365,1);
INDEXAUGDAYS (213:243) = true;
%INDEXmonthDAYS (8,213:243) = true;
INDEXSEPDAYS = false(365,1);
INDEXSEPDAYS (244:273) = true;
%INDEXmonthDAYS (9,244:273) = true;
INDEXOCTDAYS = false(365,1);
INDEXOCTDAYS (274:304) = true;
%INDEXmonthDAYS (10,274:304) = true;
INDEXNOVDAYS = false(365,1);
INDEXNOVDAYS (305:334) = true;
%INDEXmonthDAYS (11,305:334) = true;
INDEXDECDAYS = false(365,1);
INDEXDECDAYS (335:365) = true;
%INDEXmonthDAYS (12,335:365) = true;

CLEARDAYINDEX = reshape(INDEXCLEARDAY,[365,1]);
WS_data_resampled.EstimDaylySol(~INDEXDAYTIME)= nan;
WS_data_resampled.DailyZHMmntAvg = zeros(24,12);
WS_data_resampled.DailyZHMmntAvg(:,1) =
mean(WS_data_resampled.EstimDaylySol(:,INDEXJANDAYS&~CLEARDAYINDEX),2,'omitnan');
WS_data_resampled.DailyZHMmntAvg(:,2) =
mean(WS_data_resampled.EstimDaylySol(:,INDEXFEBDAYS&~CLEARDAYINDEX),2,'omitnan');
WS_data_resampled.DailyZHMmntAvg(:,3) =
mean(WS_data_resampled.EstimDaylySol(:,INDEXMARDAYS&~CLEARDAYINDEX),2,'omitnan');
WS_data_resampled.DailyZHMmntAvg(:,4) =
mean(WS_data_resampled.EstimDaylySol(:,INDEXAPRDAYS&~CLEARDAYINDEX),2,'omitnan');
WS_data_resampled.DailyZHMmntAvg(:,5) =
mean(WS_data_resampled.EstimDaylySol(:,INDEXMAYDAYS&~CLEARDAYINDEX),2,'omitnan');
WS_data_resampled.DailyZHMmntAvg(:,6) =
mean(WS_data_resampled.EstimDaylySol(:,INDEXJUNDAYS&~CLEARDAYINDEX),2,'omitnan');
WS_data_resampled.DailyZHMmntAvg(:,7) =
mean(WS_data_resampled.EstimDaylySol(:,INDEXJULDAYS&~CLEARDAYINDEX),2,'omitnan');
WS_data_resampled.DailyZHMmntAvg(:,8) =
mean(WS_data_resampled.EstimDaylySol(:,INDEXAUGDAYS&~CLEARDAYINDEX),2,'omitnan');
WS_data_resampled.DailyZHMmntAvg(:,9) =
mean(WS_data_resampled.EstimDaylySol(:,INDEXSEPDAYS&~CLEARDAYINDEX),2,'omitnan');
WS_data_resampled.DailyZHMmntAvg(:,10) =
mean(WS_data_resampled.EstimDaylySol(:,INDEXOCTDAYS&~CLEARDAYINDEX),2,'omitnan');
WS_data_resampled.DailyZHMmntAvg(:,11) =
mean(WS_data_resampled.EstimDaylySol(:,INDEXNOVDAYS&~CLEARDAYINDEX),2,'omitnan');
WS_data_resampled.DailyZHMmntAvg(:,12) =
mean(WS_data_resampled.EstimDaylySol(:,INDEXDECDAYS&~CLEARDAYINDEX),2,'omitnan');

%Daily totals from DailyZHMmntAvg
WS_data_resampled.DailyZHMmntAvgTot = zeros(12,1);
for i = 1:12
    WS_data_resampled.DailyZHMmntAvgTot(i) =
sum(WS_data_resampled.DailyZHMmntAvg(:,i),'omitnan');
end
%Scale ASHRAE clear sky to monthly average ZHM total on a horizontal
%surface on cloudy days

WS_data_resampled.DailyCldyZHMratioASH = nan(24,365);

```

```

%WS_data_resampled.DailyCldyAHSminusZHMhrly = nan(24,365);

for i = 1:24
    WS_data_resampled.DailyCldyZHMratioASH(i,INDEXJANDAYS~-CLEARDAYINDEX) =
WS_data_resampled.DailyZHMmntAvgTot(1)./WS_data_resampled.DayAverageCldCvr(8,INDEXJANDAYS~-CLEAR
AYINDEX);
    WS_data_resampled.DailyCldyZHMratioASH(i,INDEXFEBDAYS~-CLEARDAYINDEX) =
WS_data_resampled.DailyZHMmntAvgTot(2)./WS_data_resampled.DayAverageCldCvr(8,INDEXFEBDAYS~-CLEAR
AYINDEX);
    WS_data_resampled.DailyCldyZHMratioASH(i,INDEXMARDAYS~-CLEARDAYINDEX) =
WS_data_resampled.DailyZHMmntAvgTot(3)./WS_data_resampled.DayAverageCldCvr(8,INDEXMARDAYS~-CLEAR
AYINDEX);
    WS_data_resampled.DailyCldyZHMratioASH(i,INDEXAPRDAYS~-CLEARDAYINDEX) =
WS_data_resampled.DailyZHMmntAvgTot(4)./WS_data_resampled.DayAverageCldCvr(8,INDEXAPRDAYS~-CLEAR
AYINDEX);
    WS_data_resampled.DailyCldyZHMratioASH(i,INDEXMAYDAYS~-CLEARDAYINDEX) =
WS_data_resampled.DailyZHMmntAvgTot(5)./WS_data_resampled.DayAverageCldCvr(8,INDEXMAYDAYS~-CLEAR
AYINDEX);
    WS_data_resampled.DailyCldyZHMratioASH(i,INDEXJUNDAYS~-CLEARDAYINDEX) =
WS_data_resampled.DailyZHMmntAvgTot(6)./WS_data_resampled.DayAverageCldCvr(8,INDEXJUNDAYS~-CLEAR
AYINDEX);
    WS_data_resampled.DailyCldyZHMratioASH(i,INDEXJULDAYS~-CLEARDAYINDEX) =
WS_data_resampled.DailyZHMmntAvgTot(7)./WS_data_resampled.DayAverageCldCvr(8,INDEXJULDAYS~-CLEAR
AYINDEX);
    WS_data_resampled.DailyCldyZHMratioASH(i,INDEXAUGDAYS~-CLEARDAYINDEX) =
WS_data_resampled.DailyZHMmntAvgTot(8)./WS_data_resampled.DayAverageCldCvr(8,INDEXAUGDAYS~-CLEAR
AYINDEX);
    WS_data_resampled.DailyCldyZHMratioASH(i,INDEXSEPDAYS~-CLEARDAYINDEX) =
WS_data_resampled.DailyZHMmntAvgTot(9)./WS_data_resampled.DayAverageCldCvr(8,INDEXSEPDAYS~-CLEAR
AYINDEX);
    WS_data_resampled.DailyCldyZHMratioASH(i,INDEXOCTDAYS~-CLEARDAYINDEX) =
WS_data_resampled.DailyZHMmntAvgTot(10)./WS_data_resampled.DayAverageCldCvr(8,INDEXOCTDAYS~-CLEAR
DAYINDEX);
    WS_data_resampled.DailyCldyZHMratioASH(i,INDEXNOVDAYS~-CLEARDAYINDEX) =
WS_data_resampled.DailyZHMmntAvgTot(11)./WS_data_resampled.DayAverageCldCvr(8,INDEXNOVDAYS~-CLEAR
DAYINDEX);
    WS_data_resampled.DailyCldyZHMratioASH(i,INDEXDECDAYS~-CLEARDAYINDEX) =
WS_data_resampled.DailyZHMmntAvgTot(12)./WS_data_resampled.DayAverageCldCvr(8,INDEXDECDAYS~-CLEAR
DAYINDEX);
end

WS_data_resampled.DailyCldyASHScaled = nan(24,365);
WS_data_resampled.DailyCldyASHScaled =
WS_data_resampled.DailyASHRAEHoriz(:,:).*WS_data_resampled.DailyCldyZHMratioASH(:,:);

WS_data_resampled.DailyCldyASHminusZHMhrly = nan(24,365);

for i = 1:24
    WS_data_resampled.DailyCldyASHminusZHMhrly(i,INDEXJANDAYS~-CLEARDAYINDEX) =
WS_data_resampled.EstimDaylySol(i,INDEXJANDAYS~-CLEARDAYINDEX)-WS_data_resampled.DailyZHMmntAvg(i
,1);
    WS_data_resampled.DailyCldyASHminusZHMhrly(i,INDEXFEBDAYS~-CLEARDAYINDEX) =
WS_data_resampled.EstimDaylySol(i,INDEXFEBDAYS~-CLEARDAYINDEX)-WS_data_resampled.DailyZHMmntAvg(i
,2);
    WS_data_resampled.DailyCldyASHminusZHMhrly(i,INDEXMARDAYS~-CLEARDAYINDEX) =
WS_data_resampled.EstimDaylySol(i,INDEXMARDAYS~-CLEARDAYINDEX)-WS_data_resampled.DailyZHMmntAvg(i
,3);
    WS_data_resampled.DailyCldyASHminusZHMhrly(i,INDEXAPRDAYS~-CLEARDAYINDEX) =
WS_data_resampled.EstimDaylySol(i,INDEXAPRDAYS~-CLEARDAYINDEX)-WS_data_resampled.DailyZHMmntAvg(i
,4);
    WS_data_resampled.DailyCldyASHminusZHMhrly(i,INDEXMAYDAYS~-CLEARDAYINDEX) =
WS_data_resampled.EstimDaylySol(i,INDEXMAYDAYS~-CLEARDAYINDEX)-WS_data_resampled.DailyZHMmntAvg(i
,5);

```

```

        WS_data_resampled.DailyCldyASHminusZMhrly(i,INDEXJUNDAYS&-CLEARDAYINDEX) =
WS_data_resampled.EstimDaylySol(i,INDEXJUNDAYS&-CLEARDAYINDEX)-WS_data_resampled.DailyZHMmntAvg(i
,6);
        WS_data_resampled.DailyCldyASHminusZMhrly(i,INDEXJULDDAYS&-CLEARDAYINDEX) =
WS_data_resampled.EstimDaylySol(i,INDEXJULDDAYS&-CLEARDAYINDEX)-WS_data_resampled.DailyZHMmntAvg(i
,7);
        WS_data_resampled.DailyCldyASHminusZMhrly(i,INDEXAUGDDAYS&-CLEARDAYINDEX) =
WS_data_resampled.EstimDaylySol(i,INDEXAUGDDAYS&-CLEARDAYINDEX)-WS_data_resampled.DailyZHMmntAvg(i
,8);
        WS_data_resampled.DailyCldyASHminusZMhrly(i,INDEXSEPDAYS&-CLEARDAYINDEX) =
WS_data_resampled.EstimDaylySol(i,INDEXSEPDAYS&-CLEARDAYINDEX)-WS_data_resampled.DailyZHMmntAvg(i
,9);
        WS_data_resampled.DailyCldyASHminusZMhrly(i,INDEXOCTDDAYS&-CLEARDAYINDEX) =
WS_data_resampled.EstimDaylySol(i,INDEXOCTDDAYS&-CLEARDAYINDEX)-WS_data_resampled.DailyZHMmntAvg(i
,10);
        WS_data_resampled.DailyCldyASHminusZMhrly(i,INDEXNOVDAYS&-CLEARDAYINDEX) =
WS_data_resampled.EstimDaylySol(i,INDEXNOVDAYS&-CLEARDAYINDEX)-WS_data_resampled.DailyZHMmntAvg(i
,11);
        WS_data_resampled.DailyCldyASHminusZMhrly(i,INDEXDECDAYS&-CLEARDAYINDEX) =
WS_data_resampled.EstimDaylySol(i,INDEXDECDAYS&-CLEARDAYINDEX)-WS_data_resampled.DailyZHMmntAvg(i
,12);
    end
        WS_data_resampled.DailyCldySmoothed = zeros(24,365);
        WS_data_resampled.DailyCldySmoothed(:,~CLEARDAYINDEX) =
WS_data_resampled.DailyCldyASHscaled(:,~CLEARDAYINDEX)+WS_data_resampled.DailyCldyASHminusZMhrly
(:,~CLEARDAYINDEX);

    figure (1);
    %set(gcf, 'Position', [50,900,750,500]);
    set(gcf, 'Position', [10,50,2500,1400]);
    subplot (6,1,1);
    plttemp = reshape(WS_data_resampled.DailyCldySmoothed,[1,8760]);
    plot(plttemp(1:240));
    title ('DailyCldySmoothed');
    ax = gca;
    ax.XLim = [1 240];
    ax.YLim = [-100 max(plttemp)*1.1];

%figure (3);
%set(gcf, 'Position', [1750,900,750,500]);
subplot (6,1,3);
plttemp = reshape(WS_data_resampled.EstimHourlySol,[1,8760]);
%for i = 1:24
%    plttempIndex(i,1:365) = CLEARDAYINDEX;
%end
%plttempIndexC = reshape(plttempIndex,[1,8760]);
plot(plttemp(1:240));
%plot(plttemp(~plttempIndex));
title ('EstimHourlySol ZHM');
ax = gca;
ax.XLim = [1 240];
ax.YLim = [-100 max(plttemp)*1.1];

% Direct/diffuse partition using "Zhang et al. (2004) has been used to estimate the direct
normal
% radiation using a sigmoidal Gompertz function where growth
% is slowest at the start and end of the function (Parton and Innis 1972)"
% Following "Development of 3012 IWEC2Weather Files for International
% Locations (RP-1477)" Huang et al.

A1 = zeros (24,365);
A2 = zeros (24,365);
A3 = zeros (24,365);

```

```

A4 = 2.99;
SinH = zeros (24,365);
SinH = max(sin(WS_data_resampled.SolAltAngleDayly),0.2); %Zhang et al. (2004) "When Kt is
smaller than 0.2, the direct radiation Kn is almost zero"
%"Therefore values smaller than 0.3 were excluded in the modelling
% process."
A1(INDEXDAYTIME) = -0.1556*SinH(INDEXDAYTIME).*SinH(INDEXDAYTIME) + 0.1028.*SinH(INDEXDAYTIME) +
1.3748;
A2(INDEXDAYTIME) = 0.7973*SinH(INDEXDAYTIME).*SinH(INDEXDAYTIME) + 0.1509*SinH(INDEXDAYTIME) +
3.035;
A3(INDEXDAYTIME) = 5.4307*SinH(INDEXDAYTIME) + 7.2182;

WS_data_resampled.DailyTotalHorizontal = WS_data_resampled.DailyCldySmoothed +
max(WS_data_resampled.DailyClearScaledToZHM,0);

subplot (6,1,1);
plttemp = reshape(WS_data_resampled.EstimHourlySol,[1,8760]);
plot(plttemp(1:240));
title ('Global Horizontal Radiation - Raw ZHM');
ax = gca;
ax.XLim = [1 240];
ax.YLim = [-100 max(plttemp)*1.1];

WS_data_resampled.Kt = zeros (24,365);
WS_data_resampled.Kt = (WS_data_resampled.DailyTotalHorizontal./SinH)/IO;

WS_data_resampled.Knormal = zeros (24,365);
WS_data_resampled.Knormal = (A1.*A2).^(-(A3.*A2).^(-(A4.*WS_data_resampled.Kt)));

WS_data_resampled.DailyDirectNormal = zeros (24,365);
WS_data_resampled.DailyDirectNormal7 = zeros (24,365);
WS_data_resampled.DailyDirectNormal(INDEXDAYTIME) = WS_data_resampled.Knormal(INDEXDAYTIME).*IO;
WS_data_resampled.DailyDirectNormal7(INDEXDAYTIME7) =
WS_data_resampled.Knormal(INDEXDAYTIME7).*IO;

%figure (2);
%set(gcf, 'Position', [900,900,750,500]);
subplot (6,1,2);
WS_data_resampled.DailyCldySmoothed(:,~CLEARDAYINDEX) =
max(WS_data_resampled.DailyCldySmoothed(:,~CLEARDAYINDEX),0);
%plttemp = reshape(WS_data_resampled.DailyCldySmoothed,[1,8760]);
plttemp = reshape(WS_data_resampled.DailyTotalHorizontal,[1,8760]);
plot(plttemp(1:240));
%plot(WS_data_resampled.DailyCldySmoothed(:,~CLEARDAYINDEX));
title ('DailyTotalHorizontal');
ax = gca;
ax.XLim = [1 240];
ax.YLim = [-100 max(plttemp)*1.1];

%figure (4);
%set(gcf, 'Position', [50,300,750,500]);
subplot (6,1,4);
%plttemp = reshape(WS_data_resampled.DailyDirectNormal,[1,8760]);
plttemp1 = reshape(WS_data(1:8760,8),[1,8760]);
plttemp2 = reshape(WS_data_resampled.DailyTotalHorizontal,[1,8760]);
%plttemp(2:8760) = plttemp2(1:8759);plttemp(1)=plttemp2(8760);
% plttemp =
reshape(WS_data(1:8760,8),[1,8760]) - reshape(WS_data_resampled.DailyTotalHorizontal,[1,8760]);
%plttemp = plttemp1-plttemp2;
plot(plttemp1(8280:8760));
hold;
plot(plttemp2(8280:8760));
%plot(plttemp(1:240));

```



```

title ('Difference EPW global horizontal - global horizontal this model (ZHM smoothed)');
ax = gca;
%ax.XLim = [4380 4428];
ax.YLim = [-100 1400];
hold;
Kns = zeros(100,1);
Kts = zeros(100,1);
sinhangle = zeros(100,1);

for i = 1:100
    hourangle = (i-0.99)*pi/100;
    sinhangle(i) = sin(hourangle);
    A1s = -0.1556*sinhangle(i)*sinhangle(i) + 0.1028*sinhangle(i) + 1.3748;
    A2s = 0.7973*sinhangle(i)*sinhangle(i) + 0.1509*sinhangle(i) + 3.035;
    A3s = 5.4307*sinhangle(i) + 7.2182;
    Kts(i) = 0.35/sinhangle(i);
    Kns(i) = (A1s*A2s)^(-((A3s*A2s)^(-(A4*Kts(i)))));
end

%figure (5);
%set(gcf,'Position',[900,300,750,500]);
subplot (6,1,5);
plttemp = reshape(WS_data_resampled.DailyDirectNormal7,[1,8760]);
plot(plttemp);
title ('DirectDailyNormal 7');
ax = gca;
ax.XLim = [1 8760];
ax.YLim = [-100 1400];

%figure (6);
%set(gcf,'Position',[1750,300,750,500]);
%subplot (6,1,6);
%plot(Kts(2:100),sinhangle(2:100));

%           Graph results

%figure (1);
%set(gcf,'Position',[50,900,750,500]);
set(gcf,'Position',[10,50,2500,1400]);
subplot (6,1,6);
plttemp = reshape(WS_data(1:8760,8),[1,8760]);
plot(plttemp(1:240));
title ('Global Horizontal Radiation From EPW');
ax = gca;
ax.XLim = [1 240];
ax.YLim = [-100 max(plttemp)*1.1];

figure (2);
set(gcf,'Position',[10,50,2500,1400]);
plttemp1 = reshape(WS_data(1:8760,8),[1,8760]); % y axis daily from EPW
file
plttemp2 = reshape(WS_data_resampled.DailyTotalHorizontal,[1,8760]); % x axis daily ZHM estimate
hold
plot (plttemp2,plttemp1,'linestyle','none','marker','o');
hold

JoeMonthHorizTot = zeros(12,1);

```

```

ZHMonthHorizTot = zeros(12,1);

plttemp1 = reshape(WS_data(1:8760,8),[24,365]);
plttemp1(plttemp1==0)=NaN;
plttemp2 = WS_data_resampled.DailyTotalHorizontal;
plttemp2(plttemp2==0)=NaN;

JoeMonthHorizTot = zeros(12,1);
ZHMonthHorizTot = zeros(12,1);

JoeMonthHorizTot(1,1) = mean(plttemp1(:,INDEXJANDAYS), 'all', 'omitnan');
JoeMonthHorizTot(2,1) = mean(plttemp1(:,INDEXFEBDAYS), 'all', 'omitnan');
JoeMonthHorizTot(3,1) = mean(plttemp1(:,INDEXMARDAYS), 'all', 'omitnan');
JoeMonthHorizTot(4,1) = mean(plttemp1(:,INDEXAPRDAYS), 'all', 'omitnan');
JoeMonthHorizTot(5,1) = mean(plttemp1(:,INDEXMAYDAYS), 'all', 'omitnan');
JoeMonthHorizTot(6,1) = mean(plttemp1(:,INDEXJUNDAYS), 'all', 'omitnan');
JoeMonthHorizTot(7,1) = mean(plttemp1(:,INDEXJULDAYS), 'all', 'omitnan');
JoeMonthHorizTot(8,1) = mean(plttemp1(:,INDEXAUGDAYS), 'all', 'omitnan');
JoeMonthHorizTot(9,1) = mean(plttemp1(:,INDEXSEPDAYS), 'all', 'omitnan');
JoeMonthHorizTot(10,1) = mean(plttemp1(:,INDEXOCTDAYS), 'all', 'omitnan');
JoeMonthHorizTot(11,1) = mean(plttemp1(:,INDEXNOVDAYS), 'all', 'omitnan');
JoeMonthHorizTot(12,1) = mean(plttemp1(:,INDEXDECDAYS), 'all', 'omitnan');

ZHMonthHorizTot(1,1) = mean(plttemp2(:,INDEXJANDAYS), 'all', 'omitnan');
ZHMonthHorizTot(2,1) = mean(plttemp2(:,INDEXFEBDAYS), 'all', 'omitnan');
ZHMonthHorizTot(3,1) = mean(plttemp2(:,INDEXMARDAYS), 'all', 'omitnan');
ZHMonthHorizTot(4,1) = mean(plttemp2(:,INDEXAPRDAYS), 'all', 'omitnan');
ZHMonthHorizTot(5,1) = mean(plttemp2(:,INDEXMAYDAYS), 'all', 'omitnan');
ZHMonthHorizTot(6,1) = mean(plttemp2(:,INDEXJUNDAYS), 'all', 'omitnan');
ZHMonthHorizTot(7,1) = mean(plttemp2(:,INDEXJULDAYS), 'all', 'omitnan');
ZHMonthHorizTot(8,1) = mean(plttemp2(:,INDEXAUGDAYS), 'all', 'omitnan');
ZHMonthHorizTot(9,1) = mean(plttemp2(:,INDEXSEPDAYS), 'all', 'omitnan');
ZHMonthHorizTot(10,1) = mean(plttemp2(:,INDEXOCTDAYS), 'all', 'omitnan');
ZHMonthHorizTot(11,1) = mean(plttemp2(:,INDEXNOVDAYS), 'all', 'omitnan');
ZHMonthHorizTot(12,1) = mean(plttemp2(:,INDEXDECDAYS), 'all', 'omitnan');

figure (3);
set(gcf, 'Position', [10,50,2500,1400]);
hold
plot(ZHMonthHorizTot,JoeMonthHorizTot, 'linestyle', 'none', 'marker', 'o');
ax = gca;
ax.XLim = [0,1200];
ax.YLim = [0,1200];
title ('Global Horizontal Radiation ZHM(x) vs EPW(y) monthly averages IWECC vs IWECC2');
hold

for imonth = 1:12
if ZHMonthHorizTot(imonth) < 100
file_list(ifile)
end
end

end
figure(3);
xlabel('Monthly global horizontal radiation ZHM this program');
ylabel('Monthly global horizontal radiation EPW file');

figure(2);
xlabel('Daily global horizontal radiation ZHM this program');
ylabel('Daily global horizontal radiation EPW file');
ax = gca;
ax.XLim = [-400,1200];
ax.YLim = [-400,1200];

```

Referencia

1. Joe, Yu, et al. "Development of 3012 IWEC2 weather files for international locations (RP-1477)." *Ashrae Transactions* 120.1 (2014).

Apéndice 2: Simulaciones del comportamiento térmico de una casa típica con la última versión del ESP-r.

## **INFORME DE TRABAJO**

Procesamiento de los datos meteorológicos horarios para producir años típicos actualizados con los datos más recientes disponibles utilizando programas desarrollados en el ambiente Matlab. Simulación del comportamiento térmico de viviendas utilizando los datos referidos utilizando la plataforma ESP-r.

Dr. Ricardo Gallegos Ortega

Septiembre-Diciembre 2022

# CONTENIDO

- 1 Habilitación de las herramientas de cómputo.
  - 1.1 Sistema Operativo
  - 1.2 ESP-r
  
- 2 Producción de archivos típicos meteorológicos aptos para ser procesados por el programa Esp-r.
  - 2.1 Creación del archivo binario.
  - 2.2 Creación del archivo block
  - 2.3 Alimentación del archivo *climatelist*.
  - 2.4 Archivos climáticos producidos.
  
- 3 Simulación de un modelo de vivienda con los archivos producidos.
  - 3.1 Objetivo de la simulación.
  - 3.2 Proceso de simulación.
    - 3.2.1 Selección de la base de datos climática.
    - 3.2.2 Ejecución de la simulación.
  - 3.3 Revisión de resultados
    - 3.3.1 Obtención de resultados.
    - 3.3.2 Procesamiento de resultados.
  
- 4 Simulación de un modelo de vivienda para sitios seleccionados considerando madera contrachapada (CLT).
  - 4.1 Objetivo de la simulación.
  - 4.2 Archivos meteorológicos.
  - 4.3 Ejecución de la simulación.
  - 4.4 Revisión de resultados
    - 4.4.1 Obtención de resultados.
    - 4.4.2 Procesamiento de resultados.

- 5 Entregables
- 5.1 Carpeta EPW BLOCKS Y BINARIOS.
- 5.2 Carpeta RESULTADOS.
- 5.2.1 Subcarpeta HISTORICOS
- 5.2.2 Subcarpeta CLT

El trabajo realizado se llevó a cabo en cuatro etapas:

1. Habilitación de las herramientas de cómputo.
2. Producción de archivos típicos meteorológicos aptos para ser procesados por el programa Esp-r.
3. Simulación de un modelo de vivienda con los archivos producidos.
4. Simulación de un modelo de vivienda para sitios seleccionados considerando construcción con madera contrachapada (CLT)

## **1. Habilitación de las herramientas de cómputo.**

Como tarea inicial se deben actualizar y acondicionar los programas de cómputo que se usarán.

### **1.1 Sistema Operativo**

El programa de simulación usado corre en ambiente Linux, en su distribución UBUNTU, por lo que para ser usado en una máquina con sistema operativo Windows se debió crear una máquina virtual con el programa Virtual Box.

El flujo de trabajo se dio de la siguiente forma, de manera resumida.

- 1.1.1 Instalar el programa Virtual Box en su (Vbox) versión más reciente.
- 1.1.2 Descargar la imagen de UBUNTU en su versión más reciente de de:  
<https://ubuntu.com/download/desktop>
- 1.1.3 Crear una máquina virtual en Vbox y configurarla con las siguientes características:  
RAM: 5Gb. Almacenamiento dinámico: 120 Gb Memoria de Video : 16Mb  
Controlador gráfico: VMSVG.
- 1.1.4 Instalar en la máquina virtual creada, la versión de UBUNTU descargada.
- 1.1.5 Crear una carpeta compartida con el sistema Windows, para poder almacenar archivos que puedan ser leídos por tal sistema, de acuerdo a lo que se indica en :  
<https://marcosmarti.org/como-montar-una-carpeta-compartida-en-virtualbox-en-ubuntu/>

### **1.2 ESP-r**

El programa de simulación ESP-r se puede descargar en su versión pre compilada, sin embargo, este método presentó problemas y el programa no pudo instalarse. Se optó

entonces por instalar el programa mediante compilación de acuerdo a lo que se indica en: <https://www.youtube.com/watch?v=cfxPFSBV6ps>

Se creó la carpeta /home/ricardo/Modelos/Terraced y haciendo uso de la carpeta compartida se insertó el modelo de casa con colindancias ChThs00\_East .

Se verificó la integridad del modelo y se descubrieron algunos errores de topología de superficies no asignadas o asignadas correctamente. Se corrigieron tales errores y se hicieron corridas de prueba, con resultados satisfactorios.

## **2. Producción de archivos típicos meteorológicos aptos para ser procesados por el programa Esp-r.**

La suite de simulación Esp-r realiza las simulaciones térmicas y análisis climáticos con archivos climáticos binarios, que a su vez provienen de archivos tipo EPW. El nombre y ubicación del archivo climático, así como algunos datos resumidos y estadísticos del contenido del archivo se ponen a disponibilidad de los diferentes módulos de la suite al incluir esta información en una lista de archivos llamada *climatelist*. El archivo EPW de preferencia debe estar ubicado en /opt/esp-r/climate, con objeto de no especificar trayectorias largas cuando se invoque el módulo climático. Posteriormente se puede cambiar de ubicación o borrar. De esta manera el proceso para hacer disponible un archivo climático para Esp-r es el siguiente:

### **2.1 Creación del archivo binario.**

A partir de un archivo epw, se debe primero crear un archivo binario, invocando el módulo *clm* en modo text, (preferentemente hay que ubicarse con la consola en el directorio /opt.esp-r/climate) de la siguiente manera, suponiendo que el archivo epw se llame QUERETARO97,epw y el archivo binario vaya a llevar el nombre QUERETARO97:

```
clm -mode text -file QUERETARO97 -act epw2bin silent
QUERETARO97.epw
```

Con el comando anterior se ha creado el archivo binario correspondiente, falta producir el archivo que contiene la información de ubicación y resumen climático, en un archivo con terminación block, en el caso de este ejemplo sería QUERETARO97.block

### **2.2 Creación del archivo block**

Para producir el archivo block se requiere invocar el módulo *clm* en su opción interactiva, mediante:

```
clm -file QUERETARO97 (Aparece la interfaz gráfica). Opciones a usar:
```

d graphical Aunque no es indispensable para la producción del archivo block, es muy útil para tener una idea si el archivo se convirtió correctamente a binario, graficar una o dos variables

Las siguientes opciones si son indispensables para la producción del archivo block:

### l Manage files

a menu str: (Es el nombre con el que aparecerá en los módulos para ser seleccionado, se puede cambiar el nombre del archivo)

b menú aid: (Comentario sobre la fuente de los datos)

c clm file: (Ubicación del archivo, preferentemente /opt.esp-r/climate/QUERETARO97, para este ejemplo)

d available ONLINE (si aparece OFFLINE, debe cambiarse)

o list/generate/edit documentation

initialise

save

Con esto se ha creado el archivo block.

Un archivo block contiene la siguiente información:

```
*item
*name    QUERETARO97
*aide    QUERETARO97 fue producido por UAM Cuajimalpa
*dbfl    /opt/esp-r/climate/QUERETARO97
*avail   ONLINE
*winter_s 1 1 28 2 1 11 31 12 # seasons Thu-01-Jan--Sat-28-Feb &
Sun-01-Nov--Thu-31-Dec
*spring_s 1 3 30 4 1 9 31 10 # seasons Sun-01-Mar--Thu-30-Apr &
Tue-01-Sep--Sat-31-Oct
*summer_s 1 5 31 8 # summer season Fri-01-May--Mon-31-Aug
*winter_t 9 1 15 1 20 11 26 11 # typical Fri-09-Jan--Thu-15-Jan &
Fri-20-Nov--Thu-26-Nov
*spring_t 6 3 12 3 2 10 8 10 # typical Fri-06-Mar--Thu-12-Mar &
Fri-02-Oct--Thu-08-Oct
*summer_t 11 7 17 7 # typical summer Sat-11-Jul--Fri-17-Jul
*help_start
```

Weather is XOXOCOTLAN-IAP - MEX

Location: 17.00N -6.72W : 1998

Month	Minimum	Time	Maximum	Time	Mean
Jan	3.2	@ 7h00 Thu-01	30.3	@16h00 Thu-29	18.0
Feb	7.5	@ 7h00 Mon-02	31.8	@16h00 Sun-22	20.3
Mar	8.0	@ 6h00 Wed-04	33.0	@16h00 Thu-12	20.6
Apr	10.0	@ 7h00 Thu-09	38.0	@18h00 Fri-24	23.4
May	14.0	@ 6h00 Tue-19	32.8	@15h00 Wed-06	22.9
Jun	12.0	@17h00 Wed-17	31.0	@13h00 Mon-29	21.7
Jul	13.0	@ 5h00 Tue-07	30.8	@16h00 Sat-04	20.9
Aug	10.3	@ 6h00 Mon-31	30.0	@16h00 Tue-11	19.9
Sep	14.3	@ 6h00 Tue-29	29.8	@16h00 Thu-17	21.3
Oct	8.9	@ 5h00 Sat-31	31.0	@15h00 Tue-20	20.3
Nov	6.0	@ 6h00 Tue-24	30.0	@15h00 Thu-05	18.7
Dec	4.0	@ 7h00 Wed-16	29.0	@15h00 Tue-08	17.8
Annual	3.2	@ 7h00 Thu-01-Jan	38.0	@18h00 Fri-24-Apr	20.5

---Seasons & typical periods---

Winter season is Thu-01-Jan - Sat-28-Feb



```
Typical winter week begins Fri-09-Jan
Spring season is Sun-01-Mar - Thu-30-Apr
Typical spring week begins Fri-06-Mar
Summer season is Fri-01-May - Mon-31-Aug
Typical summer week begins Sat-11-Jul
Autumn season is Tue-01-Sep - Sat-31-Oct
Typical autumn week begins Fri-02-Oct
Winter season is Sun-01-Nov - Thu-31-Dec
*help_end
```

La línea *\*item* marca el inicio del archivo block para el sitio, y desde ahí hasta la línea *\*avail* contiene la información que se introdujo en el módulo *clm*. A partir de la línea *\*winter* hasta la línea *\*help start* contiene la información que el módulo *clm* calculó como las semanas típicas de cada estación, dividiendo el invierno en dos periodos, invierno de comienzo de año e invierno de fin de año. A partir de la línea *\*help start* contiene información del nombre de sitio y sus coordenadas geográficas y el año para el que corresponde la información. Hay que aclarar que la longitud geográfica está representada como la diferencia en grados positivos o negativos que separan el sitio del meridiano de tiempo estándar más cercano. Posteriormente se encuentra una tabla que contiene los valores mínimos y máximos, y su hora de ocurrencia, de la temperatura ambiente para cada mes, así como para el año completo. Las últimas líneas, muestran lo que el módulo *clm* estimó como las semanas típicas de cada periodo. La línea *\*help\_end* marca el final del archivo block.

Se crearon los archivos block de todos los epw y se insertaron en el *climatelist*.

### 2.3 Alimentación del archivo *climatelist*.

Para alimentar la base de datos *climatelist*, se debe copiar en un archivo de texto todo el contenido del archivo block, desde *\*item* hasta *\*help end* (incluyendo ambas líneas). Las líneas copiadas deben insertarse en el archivo *climatelist* después de una línea *\*help end*. Hay que hacer notar que el archivo *climatelist* solo puede albergar un número determinado de archivos block, por lo que es recomendable borrar archivos block de sitios que no sean de interés. Asimismo, se recomienda guardar una copia de la base de datos original, en caso de no realizar correctamente los pasos anteriores. A menudo surgen mensajes en los módulos de simulación o análisis climático que informan que no se encuentra el archivo solicitado, o no se puede encontrar en la lista de archivos disponibles. Esto puede deberse a las siguientes causas:

La base de datos tiene más archivos de los que se pueden presentar. En este caso, se pueden borrar archivos block no necesarios.

La información de la ubicación del archivo binario no es correcta.

El archivo está marcado como OFFLINE.

En cualquiera de los casos anteriores, es posible la corrección del *climatelist* usando un procesador de textos.

### 2.4 Archivos climáticos producidos.

Se recibieron archivos climáticos para las ciudades y años que se detallan posteriormente, pero se hace la aclaración que el nombre de los archivos fue modificado ligeramente, ya que los archivos originalmente venían nombrados como, por ejemplo:

MEX\_CANCUN-IAP\_765905\_76.epw

Esta nomenclatura aclara la ubicación del sitio (Cancún en México), la fuente de los archivos, Aeropuerto Internacional (International Airport –IAP-), la codificación de la estación (765905) y el año al que corresponden los datos, 76 (1976). Aunque esta nomenclatura es bastante descriptiva, se optó por simplificarla, ya que tal tener muchos caracteres en el nombre, la hacen propicia a errores de tipografía al referirse al archivo. Por tanto, se usó solamente el nombre del sitio y el año, por ejemplo, para el archivo anterior quedaría CANCUN76.epw

Los archivos con los que se trabajó en esta parte corresponden a las ciudades y periodos siguientes:

Cancún: de 1975 a 2013 excepto 1995 con un total de 38 archivos.

Ciudad Juárez: de 1975 a 1990 excepto 1976 con un total de 15 archivos.

Guadalajara: de 1975 a 1990 y de 2001 a 2014 excepto 2012, con un total de 28 archivos.

Mexicali: de 1991 a 2014 excepto 1995 y 2012 con un total de 22 archivos

Monterrey, estación Aeropuerto: 1975 a 2014 excepto 1995 y 2012 con un total de 38 archivos.

Monterrey, estación General Escobedo: de 1996 a 2014 excepto 2012 con un total de 18 archivos.

Monterrey, estación Ciudad: de 2001 a 2014 excepto 2012 con un total de 13 archivos.

Puebla: de 1989 a 2014 excepto 2012 con un total de 25 archivos.

Querétaro: de 1997 a 2014 excepto 2012 con un total de 17 archivos.

San Luis Potosí: de 1975 a 2014 excepto 1978 y 2012 con un total de 38 archivos.

Tijuana: de 1990 a 2014 excepto 1992 y 2012 con un total de 22 archivos.

En total se recibieron 274 archivos en formato epw, algunos de los cuales al ser analizados por el módulo *clm*, presentaron ciertos problemas, por los que se decidió no incluirlos en las simulaciones:

Todos los archivos de Ciudad Juárez presentaron datos incoherentes en temperatura y humedad relativa, por tanto, no se consideró Ciudad Juárez para las simulaciones.

Los archivos de Guadalajara de los años 1975 y 1990 no tienen información completa para varias semanas del año.

Los archivos de Puebla de 1989, 1990 y 2001 presentan datos inconsistentes de temperatura para varias semanas del año.

El archivo de San Luis Potosí de 1979 está incompleto, para este mismo sitio, los archivos de 1985, 1986 y 1987 presentan valores inconsistentes en la temperatura y los archivos de 2001, 2011 y 2013 no pudieron leerse, parecen estar corruptos.

Habiendo analizado con el módulo *clm* y descartado los archivos inusables, y siguiendo los puntos 2.1 a 2.3 se crearon los archivos binarios, los archivos block de cada uno de los sitios y años considerados y se alimentó la base de datos *climatelist*, y se procedió a realizar las simulaciones. En algunos archivos de diversas ciudades la primera línea no estaba correctamente declarada; como esta línea es solamente un encabezado con información general del sitio, se corrigió el problema copiando la primera línea de otro archivo de la misma ciudad. Hay que aclarar que no todos los archivos se alimentaron a la vez en la base de datos, debido a la capacidad limitada de esta, por lo que se tuvo que realizar varias veces el proceso de incluir archivos en ella.

### **3. Simulación de un modelo de vivienda con los archivos producidos.**

Una vez depurado el conjunto de archivos climáticos, se procedió a alimentar la base de datos *climatelist* y a simular usando el módulo *prj* de Esp-r.

#### **3.1 Objetivo de la simulación.**

El modelo de vivienda simulado es una vivienda unifamiliar de dos plantas, con construcciones y materiales convencionales, con colindancia en una de sus orientaciones. Este modelo, que se muestra en la Figura 1, fue elaborado previamente por el Dr. Christopher Heard, quien introdujo en el modelo un sensor de temperatura media radiante al nivel de la cama de la planta superior, con el fin de realizar estudios de confort. Asimismo, se introdujeron estrategias de control como la apertura de ventanas bajo ciertas condiciones.

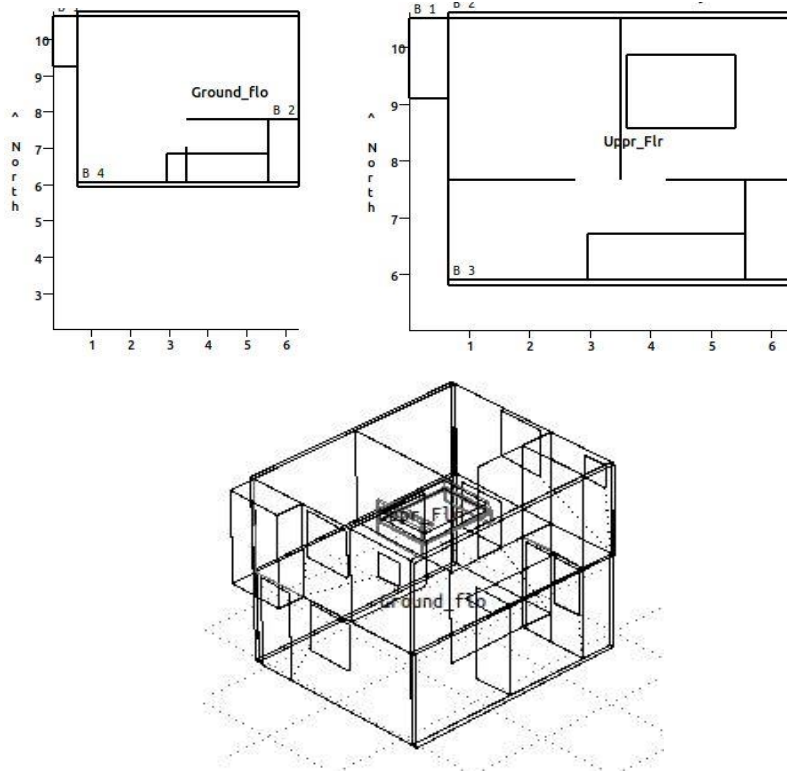


Figura 1. Plantas e isométrico de la vivienda a simular.

El objetivo de la simulación es determinar los periodos en que una persona que duerme en esa vivienda estaría en confort. Para ello el resultado que interesa es la temperatura media radiante del sensor y la humedad relativa, para posteriormente calcular el valor de PMV en una hoja de trabajo de otra aplicación.

### 3.2 Proceso de simulación.

En Esp-r la simulación de un modelo se realiza invocando el módulo *prj* que es el módulo central de la suite y que permite construir un modelo, verificarlo y simularlo, pero que también enlaza a los módulos de análisis climático y análisis de resultados.

Para evitar dar trayectorias muy largas en la ubicación del modelo, es preferible invocar el módulo *prj* desde el directorio *cfg* del modelo.

#### 3.2.1 Selección de la base de datos climática

Al invocar el módulo *prj*, Esp-r presenta inicialmente una lista de los modelos que contiene el directorio donde se invocó, de ahí la conveniencia de situarse inicialmente en el directorio *cfg* del modelo.

Una vez escogido el modelo a trabajar, aparece un menú principal que permite realizar operaciones globales y desde donde es posible escoger el archivo climático con el que se simulará el modelo escogiendo la siguiente secuencia de opciones :

```
b databases -> a anual weather -> b select another
```

Aparece entonces la lista de archivos que contiene la base de datos climatelist y se puede escoger entonces el archivo con el que se simulará el modelo.

### 3.2.2 Ejecución de la simulación.

Si el modelo contiene errores de topología o no contiene los archivos requeridos, se emitirá un mensaje y se deberán corregir, de otra manera se puede proceder a realizar la simulación. Desde el menú principal, se sigue la siguiente secuencia de opciones:

```
m browse/edit/simulate -> s simulation -> q integrated simulation  
-> automated
```

Se ejecutará la simulación del modelo y se regresará al menú anterior.

### 3.3 Revisión de resultados.

Debe seleccionarse el tipo de resultados que se desea obtener, ya que Esp-r guarda los resultados de todos los cálculos, en un archivo especial, del cual hay que obtener los resultados específicos que se desean, así como la frecuencia y el medio en que se desea obtenerlos

#### 3.3.1 Obtención de resultados.

Todos los resultados posibles de la simulación se almacenan en un archivo. La cantidad de información que contiene este archivo es muy grande, pues contiene resultados de temperaturas, flujos de calor, cargas térmicas, flujos de masa e intercambios de energía por conducción, convección, radiación, infiltración y ventilación a nivel de superficie y zona además de las variables climáticas. Esta cantidad de información hace que si consultar información directamente de este archivo, sea tardado y complicado, además de que el archivo es innecesariamente pesado. Por ello, existe la posibilidad de seleccionar la información que se desea y se pueda presentar en gráficas o tablas, o almacenar en archivos para su posterior procesamiento, mediante el módulo *res*.

En el menú se escoge la opción `t results analysis`, lo cual llama al módulo *res* que sirve para presentar los resultados mediante gráficas, listados o archivos.

En el módulo *res* es posible escoger las para las que se desea rescatar información, (opción 4). Las opciones a y c permiten elegir entre presentar la información mediante gráficas en la misma pantalla o mediante archivos. La opción d permite realizar estudios estadísticos sobre distribución de frecuencias, totales, máximos, mínimos, estadística descriptiva, etc.

En este trabajo se eligieron las siguientes opciones;

Para escoger la información que se desea, en este caso la TMR al nivel de la cama, la temperatura de la zona y la humedad relativa de la zona, para posteriormente calcular el PMV:

```
4 building zones: Upp_Flr (planta alta).
```

```
c reports -> g performance metrics -> b temperatures g sensor mean  
rianadt temperature -> b Upp_Flr : BedMRT  
b temperatures-> b dry bulb (db) temperature  
i zone RH
```

Para configurar el archivo y producir la salida de resultados:

```
>display to: file
```

```
Export file name: escribir el nombre del archivo que se desea, incluyendo la extensión csv
```

```
^delim: comma (se puede escoger el tipo de seprador entre valores, en este caso coma porque serán archivos csv
```

```
;list data con esto se produce el archivo de resultados.
```

De esta forma se produjeron archivos csv que contienen la información necesaria para calcular el PMV, que es la variable que interesa en este trabajo. Se produjeron un total de doscientos cincuenta y seis archivos csv

### **3.3.2 Procesamiento de resultados.**

La información de los archivos csv producidos se pasó posteriormente como hoja de cálculo para alimentar a la hoja de cálculo PLANTILLA.xls, desarrollada por el Dr. Christopher Heard y que contiene las ecuaciones para calcular el PMV de acuerdo a los resultados de la simulación y al nivel de arropamiento considerado (varios niveles de clo). Los resultados de PMV por cada año se concentraron a su vez en hojas de cálculo para cada ciudad. En estas hojas de cálculo se presenta un concentrado comparativo y una gráfica con el valor de PMV para cada año y nivel de clo.

También se produjo una hoja de cálculo con las tablas y gráficas concentradas de cada ciudad, para fines comparativos.

## **4. Simulación de un modelo de vivienda para sitios seleccionados considerando madera contrachapada (CLT).**

Se realizó una serie de simulaciones considerando madera contrachapada (CLT) como material de construcción, para sitios seleccionados en el sureste.

### **4.1 Objetivo de la simulación.**

La simulación tuvo como objetivo estimar el efecto en la carga térmica de una vivienda usar madera contrachapada (CLT) como material para muros, entresijos y techos. En este caso los resultados de interés son las cargas térmicas del modelo con construcción convencional y usando CLT. La vivienda a simular es la misma que la del punto 3.1

### **4.2 Archivos meteorológicos.**

Para el caso de esta simulación se usaron archivos típicos meteorológicos del tipo TMY3 en formato epw enviados por el Dr. Christopher Heard, correspondientes a las siguientes ubicaciones:

Cancún, Q.Roo

Mérida, Yuc.

Progreso, Yuc.  
Valladolid, Yuc.  
Bahías de Huatulco, Oax.  
Huajuapán de León, Oax.  
Oaxaca, Oax.  
Puerto Escondido, Oax.  
Puerto Ángel, Oax.  
Xococotlán, Oax.

Para estos archivos se siguió el procedimiento descrito en los puntos 2.1 a 2.3 para producir los archivos binarios y los archivos block, con los cuales se alimentó la base de datos *climatelist*.

### 4.3 Ejecución de la simulación

Para cada sitio se realizaron dos simulaciones, una con los materiales y construcciones de origen del modelo, y otra usando madera contrachapada (CLT) en muros, entrepisos y techos, con las propiedades termofísicas que se encuentran en :

Prata, Simões, Tadeu, *Heat transfer measurements of a linear thermal bridge in a wooden building corner.* <https://doi.org/10.1016/j.enbuild.2017.09.073>

Conductividad Térmica: 0.13 W/m K

Densidad: 574.69 kg/m<sup>3</sup>

Calor Específico: 1406.6 J/kg K

Las construcciones consisten en:

Muros Exteriores:

Emplaste 0.0127 m de espesor.

Chapa de madera 0.006 m de espesor

Aislante EPS 0.0254 m de espesor.

CLT 0,12m de espesor

Entrepisos:

CLT 0.10 m de espesor

Linóleo 0.006 m de espesor.

Techo:

Cartón asfaltado: 0/002 m de espesor

Chapa de madera 0.006 m de espesor

Aislante EPS: 0.0508 m de espesor

CLT 0.012 m de espesor.

Las simulaciones procedieron de acuerdo a los puntos.2.1 y 3.2.2

#### 4.4 Revisión de resultados

En este caso los resultados de interés fueron solamente las cargas térmicas totales, tanto de refrigeración como de calefacción tanto para el caso base, con construcción convencional, como para el caso de usar CLT.

##### 4.4.1 Obtención de resultados.

En este caso como lo que interesa es el total anual de la carga, se pide un concentrado estadístico, con la opción `enquire about` Por lo tanto, en el módulo *res* se siguió la siguiente secuencia en los menús:

```
4 building zones: *all-> d enquire about -> g performance metrics-
> a summary statistics -> h heat/cool/humidity ->g all sensible +
latent load
* (all )
>display to: (dar nombre del archivo)
^delimiter : comma
-exit menú
-exit module
```

Con esto se han creado los archivos csv que contienen la información de la carga térmica máxima por enfriamiento, por calefacción y total para cada zona.

##### 4.4.2 Procesamiento de resultados.

La información de los archivos csv producidos se pasó a una hoja de cálculo en la que se presentan tres tablas. La primera tabla presenta para cada ciudad un concentrado donde de la carga de calentamiento máxima, la carga de enfriamiento máxima para cada zona, la carga máxima total para el caso base. La segunda tabla es similar a la primera pero la información corresponde al caso de usar CLT. La tercera tabla presenta para cada ciudad la diferencia en la carga entre los dos casos.

## 5. Entregables.

Como producto de este trabajo se entregan los siguientes productos:

Un archivo comprimido llamada ENTREGABLES UAM 2022, que a su vez contiene dos carpetas llamadas:

EPW BLOCKS y BINARIOS



## RESULTADOS

### 5.1 Carpeta EPW BLOCKS Y BINARIOS.

En esta carpeta se guardan los archivos producidos en el punto 3, los binarios, los block y los epw de cada sitio, así como los producidos para las simulaciones del punto 4.

La carpeta contiene diez subcarpetas, nombradas de acuerdo a la ciudad y contiene:

Los archivos epw, con el nombre modificado y en algunos casos con la primera línea corregida.

Los archivos binarios producidos.

Los archivos block producidos.

Existe también una carpeta llamada TMY3SURESTE que contiene los archivos epw, block y binarios para las diez ciudades consideradas en el punto 4.

El total de archivos de esta carpeta es de setecientos veintiséis (726).

### 5.2 Carpeta RESULTADOS.

Esta carpeta contiene los archivos de resultados, tanto los csv producidos por la simulación como las hojas de trabajo con la información procesada.

La carpeta contiene dos subcarpetas llamadas HISTORICOS y CLT. Aquí también se encuentra el archivo llamado COMPARATIVO.xls que es una hoja de trabajo con el concentrado de información y gráficas y tablas comparativas para las ciudades consideradas.

#### 5.2.1 Subcarpeta HISTORICOS.

En esta carpeta están almacenados los resultados del punto 3, contiene dos subcarpetas: CSV y PMV.

En la carpeta CSV se encuentran los archivos producidos por el módulo *res*

En la subcarpeta PMV se encuentran las hojas de trabajo para cada ciudad donde se calcula el PMV.

Esta carpeta contiene doscientos cuarenta y tres archivos (253)

#### 5.2.2 Subcarpeta CLT

En esta subcarpeta se encuentran los archivos csv producidos por las simulaciones del punto 4 y además el archivo COMPARATIVOCLT.xls, que contiene las tablas a las que se hace referencia en el punto 4.4.2. Esta carpeta contiene once (11) archivos

Se entregan entonces un total de novecientos noventa archivos (990), los cuales han sido enviado por correo electrónico al Dr, Christopher Hdeard.

Article

---

# Heat Transfer and Pressure Drops in a Helical Flow Channel Liquid/Solid Fluidized Bed

---

Oscar García-Aranda, Christopher Heard, José Javier Valencia-López and Francisco Javier Solorio-Ordaz

Special Issue

New Advancement in Heat and Mass Transfer: Fundamentals and Applications

Edited by

Dr. Guojun Yu and Dr. Huijin Xu



<https://doi.org/10.3390/en15239239>

## Article

# Heat Transfer and Pressure Drops in a Helical Flow Channel Liquid/Solid Fluidized Bed

Oscar García-Aranda <sup>1</sup>, Christopher Heard <sup>2,\*</sup>, José Javier Valencia-López <sup>3</sup>  and Francisco Javier Solorio-Ordaz <sup>4</sup>

<sup>1</sup> División de Ciencias Naturales e Ingeniería, Universidad Autónoma Metropolitana Unidad Cuajimalpa, Ciudad de México 05348, Mexico

<sup>2</sup> Departamento de Teoría y Procesos de Diseño, DCCD, Universidad Autónoma Metropolitana Unidad Cuajimalpa, Ciudad de México 05348, Mexico

<sup>3</sup> Departamento de Procesos y Tecnología, DCNI, Universidad Autónoma Metropolitana Unidad Cuajimalpa, Ciudad de México 05348, Mexico

<sup>4</sup> División de Ingeniería Mecánica e Industrial, Universidad Nacional Autónoma de México, Ciudad de México 04510, Mexico

\* Correspondence: [heard@correo.cua.uam.mx](mailto:heard@correo.cua.uam.mx)

**Abstract:** Industrial liquid/solid fluidized bed heat exchangers are commonly used with particle recycling systems to allow an increased superficial velocity and higher heat transfer rates. Here, experimental results are reported on a novel helical flow channel geometry for liquid/solid fluidized beds which allow higher heat transfer rates and reduced complexity by operating below the particle transport fluid velocity. This eliminates the complexity of particle recycle systems whilst still delivering a compact heat exchanger. The qualitative character of the fluidization was studied for a range of particle types and sizes under several inclinations of the helices and various hydraulic diameters. The best fluidization combinations were further studied to obtain heat transfer coefficients and pressure drops. Improvements over the heat exchange from a plain concentric tube in an annulus were obtained to the following degree: vertical fluidized bed, 27%; helical baffles, 34 to 54%; and fluidized bed with helical baffles, 69 to 89%.

**Keywords:** liquid/solid circulating fluidized bed; sphericity; non-spherical particle; porosity; surface cleaning; enhanced heat transfer



**Citation:** García-Aranda, O.; Heard, C.; Valencia-López, J.J.; Solorio-Ordaz, F.J. Heat Transfer and Pressure Drops in a Helical Flow Channel Liquid/Solid Fluidized Bed. *Energies* **2022**, *15*, 9239. <https://doi.org/10.3390/en15239239>

Academic Editors: Huijin Xu and Guojun Yu

Received: 31 October 2022

Accepted: 29 November 2022

Published: 6 December 2022

**Publisher's Note:** MDPI stays neutral with regard to jurisdictional claims in published maps and institutional affiliations.



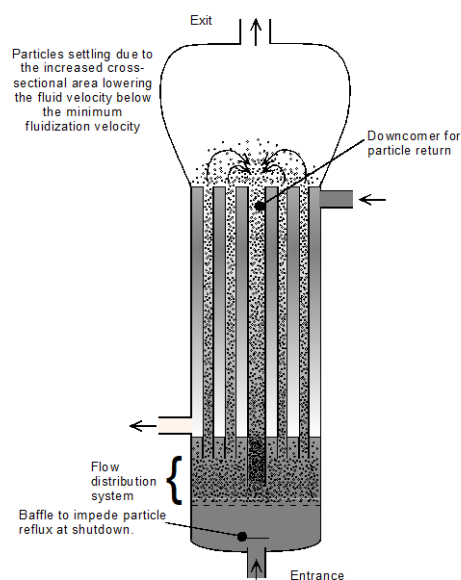
**Copyright:** © 2022 by the authors. Licensee MDPI, Basel, Switzerland. This article is an open access article distributed under the terms and conditions of the Creative Commons Attribution (CC BY) license (<https://creativecommons.org/licenses/by/4.0/>).

## 1. Introduction

Liquid/solid fluidized beds are well known for their characteristics of providing a self-cleaning effect when the fluidizing phase is a liquid with a propensity to deposit scale or fouling on the surfaces submerged in the bed. When such surfaces are employed for heat exchange, not only are they kept clean, but the heat transfer coefficients obtained are significantly higher than would be the case without the fluidized bed. However, to obtain high enough heat transfer rates to be commercially viable, it is usually necessary to use superficial velocities, for the continuous phase, which are in the particle transport regime. Consequently, such heat exchange systems are equipped with particle separation and recycling systems. These systems need to be controlled to ensure that the particle recycle rate is appropriate to maintain the desired porosity in the bed and to minimize the amount of continuous phase that is recycled. Both the particles and the continuous phase (about 40% of the volume of recycled material) would be approximately at the exit temperature of the heat exchanger and be mixed with the main inlet flow, thus affecting the approach temperatures and thermodynamic efficiency of the heat exchanger in a disadvantageous manner. Klaren recognizes that this is a disadvantage in recirculating particles and the associated fluid [1].

Notwithstanding the above-mentioned thermodynamic disadvantage, there has been considerable development work over a significant period. One of the earliest designs was

that of Klaren who proposed an internal recycle system with a central return duct and multiple small diameter beds in tubes within a shell or multiple external recycle ducts, both with control valves to avoid liquid short circuiting [2] (Figure 1). Over an appreciable period, Klaren [3–8] developed a series of means of controlling and improving the behavior of the particle recycling with ever more sophisticated and complex schemes including mechanically driven systems of valves, screw conveyors, etc. The increasing complexity of these proposed systems shows that the practical implementation of particle re-circulation is difficult and not fully resolved.



**Figure 1.** Liquid/solid fluidized bed heat exchanger with internal particle re-circulation.

Fluidized bed continuous phase superficial velocities can be increased by several methods, as discussed below. The one mentioned above is that of operating a bed in the transport regime. Beds can also have their apparent gravitational force increased by using a cylindrical geometry with a radial inflow of the continuous phase whilst under rotation around a vertical axis [9]. This arrangement, at the cost of considerable mechanical complexity, can increase the apparent gravity (centripetal force) that the bed is subjected to, by several multiples of normal gravitation force. It has been successfully demonstrated in gas–solid fluidized bed combustors with up to 100 g centripetal force. In the work reported by Demirçan et al., heat transfer coefficients were not measured directly, but combustion intensity was measured at almost an order of magnitude higher than a normal vertical fluidized bed combustor at atmospheric pressure. The heat transfer rates were calculated for various fuels. These were for a gas/solid fluidized bed and thus difficult to compare with those of a liquid/solid bed. The heat transfer coefficient was found to be proportional to the apparent gravity to the power of one fifth ( $g^{0.2}$ ). For liquid/solid fluidization in a centrifugal field, there are no experimental studies of heat transfer; however, some studies of the hydrodynamics have been carried out, including those by Margraf and Werther [10,11]. In their work, it can be seen that although the pseudo gravitational acceleration (i.e., the centripetal force) achieved was in the range 20 to 500 g, the system was mechanically highly complex even without heat transfer elements. If centrifugally enhanced fluidized bed heat exchangers were to be developed, the Achilles’ heel would be the reliability and maintenance caused by the rotating seals and drives.

O’Dea et al. [12] experimented with gas/solid fluidization of fine particles in an inclined tube. The particle diameters ranged from 0.06 to 0.5 mm with densities in the range 1450 to 2620 kg/m<sup>3</sup>. The tube diameter was 83 mm, which gave ratios of particle to tube diameter from  $7.2 \times 10^{-4}$  to  $6 \times 10^{-3}$ . They identified three flow regimes from a fixed bed to a channeled bed with inclinations between 45° and vertical. However, the

authors concluded that the applicability of their model needed to be confirmed for a wider range of properties. Their results could not be directly applied to liquid/solid fluidized beds. A prior study by Zenz, which was summarized by Zabrodsky [13], reported a similar classification of flow regimes in inclined tubes for pneumatic transport of particulate solids.

Galvin and Nguyentranlam [14] observed that inclined parallel plates in a liquid/solid fluidized bed allow a wide range of bed porosities and fluid speeds higher than the particles' terminal velocities. The option of operating a liquid/solid fluidized bed in a tilted vessel with flow vectors in both the horizontal and vertical directions would be expected to allow higher continuous phase flow speeds with a lower vertical velocity component. The vertical component of the flow velocity is that which predominantly provides the fluidizing effect. Thus, higher superficial velocities over immersed heat transfer surfaces could be obtained without entering a particle transport regime.

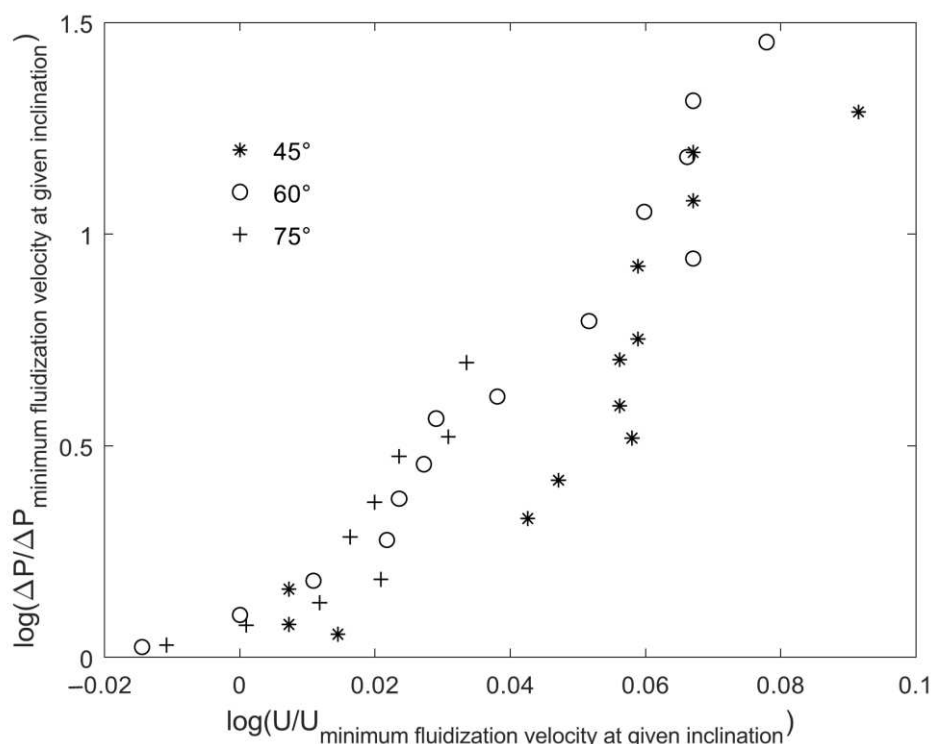
Hudson et al. [15] reported the velocity profiles in liquid/solid fluidized beds with a maximum inclination of  $10^\circ$  from the vertical and showed a solids re-circulation pattern that favored mixing of the particles. Yakubov et al. [16] reported up to a 30% increase in the critical velocity for bed escape with an inclination of  $45^\circ$  of a cylindrical liquid/solid fluidized bed. It was also found that the fluidization in an inclined cylinder developed recirculation cells with regions of very low particle concentrations between such cells.

Murata et al. [17] found that an inclined gas/solid fluidized bed at  $15^\circ$  to the vertical can have substantially increased heat transfer coefficients for electrically heated plates with the same inclination as the tube containing the bed, compared to the vertical state. The authors attributed some of the increase to the higher level of contact between heater plates and particles in the inclined case. Ashok Kumar et al. [18] carried out a study of the inclination of a tube with liquid/solid fluidization in order to ascertain the maximum angle at which a homogenous fluidization could be sustained. They used 1.5 mm diameter sand particles and inclinations from  $30^\circ$  to  $90^\circ$  to the horizontal. They reported five types of flow patterns and concluded that  $70^\circ$  to the horizontal was the minimum angle to sustain fluidizing conditions for inclined pipe connectors in process industries.

Chong et al. [19] researched flow regimes for a liquid/solid fluidized bed in an inclined pipe and identified four conditions: fixed bed, initial fluidization, partial fluidization and fully fluidized bed. They covered inclinations of  $45^\circ$ ,  $60^\circ$  and  $70^\circ$  for water/solid systems with glass particles from 0.42 to 0.5 mm diameter in a 76 mm internal diameter tube. They found that the initial fluidization velocity for both gas/solid and liquid/solid has the same ratio to the vertical bed minimum fluidization velocity for a given angle of inclination. The authors developed models of the relationship between the behavior of a vertical bed and inclined beds for fluidization velocities and pressure drops. They showed that the ratio of complete fluidization velocity to minimum fluidization velocity is always greater for a given inclined bed in liquid/solid systems than it is in gas/solid systems. A linear relationship on a log–log plot between the ratio of fluidized pressure drop to minimum fluidization pressure drop and the ratio of superficial velocity to minimum fluidization velocity was shown. Figure 2 shows the Chong et al. data plotted in function of the ratio of fluid velocity to minimum fluidization velocity for the specific inclination and the corresponding ratio of pressure drops instead of the original form where the data were plotted as ratios to the vertical bed minimum fluidization conditions for all the inclinations. Each inclination should be considered as a different flow channel geometry and so the behavior of the bed should be compared to the minimum fluidization conditions of that particular inclination, rather than that of the vertical bed. It should be noted that for industrial liquid/solid fluidized bed heat exchangers, the particle sizes employed are much larger and the flow channels much narrower than those used by Chong et al. It can be observed that the data do not extend to velocity ratios ( $U/U$  minimum fluidization for given inclination) of more than 1.25.

Similarly, Figure 3 shows the data from Yakubov et al.'s work (Figure 7 in Yakubov's paper [16]), for larger particles in a 2.78 cm diameter column with 3.2 mm diameter particles ( $D_p/D_h = 0.11$  compared to 0.0055 to 0.0066 in the case of Chong et al.). The same kind

of changes were applied to these data so that it is also shown relative to the minimum fluidization conditions for each bed inclination rather than relative to the vertical bed minimum fluidization conditions. There is a clear difference between these results and those of Chong et al. The range of relative velocities (Relative to the minimum fluidization velocity of each inclination) is much greater. The ratio of particle diameter to hydraulic diameter is much greater for this data set. And the curves in the figure show a clear plateau in the pressure drop ratio as the velocity ratio reaches values between 1.25 and 1.4.



**Figure 2.** Chong et al. re-plotted as a function of minimum fluidization velocity and pressure drop for each inclination, instead of considering that of a vertical bed as the reference condition.

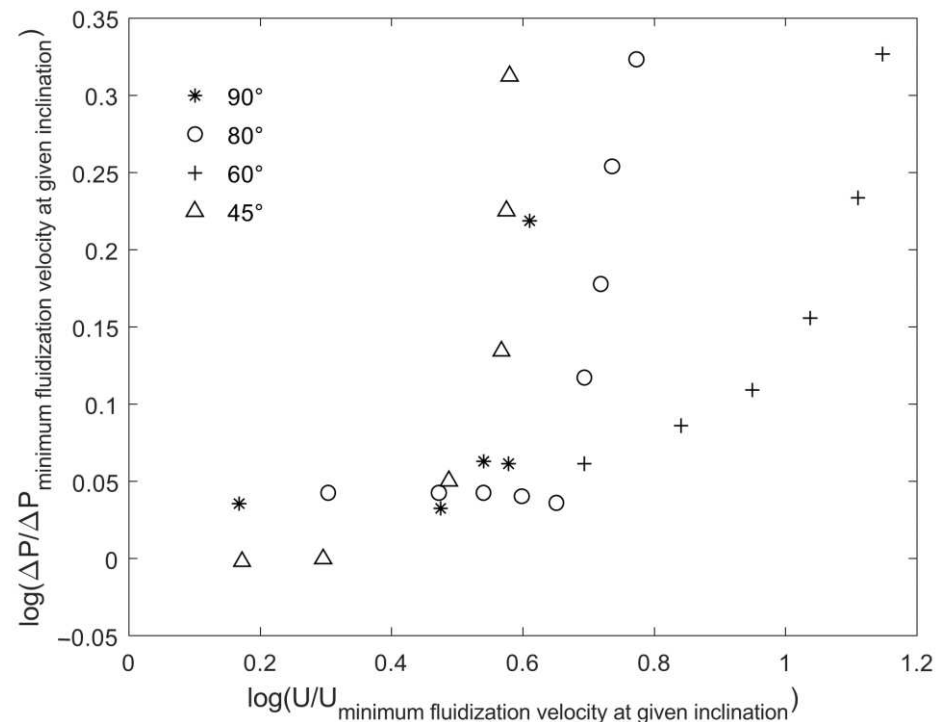
Nonetheless, in both cases, it is clear that at an inclination of  $45^\circ$  the relative pressure drop is lower than for the other reported angles for the conditions of stable fluidization. Yakubov et al. report that the proportion of the pressure drop attributable to water friction (without a fluidized bed) was less than 4% of the total measured pressure drop.

Galvin and Dickinson [20] reported a study of the separation and transport of particles in inclined channels under centrifugal forces. They achieved centripetal forces of up to 73 g obtaining good results for particle classification. In this work, multiple narrow channels were used to obtain a synergy between the effects of high centripetal force and the inclination of the bed. However, for heat transfer, it is unlikely that such an approach would be profitable due to the great mechanical complexity that would be entailed.

Hashizume and Matsue [21] have shown that to maintain a homogeneous fluidization for vertical liquid/solid fluidized beds, the critical ratio of particle diameter to circular bed diameter is 0.220. There is very little information available on the effect of inclining the bed duct on the critical particle diameter to duct diameter or bed hydraulic diameter ratio. Chong et al. used a single particle size. Yakubov et al. used a range of particle sizes giving ratios of particle diameter to tube diameter from 0.054 to 0.124, which is well below the value of 0.2 reported by Hashizume and Matsue.

From the above literature review it can be seen that there is not a large body of research on inclined liquid/solid fluidized beds. However, that which does exist shows that an inclined liquid/solid fluidized bed allows higher superficial velocities to be achieved before particle transport occurs without resorting to active mechanical systems. Given this, it

might be expected that heat transfer coefficients for surfaces in contact with these fluidized beds would be higher than for simple vertical flow. However inclined tubes would have a larger footprint within a process plant. Therefore, it was thought that wrapping the inclined channel in a circle (helical form) might be useful to reduce the flow area necessary for an inclined channel fluidized bed configuration. No studies were found which reported experimental results for such a configuration.



**Figure 3.** Yakubov et al. re-plotted as relative pressure drop as a function of relative superficial velocity for each inclination.

Pronk et al. [22] found that for stationary liquid/solid fluidized beds, the maximum fouling and scaling prevention effect was achieved with larger particles (in their case, 2 mm diameter) at the highest bed porosity consistent with homogeneous fluidization. They reported that it is believed that the impulse and energy of particle impacts at higher superficial velocities was associated with, in their case, higher particle density. Using the helical flow pattern, higher superficial velocities are also obtained with respect to a plain vertical flow regime.

Wu et al. [23], in their 2022 review of fluidized bed heat exchange technology for liquid/solid and vapour/liquid/solid systems, made no mention of geometries that cause a helical flow to enhance superficial velocities and, thus, heat transfer and self-cleaning. However, mention is made of a gas/solid spiral plate heat exchanger studied by Jiang et al. [24]. The experimental system was not an inclined helical flow but a traditional spiral plate heat exchanger with particles added to the gas flow. A maximum heat transfer enhancement of nearly 30%, with respect to a simple gas flow was reported.

It is clear that there has been considerable interest in the use of liquid/solid fluidized bed heat exchangers for heat recovery from highly fouling and scaling fluids such as geothermal brines, Tan et al. [25]. However, their economic feasibility has been hampered by their large size and thus, their cost.

## 2. Objectives

This experimental study sought to answer the following questions. Would there be significant changes in the fluidization behavior in a helical flow channel? Can a good quality of fluidization be established in a helical flow channel? Does this enable higher heat

transfer coefficients for surfaces immersed in the bed than would be the case in a simple vertical bed? What are the pressure drop implications of this bed geometry?

### 3. Experimental System

Figure 4 shows the basic experimental system. Due to vertical space limitations, a means of reducing the flow stabilization tube length before the distributor was necessary. The two elbows immediately before the distributor included flow control elements based on the Cheng rotating vane [26]. A modified form was manufactured with continuous flow control channels into, through and out of the elbow assuring the 180° rotation of the flow streams around the flow axis within the elbow and the removal of the swirl at the exit (By ‘unwinding’ the flow channels). The distributor consisted of an elongated honeycomb of flow channels. The test section of the apparatus was made of a 1.87 m long transparent acrylic tube with an internal diameter of 43.8 mm. For the heat transfer experiments, a 14 mm diameter, 240 mm length, concentric bayonet ceramic electric heater from Electrothermal was used. This had an approximate heat output of 400 W (The use of a heat flux sensor makes the exact heat output unimportant).

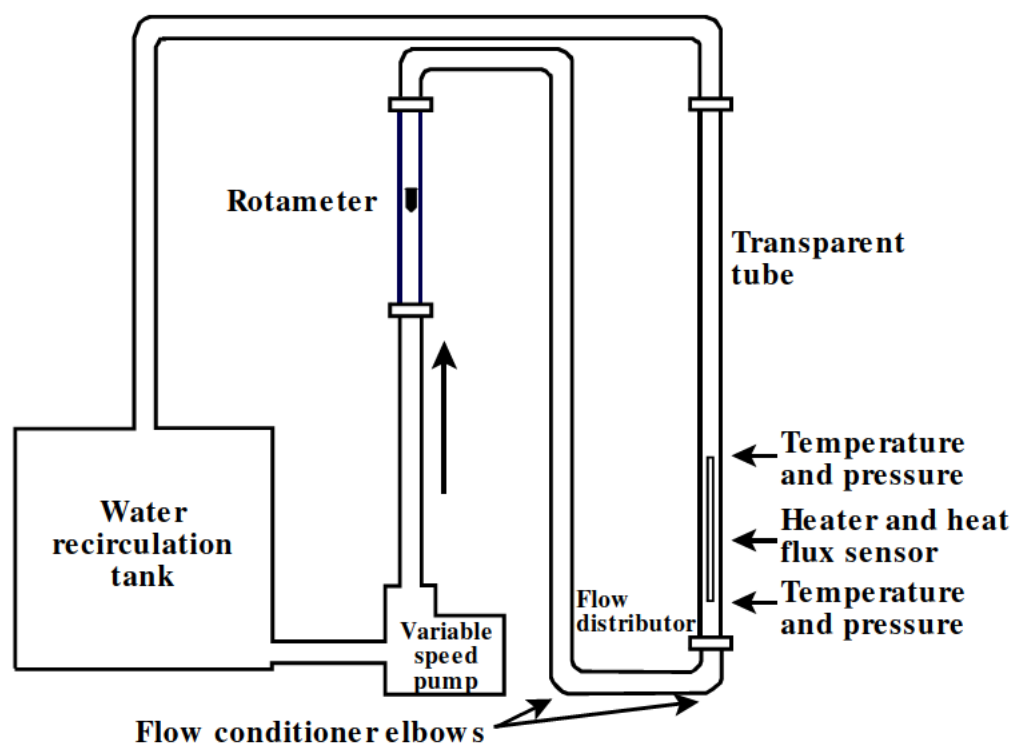


Figure 4. Experimental system layout.

Two type T thermocouple temperature sensors were used to measure the bulk fluid temperature at the foot of the bed and immediately above the heated section. These thermocouples were Special Limits 24AWG Omega Engineering type T thermocouple wire with PTFE insulation and an error limit of 0.4% and the junctions were made using a capacitive discharge thermocouple welding system (HotSpot II Heavy Duty Welder).

Heat flux was measured at a central point along the length of the heater where thermographic imaging showed a uniform temperature field. A RdF 20457-2 micro-foil heat flux sensor (Thickness 0.127 mm, thermal impedance of 0.017 W/m<sup>2</sup> K and 25 by 20 mm) with manufacturer’s individual calibration (Output per unit heat flux and correction for the surface temperature as measured by the integrated type T thermocouple: calibrated per ANSI MC96.1-1975 and NBS Monograph 125) was glued to the heater.

Pressure drops were measured with a differential pressure sensor from Validyne Engineering (DP15 Variable Reluctance Pressure Sensor and CD280 Multi-Channel Carrier



Demodulator) which was calibrated with a dead weight calibrator (Dewitt, range 0–26 kPa and a resolution of 0.9 kPa).

The above-described sensors (Temperature, pressure and heat flux) were connected to a data logger (Omega Engineering OMB-DAQ-2416). Flow rates were measured with a rotameter (Dwyer type LFM) with a custom fabricated float which was calibrated with the weight-time method for a flow range of 0.9 to 9 m<sup>3</sup>/h. The flow rates were controlled by means of using a centrifugal pump with a variable frequency velocity control.

#### 4. Methods

One of the basic parameters to be measured in a fluidized bed system is the minimum fluidization velocity and the concomitant pressure drop. In a vertically oriented fluidized bed with small wall effects (i.e., the bed diameter is large with respect to the particle diameter), the pressure drop tends to be almost constant from the onset of fluidization up to the point where transport of bed particles sets in. Figure 5 shows an idealized version of pressure drop vs superficial velocity for the expansion of a fluidized bed. From this, it can be observed that the simultaneous measurement of flow rate and pressure drop for rising and falling flow rate can reveal the minimum fluidization velocity.

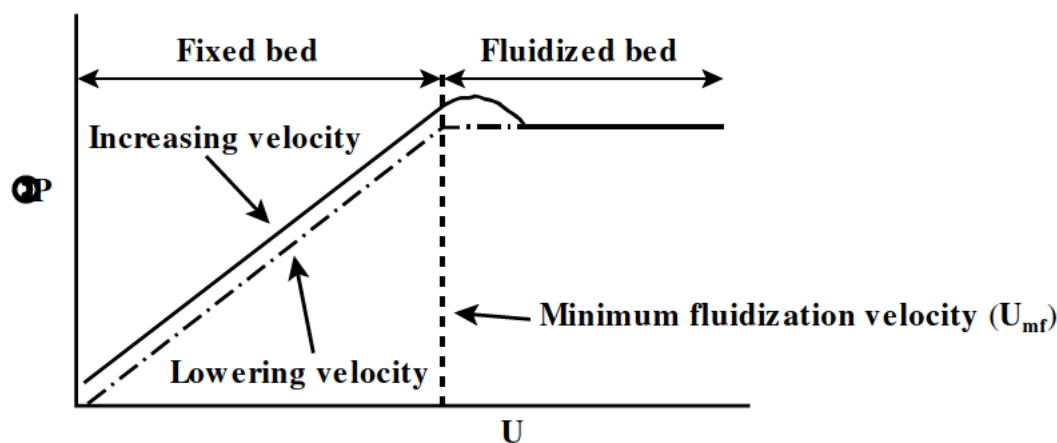


Figure 5. Pressure drop as a function of superficial velocity for an idealized fluidized bed.

Industrial practice seldom uses spherical particles in fluidized beds; thus, several available particle forms were obtained in order to evaluate their qualitative behavior in a helical channel bed (Table 1).

Table 1. Particle characteristics.

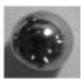



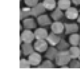
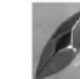

	P#1	P#2	P#3	P#4	P#5	P#6	P#7
							
	Sphere	Sphere	Saturn	Diagonal Cut Cylinder	Straight Cylinder	Needle	Sphere
Density (kg.m <sup>-3</sup> )	10,031	9570	8250	8240	7325	8260	6900
Mass (g)	443	450	329	352	350	334	315
Fixed bed porosity	0.284	0.242	0.236	0.184	0.222	0.358	0.264
Sphericity	1.0	1.0	0.808	0.923	0.873	0.891	1.0
Minimum fluidization velocity (m.s <sup>-1</sup> )	0.353	0.602	0.463	0.381	0.332	0.384	0.528

Figure 6 shows the bed expansion behavior of the particles as a function of Reynolds number based on the particle equivalent diameter (i.e., the diameter of a sphere of the same volume). This concurs with that reported by Richardson and Zaki [27].

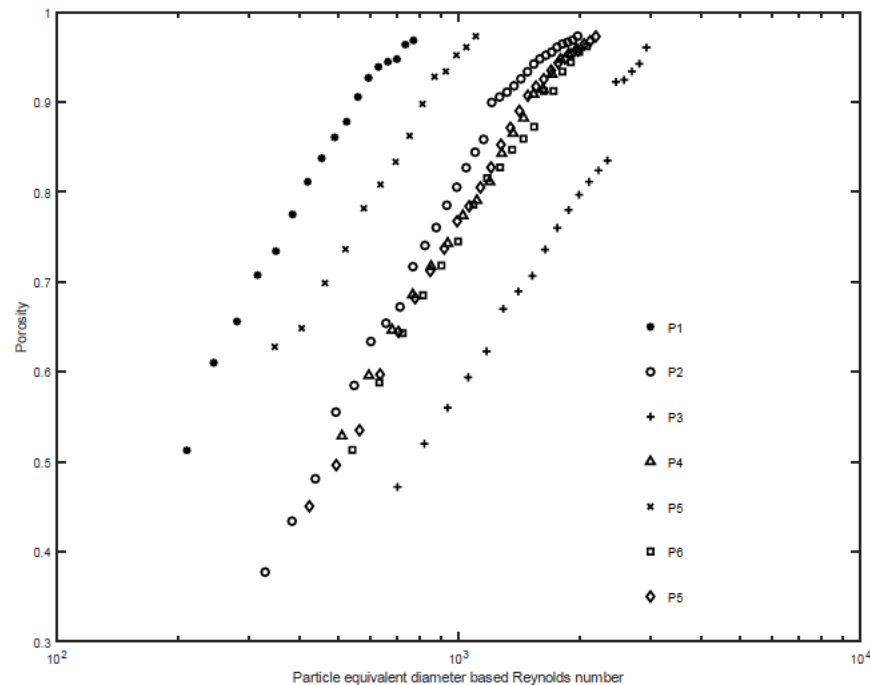


Figure 6. Porosity as a function of particle Reynolds number for a range of particles of varying density, size and sphericity.

## 5. Helical Flow Apparatus

Having assured that all the particles behave in a regular fashion in a vertical bed, all were tested for the quality of fluidization in helical flow channels.

A helical flow is composed of an axial velocity and a circular or angular movement perpendicular to the axial velocity, i.e., a tangential velocity. However, the tangential velocity is not independent of the radial position in the flow field. There are several effects that influence the flow in a full helical channel or duct.

Nine helical baffle configurations were manufactured by means of fused deposition modelling with plastic. Three inclinations of the helical channels were developed, each with three different hydraulic diameters obtained by using spirals with three, four and five starts for the baffles. A selection of these baffles is shown in Figure 7.

All the particles were tested for the quality of fluidization that could be obtained with the range of helical baffle geometries.

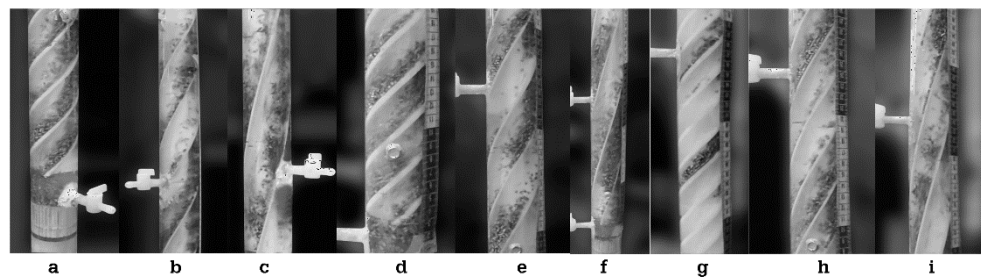
Similar effects, as mentioned above, to those that previous researchers had found in inclined liquid/solid fluidized beds were observed (Figure 8). That is: groups of particle concentrations in waves under some conditions together with particle re-circulation with the backflow in the upper part of the channel. However, under some conditions with a selected set of particles a good degree of fluidization quality was achievable. Three conditions were chosen for further study: two hydraulic diameters at 45° inclination (Figure 8a,d) and one at 60° inclination (Figure 8h). The first two correspond to baffles with three and four starts and the latter to four starts. The chopped stainless steel wire particles were chosen for further study given that they provided a good quality of fluidization and are representative of particles likely to be used in an industrial application.

A computational fluid dynamics (CFD) model using COMSOL was developed from prior work by López-Mata et al. [28] to obtain the tangential and axial velocity components ( $v_t$  and  $v_a$ , respectively) under the experimental conditions. Models were developed of 3, 4 and 5 baffles at inclinations of 45°, 60° and 75°. Steady state incompressible flow was

considered with a RANS  $k-\epsilon$  turbulence model. The model conditions were obtained from the experimental results (Flow rates and channel geometry) and are shown in Table 2.



**Figure 7.** Helical baffles used in the experiments.

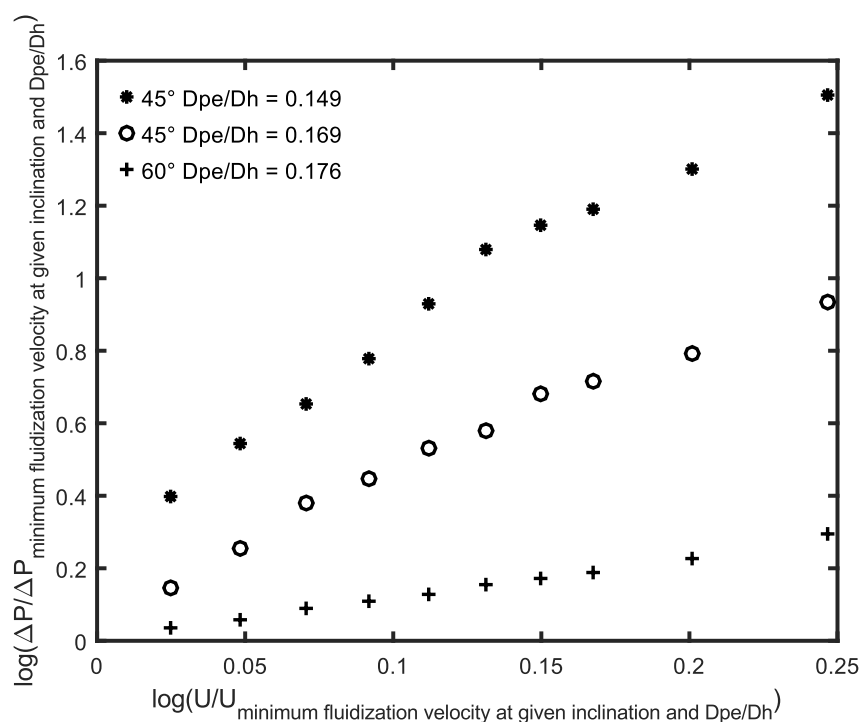


**Figure 8.** Examples of the quality of fluidization under inclinations of  $45^\circ$ ,  $60^\circ$  and  $75^\circ$  and a series of hydraulic diameters achieved by using three, four and five starts for the baffles as follows: (a)  $45^\circ$ , three starts, (b)  $60^\circ$ , three starts, (c)  $75^\circ$ , three starts, (d)  $45^\circ$ , four starts, (e)  $60^\circ$  four starts, (f)  $75^\circ$ , four starts, (g)  $45^\circ$ , five starts, (h)  $60^\circ$ , five starts and (i)  $75^\circ$ , five starts.

**Table 2.** Maximum axial and tangential velocities in tested configurations as modelled in COMSOL.

Number of Baffle Starts	$45^\circ$ Baffle Inclination	$60^\circ$ Baffle Inclination	$70^\circ$ Baffle Inclination
3	$v_t$ : $0.340 \text{ m.s}^{-1}$	$v_t$ : $0.200 \text{ m.s}^{-1}$	$v_t$ : $0.200 \text{ m.s}^{-1}$
	$v_a$ : $0.540 \text{ m.s}^{-1}$	$v_a$ : $0.519 \text{ m.s}^{-1}$	$v_a$ : $0.519 \text{ m.s}^{-1}$
4	$v_t$ : $0.380 \text{ m.s}^{-1}$	$v_t$ : $0.230 \text{ m.s}^{-1}$	$v_t$ : $0.105 \text{ m.s}^{-1}$
	$v_a$ : $0.550 \text{ m.s}^{-1}$	$v_a$ : $0.540 \text{ m.s}^{-1}$	$v_a$ : $0.545 \text{ m.s}^{-1}$
5	$v_t$ : $0.350 \text{ m.s}^{-1}$	$v_t$ : $0.239 \text{ m.s}^{-1}$	$v_t$ : $0.110 \text{ m.s}^{-1}$
	$v_a$ : $0.570 \text{ m.s}^{-1}$	$v_a$ : $0.560 \text{ m.s}^{-1}$	$v_a$ : $0.565 \text{ m.s}^{-1}$

Figure 9 shows the relationship between the relative pressure drop as a function of relative fluidization velocity. These relative values are relative to the conditions at incipient fluidization for each inclination and hydraulic diameter for the three conditions further researched. The ratio of particle equivalent diameter to hydraulic diameter for these cases is well within the limit indicated from Hashizume et al. (0.2 maximum). As a comparison, for instance, image g in Figure 8; the equivalent particle diameter to hydraulic diameter ratio is 0.193, near enough to 0.2, which shows very clear evidence of bunching or slugging of particles.



**Figure 9.** Relative pressure drop as a function of relative superficial velocity under two inclinations and three hydraulic diameters for particle P# 5.

## 6. Heat Transfer Measurements

The heat transfer measurements were carried out with sets of baffles incorporating a central heating element as described above and shown in Figure 10.

Initially, measurements were performed over the same range of superficial flow rates as used for the fluidization of the particles (P #5) but without baffles or particles. Subsequently measurements were made with a simple vertical fluidized bed. These were used as base cases for comparison with the results from measurements with the helical baffles without and with a fluidized bed. The measurements were made after a period of 20 min to stabilize the flow and temperature conditions. The amount of heat added to the water circuit was unimportant compared to the amount of water in the circuit.

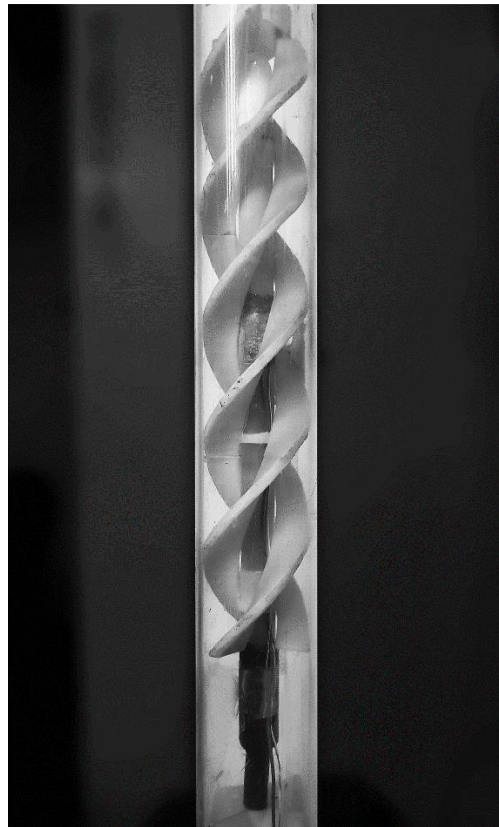
There was approximately 50 kg of water in the circuit and the heater provided 400 W power giving a temperature rise of the order of 2 K over 20 min. The measurements of heat flux, temperature of the heat flux sensor surface and the bulk water temperature at the bottom and top of the heated section allowed the direct calculation of the heat transfer coefficient.

Table 3 shows the results from the heat transfer measurements. The estimated uncertainty in the heat transfer coefficients (mostly due to the use of thermocouples as temperature sensors) has a maximum of 4.1%.

**Table 3.** Results of heat transfer measurements.

	No Baffle Nor Particles	No Baffle With Particles	Baffle Three Start 45°		Baffle Four Start 45°		Baffle Five Start 60°	
			No Bed	With Bed	No Bed	With Bed	No Bed	With Bed
$v$ [m.s <sup>-1</sup> ]	0.37	0.37	0.34	0.34	0.38	0.38	0.24	0.24
Re *	10,952	10,952	5554	5554	5866	5866	3547	3547
$\Delta P$ [Pa]	2157	4217	2746	4511	3825	5884	4315	5982
$h$ [W. m <sup>-2</sup> K <sup>-1</sup> ]	512	650	689	897	745	860	789	968
Porosity		0.853		0.814		0.802		0.825

\* Based on flow channel hydraulic diameter.



**Figure 10.** Helical baffle with concentric heater.

## 7. Discussion

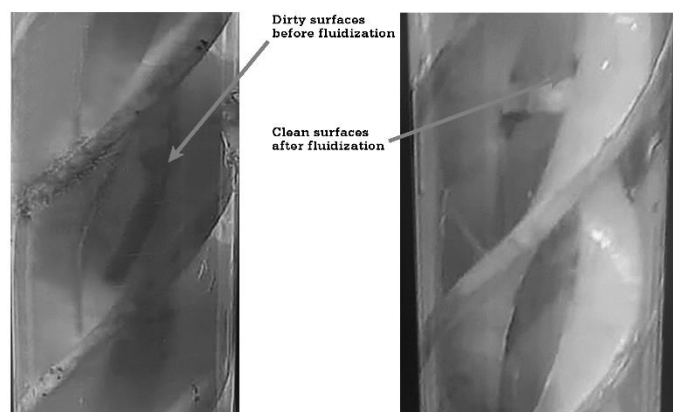
Fluidized beds can be improved by the use of interaction with inclined plates allowing a wider range of suspension conditions. This aids particle retention in the bed permitting higher superficial velocities and attenuates fluidization fluctuations. Forming inclined plates into a circle makes helical channels that can be fitted into a vertical tube. Dense beds can be formed with higher superficial velocities than the terminal velocity of the particles. The expansion of the bed is changed with respect to a vertical bed or even a simple inclined bed as shown by comparing Figures 2, 3 and 9. The differences may be a result of increased wall effects and Coriolis forces. However, the low radial velocities mean that the Coriolis forces were very low.

The use of a helical flow path allows higher velocities whilst avoiding using particle re-circulation and the consequent mechanical complications and higher probabilities of equipment breakdowns.

The measured heat transfer coefficients show substantial improvements over a stationary vertical liquid/solid fluidized bed. The best case was 49% better than the vertical bed (Table 3) but even the worst case was a 30% improvement. This case was with a type of particle that is likely to be of industrial use (chopped stainless steel wire). With larger particles, higher superficial velocities could be obtained but the channel hydraulic diameter would need to be increased. With respect to a simple concentric tube heat exchanger without a fluidized bed, the helically baffled fluidized bed can achieve an improvement of from 68 to 89%.

The cost in terms of increased pressure drop with respect to a vertical fluidized bed range from 7 to 42%, with the highest pressure drop penalty corresponding to the highest heat exchange coefficient improvement.

It should be noted that a simple heat exchanger will suffer performance degradation due to fouling over time, whereas a fluidized bed heat exchanger will maintain the cleanliness of the heat exchange surfaces and hence the heat transfer coefficient (Figure 11).



**Figure 11.** Cleaning effect of fluidized bed.

## 8. Conclusions

With some restrictions, in terms of the ratio of equivalent particle diameter to flow channel hydraulic diameter, it is possible to establish a good quality (i.e., reasonably homogeneous) liquid/solid fluidization in a single helical channel or several helical channels in parallel.

Employing baffles to form parallel helical channels wrapped around a concentric heat source can greatly increase the heat transfer coefficient to the fluidizing medium compared with the case of no fluidized bed and no baffles and a considerably increase the heat transfer coefficients compared to a vertical fluidized bed.

The pressure drop characteristics of a helical channel fluidized bed are similar to an inclined straight bed channel, but somewhat higher. There is an absence of a pressure drop plateau. This might be attributable to wall effects and secondary flow forces such as Coriolis. This pressure drop penalty is commensurate with the improved heat transfer rates obtained.

The use of helical baffles in place of an inclined concentric tube fluidized bed heat exchanger would lower the footprint in a process plant for a given service such as, for example, cooling or heating untreated seawater or effluent.

**Author Contributions:** Conceptualization, O.G.-A. and C.H.; Data curation, O.G.-A.; methodology, O.G.-A., C.H. and J.J.V.-L.; software, O.G.-A. and J.J.V.-L.; formal analysis, O.G.-A. and C.H.; investigation, O.G.-A.; resources, C.H.; writing—original draft preparation, O.G.-A. and C.H.; writing—review and editing, C.H., J.J.V.-L. and F.J.S.-O.; supervision, C.H., J.J.V.-L. and F.J.S.-O.; funding acquisition, C.H. and O.G.-A. All authors have read and agreed to the published version of the manuscript.

**Funding:** Funding for the experimental equipment used in this work was supplied by the Apoyo a la incorporación de nuevos PTC of the Programa de Mejoramiento del Profesorado of the Secretaría de Educación Pública, Mexico (48410163); Universidad Autónoma Metropolitana, Unidad Cuajimalpa, Programa de Investigación Interdisciplinaria, convocatoria 2014 (DCNI-05-120-15), Mexico and Eficiencia Thermoe S.A. de C.V. The latter also provided laboratory space and technical support. The first author was supported by a grant for tuition fees and living expenses from the Programa Nacional de Posgrados de Calidad, Consejo Nacional de Ciencia y Tecnología, México (645426).

**Informed Consent Statement:** Not applicable.

**Data Availability Statement:** The experimental data may be requested from the first author.

**Acknowledgments:** The authors acknowledge the enthusiastic technical, moral and material support of Jan Pardubicky† former Director General of Eficiencia Thermoe S.A de C.V.

**Conflicts of Interest:** The authors declare no conflict of interest. The funders had no role in the design of the study; in the collection, analyses or interpretation of data; in the writing of the manuscript; or in the decision to publish the results.

## References

1. Klaren, D.G. Apparatus for Carrying out Physical and/or Chemical Processes, More Specifically a Heat Exchanger of the Continuous Type. European Patent EP0228144A1, 8 July 1987.
2. Klaren, D.G. Dispositif Pour la Réalisation de Procédés Physiques et/ou Chimiques, en Particulier d'un Échangeur de Chaleur du Type Continu. European Patent EP0132873B1, 9 September 1987.
3. Klaren, D.G. Appareil Pour la Mise en Oeuvre d'un Processus Physique et/ou Chimique, par Exemple un Echangeur Thermique. European Patent EP0694152B1, 13 November 1996.
4. Klaren, D.G. Apparatus for Carrying out a Physical and/or Chemical Process, such as a Heat Exchanger. European Patent EP0694153B1, 13 November 1996.
5. Klaren, D.G. Device for Carrying out a Physical and/or Chemical Process, such as a Heat Exchanger. Netherlands Patent NL1005517C2, 15 September 1998.
6. Klaren, D.G. Device for Carrying out a Physical and/or Chemical Process, such as a Heat Exchanger. Netherlands Patent NL1005518C2, 15 September 1998.
7. Klaren, D.G. Apparatus for Carrying Out a Physical and/or Chemical Process, in Particular a Heat Exchanger. WO 2016/099277 A1, 23 June 2016.
8. Klaren, D.G. Apparatus and Method for Carrying out a Physical and/or Chemical Process. WO 03/069247 A1, 21 August 2003.
9. Demircan, N.; Gibbs, B.M.; Swithenbank, J.; Taylor, D.S. Rotating fluidised bed combustor, Fluidization. In Proceedings of the Second Engineering Foundation Conference, Trinity College, Cambridge, UK, 2–6 April 1978; Davidson, J.F., Keairns, D.L., Eds.; pp. 270–275.
10. Margraf, J.; Werther, J. Fluid mechanics of liquid–solid fluidization in the centrifugal field. *Can. J. Chem. Eng.* **2008**, *86*, 276–287. [[CrossRef](#)]
11. Margraf, J.; Werther, J. Continuous classification in a centrifugal fluidized bed apparatus. *J. Taiwan Inst. Chem. Eng.* **2009**, *40*, 669–681. [[CrossRef](#)]
12. O'Dea, D.P.; Rudolph, V.; Chong, Y.O.; Leung, L.S. The effect of inclination on fluidized beds. *Powder Technol.* **1990**, *63*, 169–178. [[CrossRef](#)]
13. Zabrodsky, S.S. *Hydrodynamics and Heat Transfer in Fluidized Beds*; Zenz, F.A., Translator; The MIT Press: Cambridge, MA, USA, 1966.
14. Galvin, K.P.; Nguyentranlam, G. Influence of parallel inclined plates in a liquid fluidized bed system. *Chem. Eng. Sci.* **2002**, *57*, 1231–1234. [[CrossRef](#)]
15. Hudson, C.; Briens, C.L.; Prakash, A. Effect of inclination on liquid-solid fluidized beds. *Powder Technol.* **1996**, *89*, 101–113. [[CrossRef](#)]
16. Yakubov, B.; Tanny, J.; Maron, D.M.; Brauner, N. The dynamics and structure of a liquid–solid fluidized bed in inclined pipes. *Chem. Eng. J.* **2007**, *128*, 105–114. [[CrossRef](#)]
17. Murata, H.; Oka, H.; Adachi, M.; Harumi, K. Effects of the ship motion on gas–solid flow and heat transfer in a circulating fluidized bed. *Powder Technol.* **2012**, *231*, 7–17, Corrected on *Powder Technol.* **2014**, *254*, 114. [[CrossRef](#)]
18. Ramesh, K.V.; Chandra, K.S.; Kumar, K.A. Flow Regime Mapping of Liquid-Solid Inclined Fluidized Beds. *Int. J. Eng. Appl. Sci.* **2016**, *3*, 56–57. [[CrossRef](#)]
19. Chong, Y.O.; Leung, L.S.; Nguyen, T.H.; Teo, C.S. *Inclined Fluidized Bed*; InAIChE Symp. Ser. Department of Chemical Engineering, University of Queensland: St. Lucia, QLD, Australia, 1984; Volume 80, pp. 149–155.
20. Galvin, K.P.; Dickenson, J.E. Particle transport and separation in inclined channels subject to centrifugal forces. *Chem. Eng. Sci.* **2013**, *87*, 294–305. [[CrossRef](#)]
21. Hashizume, K.; Matsue, T. Heat Transfer in Liquid-Fluidized Beds Affected by Column Wall. *Heat Transf.-Asian Res.* **2000**, *29*, 598–608. [[CrossRef](#)]
22. Pronk, P.; Ferreira, C.A.I.; Witkamp, G.J. Prevention of fouling and scaling in stationary and circulating liquid–solid fluidized bed heat exchangers: Particle impact measurements and analysis. *Int. J. Heat Mass Transf.* **2009**, *52*, 3857–3868. [[CrossRef](#)]
23. Wu, C.; Yang, H.; He, X.; Hu, C.; Yang, L.; Li, H. Principle, development, application design and prospect of fluidized bed heat exchange technology: Comprehensive review. *Renew. Sustain. Energy Rev.* **2022**, *157*, 112023. [[CrossRef](#)]
24. Jiang, F.; Dong, X.; Qi, G.; Mao, P.; Wang, J.; Li, X. Heat-transfer performance and pressure drop in a gas-solid circulating fluidized bed spiral-plate heat exchanger. *Appl. Therm. Eng.* **2020**, *171*, 115091. [[CrossRef](#)]
25. Tan, M.; Karabacak, R.; Acar, M. Experimental assessment the liquid/solid fluidized bed heat exchanger of thermal performance: An application. *Geothermics* **2016**, *62*, 70–78. [[CrossRef](#)]
26. Mattingly, G.E.; Yeh, T.T. NIST Special Tests of the Pipe Flows Produced by the Cheng Rotating Vane in Two Selected Elbow Configurations. Available online: [http://www.chengfluid.com/yahoo\\_site\\_admin1/assets/docs/NIST\\_CRV\\_Special\\_Flow\\_Test\\_Report.142144451.pdf](http://www.chengfluid.com/yahoo_site_admin1/assets/docs/NIST_CRV_Special_Flow_Test_Report.142144451.pdf) (accessed on 8 July 2021).
27. Richardson, J.F.; Zaki, W.N. Sedimentation and fluidization, Part I. *Trans. I Chem. Eng.* **1954**, *32*, S83–S100.
28. López Mata, F.A.; Heard, C.; García Aranda, O.; Valencia López, J.J. Simulación en 2D de la hidrodinámica de una columna de lechos fluidizados. In Proceedings of the Memorias del XXXVII Encuentro Nacional de la AMIDIQ, Puerto Vallarta, Mexico, 3–6 May 2016; pp. PRO-132–PRO-137.



Article

---

# Social Acceptance of a Thermal Architectural Implementation Proposal

---

Esperanza García López and Christopher Heard

## Special Issue

Selected Papers from International Conference on Innovations in Energy Engineering & Cleaner Production (IEECP'21&22)

Edited by

Prof. Dr. Bo Jin, Prof. Dr. Fei Wang, Dr. Feng Lin and Dr. Saifur Rahman Sabuj





## Article

# Social Acceptance of a Thermal Architectural Implementation Proposal

Esperanza García López and Christopher Heard \*

Departamento de Teoría y Procesos del Diseño, Universidad Autónoma Metropolitana-Unidad Cuajimalpa, Mexico City 05348, Mexico

\* Correspondence: [cheard@cua.uam.mx](mailto:cheard@cua.uam.mx)

**Abstract:** The social acceptance of introducing an improved and sustainable roofing material in multicultural communities in Mexico was addressed. A case history of a community “La Cañada” in Huixquilucan, State of Mexico (19°19′02.81″ N, 99°22′23.21″ W, 3025 m above mean sea level), a village very close to the eastern edge of Mexico City and representative of strong social and transcultural pressures similar to surrounding communities in Mexico City, is reported. The approach considered developing a double-layered roof to reduce the energy demand for space heating in this predominantly cold region, thus significantly contributing to indoor thermal comfort, reducing the need for cutting wood and helping to alleviate the accelerating impacts of deforestation in the area. Two parallel studies were used, whereby the then-current awareness levels of citizens and the factors impacting their commitment to energy sustainability were analysed using multicriteria social parameters, while the second study focused on the analysis of improved comfort when the proposed double roof was implemented, based on the feedback received from a pool of citizens who experienced living in the improved prototype dwellings. Results showed that while the level of awareness on energy efficiency was still low, the influence of media on their decisions and aspirations was strong and this could be constructively used to support the shift towards a more sustainable society and a “solar culture”. Moreover, the developed sustainable double-roof prototype has significantly improved indoor comfort and energy savings for heating, while demonstrating a fast and easy replicability potential in similar dwellings.

**Keywords:** alternative architecture; comfort; social assimilation



**Citation:** García López, E.; Heard, C. Social Acceptance of a Thermal Architectural Implementation Proposal. *Sustainability* **2023**, *15*, 4121. <https://doi.org/10.3390/su15054121>

Academic Editors: Bo Jin, Fei Wang, Feng Lin and Saifur Rahman Sabuj

Received: 30 November 2022

Revised: 30 January 2023

Accepted: 1 February 2023

Published: 24 February 2023



**Copyright:** © 2023 by the authors. Licensee MDPI, Basel, Switzerland. This article is an open access article distributed under the terms and conditions of the Creative Commons Attribution (CC BY) license (<https://creativecommons.org/licenses/by/4.0/>).

## 1. Introduction

There are few studies in the literature that investigate the social assimilation of a low cost, simple, occupant installable thermal comfort improvement in vernacular log-cabin-type construction. The building used as a test bed in this study has been previously described and its dynamic thermal performance modelled with and without the thermal comfort improvement. Detailed results of the thermal evaluation were given, comparing field measurements and modelling, and a brief report of a small subset of the surveys herein reported was included in a prior publication [1]. However, there are few studies which investigate the acceptability of such simple measures for a traditional wood dwelling in a rural community. There are studies, such as that of the acceptance of smart-home technologies, which do not reflect the kind of occupier or housing that are the subject of the present work. For example, Tirado Herrero et al. [2] observed that smart-home technologies may be less available to disadvantaged households because they lack good internet connections and the latest mobile phones. Studies related to the use of smart electricity meters in social housing in a European context, such as that of Balest and Vettorato [3], were of tenants of flats in a middle-sized Italian city and not of owner-occupiers of traditional housing in a rural community. Guo [4] reported that they found data on occupant attitudes and perceptions to be more useful than just scientific data alone in the study of traditional stilt houses in Southeast Chongqing, China. It was found that most of those interviewed were satisfied with the thermal comfort of their dwellings, yet

the survey results purported a contrary result. Three reasons were given for this: Firstly, the general rural poverty and lack of comprehensive public services. Secondly, thermal problems due to occupants' modifications, lack of maintenance and/or behaviour and, thirdly, issues of lack of cleanliness, dampness and the use of combustion-based heating in interiors. Valderrama-Ulloa et al. [5], on reviewing one hundred selected papers on indoor environmental quality in Latin American buildings, commented that there was a sustained discrepancy between measured and perceived thermal comfort conditions. Valderrama-Ulloa et al. reported that about a quarter of the papers consulted in their review only used temperature as a comfort criterion.

Whilst timber construction is not predominant in Latin America, there are specific places where it is traditional [6]. In the case of Mexico, it is used in rural communities in forested regions. About 3% of housing has wood walls and about 2% has wood or wood-shingle roof construction [7].

From the start of this research, the members of the community were always in mind and the proposals were presented to them. Once the prototype was built, measured and put into operation, the following questions were then asked: Is the design really for the inhabitants of "La Cañada" or was it only supposed that it would be an example for them? Is it true that the residents of the community would, when building, identify with our objectives of lower energy consumption, better thermal comfort and sustainability? And does our proposal have sufficiently attractive characteristics to be adopted and owned by the community and multiplied?

To answer these questions, a social investigation based on questionnaires with two aspects was decided upon. The first investigated the possibilities of reproducing the design with the help of advice. The second had the objective of finding out if the residents were conscious of thermal comfort and the concept of energy saving.

The theories of Carrera [8] were used as the basis, where the initial point is that common education-based reasoning starts with detailed local knowledge and practices. These, in turn, help people to develop theoretical and critical knowledge about their situation in each context [9].

The motive was to convey the idea that a reassessment of well-founded local knowledge is a basis for organizing sustainable communities.

## 2. Materials and Methods

The study was carried out in the community of "La Cañada", in the municipality of Huixquilucan, which is a village settled to the west of Mexico City (Figure 1). This place was chosen since it was an average community of the city hinterland. It has the same real-estate speculation, social and cultural transformation and environmental impact characteristics as these surroundings. The results obtained can be extrapolated to the entire forested periphery.



Figure 1. Location of the community "La Cañada".

### 2.1. Physical Aspects

The climate is semicold with summer precipitation. According to the Köppen-García scale, this corresponds to Cw [10]. That is why the main strategy in houses is to heat. To achieve this, their main fuel is firewood, which is provided free of charge from the forest.

Land use is mainly forestry; however, because of its scenic beauty, its short distance from Mexico City and its resources, the area suffers from multiple speculation. These include, use and sale of land, commercial interests such as clandestine timber felling, firewood cutting for restaurants (traditional pit-cooked lamb and quesadillas), communal tourist developments—trout-fishing zones, pony trekking, off-road motorcycling, quadbike tracks and the sale of forest topsoil leaf mulch, which is essential for the life of forest communities.

All of this has produced deforestation with the consequent problems of erosion and changes in rainfall, accumulation of rubbish and bad pollution of the small river that runs through the community, which today is only used to dispose of sewage [11]. The village is in a designated ecological conservation area since it is within the range of 2700 to 3200 m above sea level, which conflicts with current legislation and has not been considered. The ecological degradation is important both from the economic point of view as well as from the social point of view.

### 2.2. Social Aspects

This community is part of the municipality of Huixquilucan, one of the most economically contrasting. The highest social classes and the lowest live in the same territory. The total municipality population was 1858 inhabitants, where 52% were women for the whole commoner zone, which covers several villages. A local census gave 520 inhabitants for the “La Cañada” village.

In terms of education, at least 1% of the population was illiterate, most had completed primary school and only 10% had completed secondary or high school. No one spoke an indigenous language nor had direct prior experience that allowed them to conserve traditions or rituals [12]. Knowledge of ancestral practices did not exist in the community.

The economic class level for the community, according to government information for “La Cañada” was “D” or “D minus” [13]. These data were of great importance for the study, given that the survey tried to see what the residents’ classes of aspirations were. It is to be noted that the economic class to which they belonged makes the probability of gaining a higher social class 30%.

The form of land possession comes from the Mexican revolution (1910–1920) and is called “communal land”, where the commoners are those who have rights over land exploitation under their own rules. The local government has no policies pertaining to cleaning or conserving the environment. This is based on social or family connections or financial pressure, where the commoners are the beneficiaries [14].

The majority were from farming families or were still working as farmers. The traditional economic activity in the region is based on ancestral customs and is the sowing of maize. However, the young have started to have other sources of income. The activities are changing, above all, to informal work, such as unskilled building and general workers or impromptu tourism activity, such as food sales, pony trekking, trout fishing or setting up a restaurant.

In three generations, they have gone from farmers to new jobs where they still sow maize by custom, but they can no longer make a living from this. No member of the community is self-sufficient based on the grain, and all the inhabitants have to make up their diets with purchases in the local market.

They consider that working on weekends is sufficient to make a living and during the week they till the little land that they have (except those who have a skilled trade), which is insufficient for the sustenance of a family. Failing this, they prepare inputs for the weekend trade.

Population growth has been exponential, increasing 84% from the nineteen thirties to the present day, when 600,000 ha of communal lands were declared sufficient for subsistence. The increase in population and the nearness of the city has caused a need for more and more buildings [15]. Thus, small agricultural plots have been converted to this new use.

### 2.3. Methods

The community has undergone very important changes. Thus, it was decided to apply a social survey methodology, which went in two directions: a statistical one, which sought to measure the degree of transculturation based on the architectural aspirations of the inhabitants, evaluating the level of commitment they had towards the preservation and conservation of their environment and to find out their knowledge about the concepts that must be applied to achieve it.

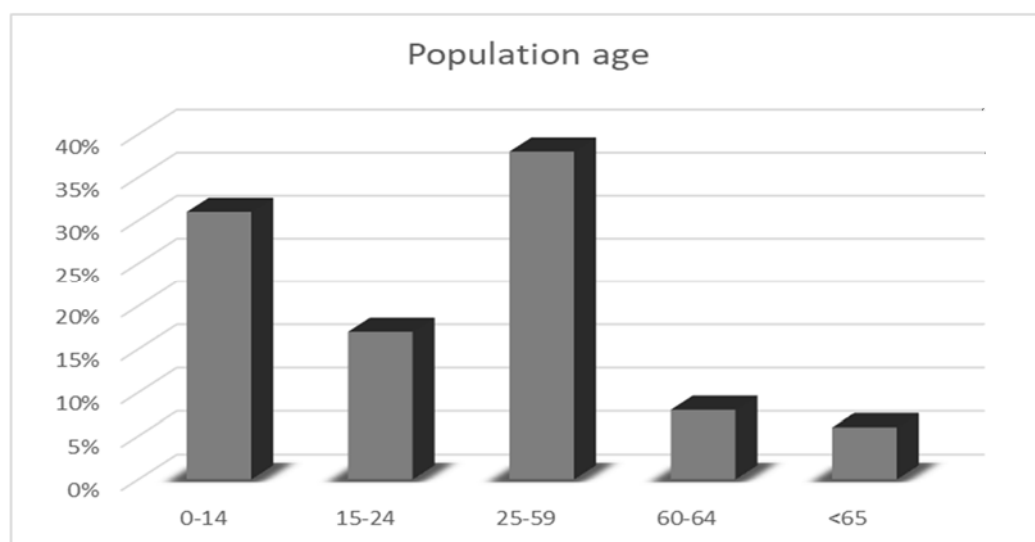
A second, more specific one, was designed to find out about the aesthetic acceptance of the proposal and its reproduction; to enquire if the proposed technology and materials could feasibly be appropriated by residents in the community; and to investigate the degree of environmental awareness concerning energy saving and understanding of the benefits of better thermal comfort.

To be sure that these surveys (Appendix A) provided reliable information, they were based on Hyman methodology for the type of questions [16] and Pardinás in the selection of the subjects [17]. Two types of mutually exclusive survey were designed, one statistical and the other qualitative.

Both questionnaires considered verification answers and care was taken that there were no leading questions. The quantity and characteristics of the survey subjects were also considered.

#### 2.3.1. Survey 1

A ten percent sample of the population above the age of consent (15 years) was taken; according to the site population curve. This resulted in 39 interviews (52% women and 48% men). Among them, 9 were subjects between 15 and 24 years old, 21 were people between 25 and 59 years old, 6 were between 60 and 64 years old and only 3 were over 65 years old (Figure 2).



**Figure 2.** Age ranges of the population.

The questionnaire had nineteen questions divided into three themes: five questions about their current home, five about awareness of the thermal characteristics of their home and nine questions about concepts, sustainable actions and environmental education.

The survey was one where the questions were mostly closed or multiple-choice. No demographic or social questions were asked, except for name and gender. The form was designed as a rapid survey, given that it was to be applied to a large number of residents. One-in-three dwellings was selected randomly and family members that complied with the survey's age and gender requirements were asked to participate.

### 2.3.2. Survey 2

The sample was of 13 persons from the community who were invited to stay for two days in the prototype building. The questionnaire tackled aspects of the physical sensation of comfort experienced, the aesthetic perception, the feasibility of implementation and their ideal home aspirations. This was a survey with eight questions, of which two were open and six used the five-level Likert scale [18].

The stays were programmed for December and January, as these are the coldest months (Figure 3). The provision of a "double skin" in the ceiling was designed to reduce the temperature swings in the living space. The best way to survey the impact of the proposal was to submit the participants to the most extreme climate of the year. In all cases, there was no active heating system, neither combustion-based nor electrical, just the blankets and clothing that the visitors supplied. The participants were asked to leave the building as little as possible so that they were inside for almost the entire two days. This was not difficult to achieve since the participants or their offspring were farmers and at that time of year, there was very little agricultural activity.

Persons invited	Visit dat	Adult man	Adult woman	Total each visit
Visit 1	Jan 7 to 9	1	1	2
Visit 2	Jan 1 to 23	1	1	4-2=2
Visit 3	Aug 10 to 12		2	2
Visit 4	Sept 8 to 10	1		1
Visit 5	Dec 8 to 10	1	2	3
Visit 6	Dec 27 to 29	2	1	3
Total by gender		6	7	13

Figure 3. Visit calendar.

## 3. Results

### 3.1. Survey 1

What the residents have and what they would like in their dwellings can be seen from the results. At present, the constructions of residents of La Cañada are very close to what they aspire to. However, the tendency to use wood as a material for walls has diminished, contributing to an increase in the use of concrete and brick. Adobe is a material whose use has changed little. It is not appreciated by many, but those who have used it in the past continue to do so.

The results show that concrete floors were the most used (74.4%), followed by ceramic floor tiles (12.8%) and compacted earth (12.8%) (Figure 4). However, to the question of "What would you like your floor to be made of?" 64.1% answered that they preferred ceramic floor tiles. Nonetheless, 35.9% answered that they would like visible concrete floors, with compacted earth completely disappearing. Ceramic tiles on a concrete base were considered to be a floor covering with the best finish.

Roof construction was mainly reinforced concrete (65%), with galvanized corrugated iron coming a distant second in preference (20.5%) and traditional wood in third place (17.9%). All these materials are still in use but there is a marked tendency to prefer reinforced concrete (82.8%), leaving behind other materials.

In the case of window frames, the predominant materials were steel sections (56.4%), aluminium (20.5%) and wood (15.4%). The preferences expressed by those surveyed were

for aluminium (51.3%) and secondly for wood (17.9%). In third place was steel (23.1%), which is widely used but no one wanted it (Figure 4).

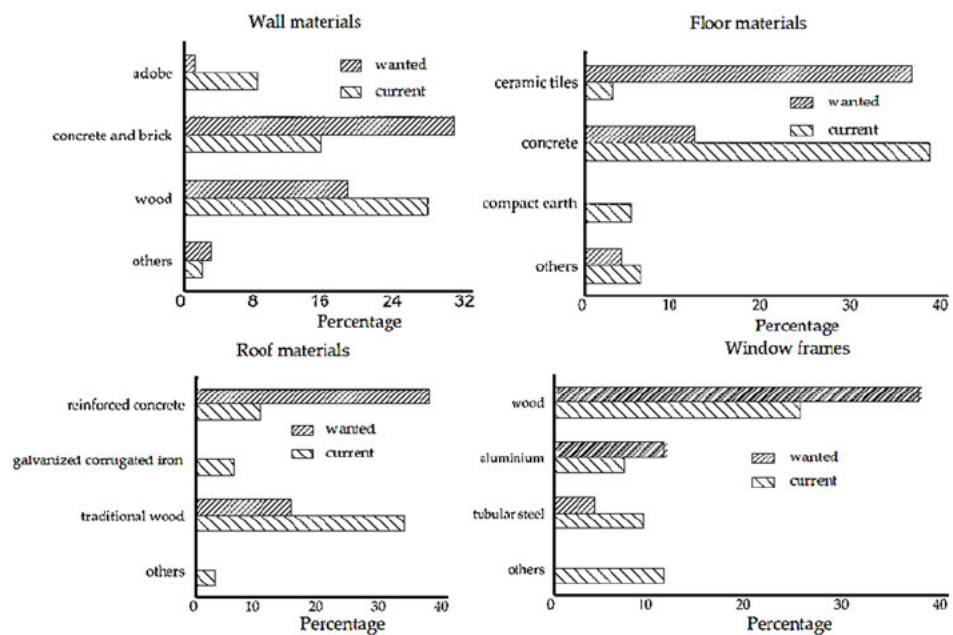


Figure 4. Construction materials.

In Figure 5, the lighter bars represent the materials that were present in their homes, and the darker bars represent what those surveyed would have liked to have in their homes. At the time of the survey, the majority of homes were single-storey, and none were more than two storeys. It can be appreciated that there is a tendency to continue building but on a single floor.

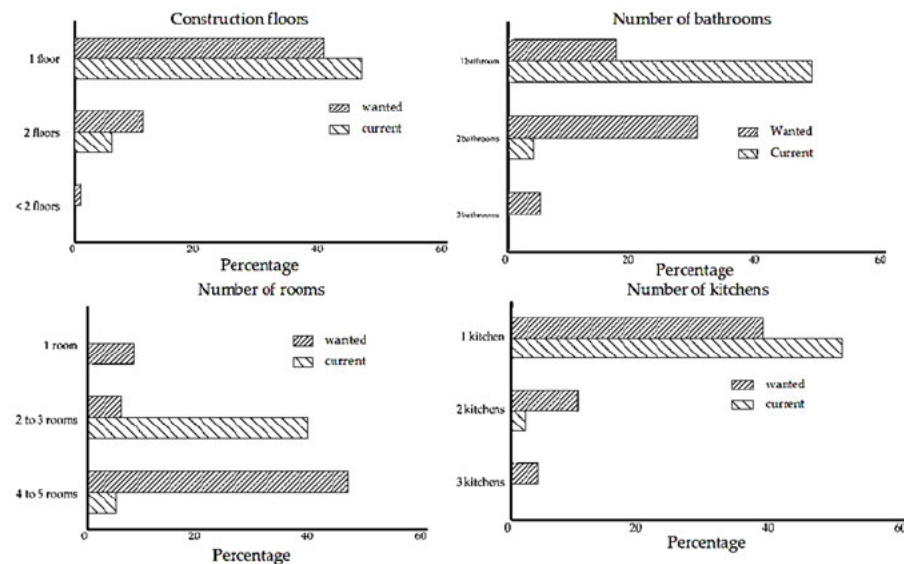


Figure 5. Material preferences.

It is very important to note that the number of bathrooms is closely related to the number of bedrooms in the house. That is, that houses with two or three bedrooms have a need for two or more bathrooms. At the same time, the growth in the size of a house implies an increase in the number of bedrooms. As a family increases in size, then so does the house.

The kitchen was an important element for those surveyed. When they were asked how many kitchens they had, 48.7% answered that they had two kitchens, 38.5% had one and 12.8% had three. However, to the question “How many kitchens would you like to have?” 43.6% answered two, the same percentage as answered three and 12.8% answered one. What can be seen is that those who wish for more kitchens are directly related to local tourism. They do not work in agriculture but in the prepared food trade, such as traditional pit-oven-cooked lamb and/or quesadillas.

On the question of thermal comfort (Figure 6) in the interior of dwellings, the survey asked for a ponderation from 1 to 5, where 1 was very cold and 5 representing very hot [19]. A majority of those surveyed (38.5%) responded that the conditions were mild. However, 23.1% said that their home was very cold, and at the other extreme, only 5% thought that their home was very hot (Figure 6). These latter cases coincided with their house being built of adobe, which has a much higher thermal time lag than the other construction types.

Those surveyed were also asked, on a scale from 1 to 5, where 1 was very damp and 5 was very dry, how was the humidity in their home? Of those surveyed, 35.9% responded that their home was semidamp and 25.6% considered their home to be dry. It was found that those interviewed associated humidity with temperature in that they thought that if the house was damp then it would be cold.

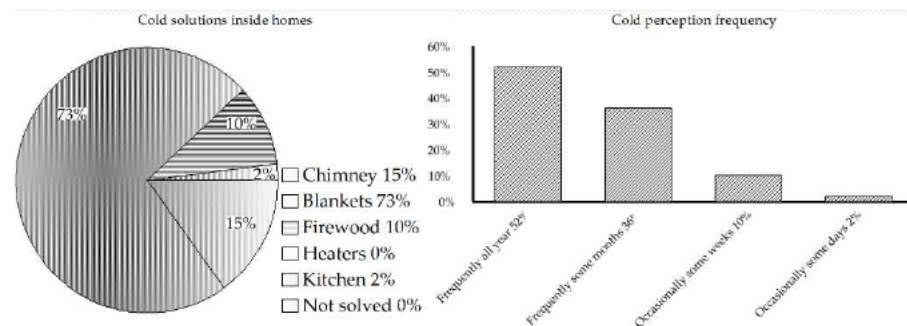


Figure 6. Thermal comfort perceptions.

A list of words was given, where the interviewees were asked to indicate if they had heard of them or not and where: television, radio or school [20] (Figures 7 and 8).

**Environmental education.** A total of 76.9% of respondents had heard of the term, whereas 23.1% said that they had not heard the term. When asked where they had heard the term, 51.3% replied on the television, 7.7% on the radio, 8% at school and 33% did not remember where.

**Ecology.** All interviewees (100%) had heard the term; 64.1% had heard the term on the television, 5.2% at school, 5.1% on the radio and 25.6% did not remember where.

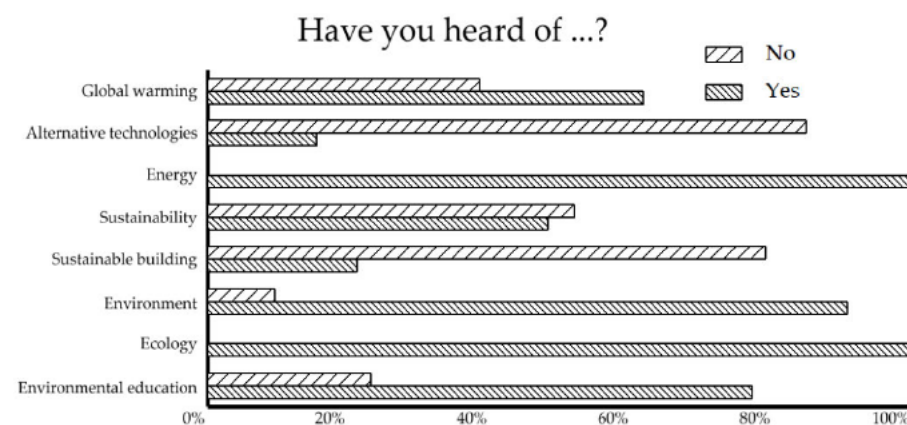
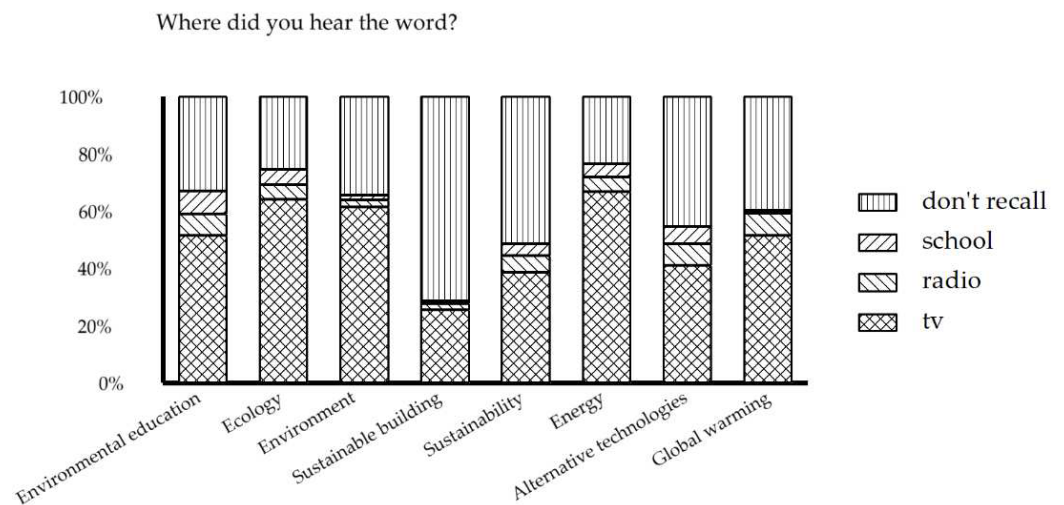


Figure 7. Words related to sustainability.



**Figure 8.** Words related to sustainability.

**Environment.** The majority (90.4%) had heard of the term and 9.6% had not; 61.5% had heard it on the television, 2.3% on the radio, 1.8% at school and 34.4% did not remember where.

**Sustainable building.** Just 21.2% had heard the word and 78.8% never had; 25.5% had heard it on the television, 2% on the radio, only 1.2 at school, and 71.3% never had heard of it.

**Sustainability.** A proportion of 48.1% had heard the term, mainly on the television (38.5%), at school (4%) or on the radio (5.9%), and 51.6% did not remember where, whereas 51.9% had never heard the term.

**Energy.** All the interviewees had heard the word (100%). Most had heard the word on the television (66.7%), 5.1% had heard it on the radio, 4.6% at school and 23.6% did not remember where they had heard it.

**Alternative technologies.** Only 15.4% responded that they had heard the term, mostly on the television (41%), to a much lesser extent on the radio (7.6%) and just 6% at school. However, there were 84.6% of interviewees who did not know of the term and 45.4% who did not remember where they had heard it.

**Global warming.** A proportion of 61.5% reported having heard the term and 38.5% reported not. The sources of having heard the term were similar to the others, with 51.3% on the television, 7.8% on the radio and just 1% at school, and 39.9% did not remember.

From the above, the majority of the interviewees had heard of these words, above all on the television and, to a lesser degree, on the radio and at school. Even so, when asked if they could describe these words, most replied that they could not (75%), whilst the remaining 25% tried to respond but were not able to explain the meanings of these terms.

These results are not disappointing. On the contrary, they show that a large part of the interviewees keep a close eye on what happens in the world via mass media.

When they were asked if the knowledge that they had acquired was of use to them in their daily life, two-thirds said that it was. In the same tenor, they considered that environmental education [21] was very important for the community to help within the family and especially for their children's homework.

### 3.2. Survey 2

From the 52 interviews in the first survey, 13 people were randomly selected to stay in the prototype building for 48 h. The second survey provided further information [18].

The guests were asked if they felt cold, hot, damp, draughts or comfortable (Figure 9). Of the guest responses, 76.9% responded that they did not feel cold and 92.3% did not feel hot. No one reported feeling damp nor draughts. It can thus be assumed that 94.9% of participants were in their comfort zone. The lack of reports of cold or heat could be



attributed to the mild weather during the test period. Due to the altitude and latitude of the site the diurnal temperature range at the time of year of the tests was around 10 K, with a minimum night-time temperature of about 7 °C. The double-skinned roof construction was used to attenuate the daily temperature variations and maintain the interior temperature at night. The interior skin allowed the building to breathe and permitted ventilation without draughts but at the same time retain heat during the night.

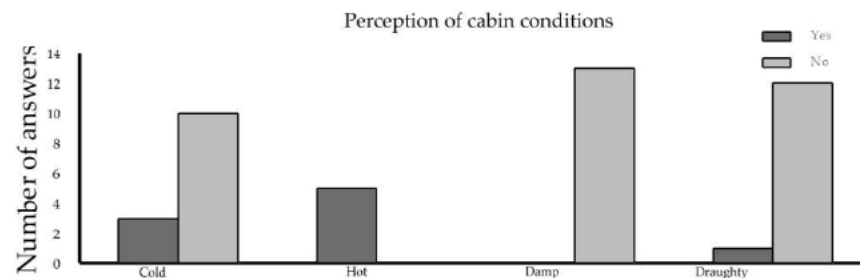


Figure 9. Perception of conditions in the cabin.

The second question was “Did you sleep well?”, to which 92.3% answered yes, that they slept as usual. The interior roof skin was not an aggressive change to what they were accustomed to, and many commented that it was an aesthetic improvement.

The testers were asked to evaluate the cabin on a scale of 1 to 5, from agreeable to disagreeable, considering the ceiling, walls, floor, temperature, noise, humidity, draughts and the installations (Figure 10). The term installations referred to the solidity of the construction and the finish, in that it did not look improvised, but rather properly integrated. None of the testers responded with extremes; 84.6% considered the cabin to be agreeable; 92.3% considered the ceiling to be agreeable; and 84.6% thought that the walls, the floor and the humidity were agreeable. On the question of noise, 53.8% considered the level to be agreeable and, finally, 92.3% thought the installations to be agreeable.

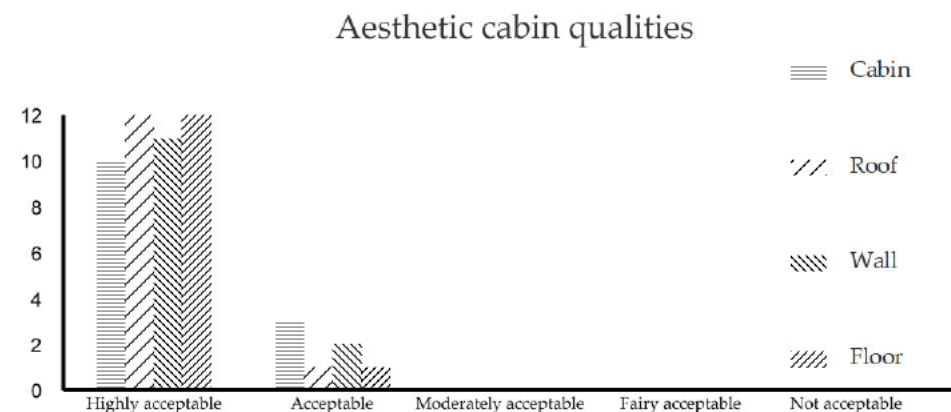


Figure 10. Perceived aesthetic qualities of the cabin.

Although the roofing was designed with practical considerations in mind, three out of four responded that they would copy this system. This question had the objective of measuring the acceptability of the proposed solution and the impact that it could achieve. However, many replies mentioned that the prototype “looked nice”. The testers were aware that the materials involved were not expensive and were readily available in the community. They also had the abilities necessary to incorporate this system in their own constructions.

When they were asked if they would use the system for the roof of their own home, then the replies changed dramatically. They showed a great lack of interest in the idea. The replies were very much in the tone of “Why would I do it?” or “What use is it to me?”. These replies were in the context of considerations of status and competition within

the community [22]. If they considered that the use of the proposed improvement would increase their social status, then they were willing to use it.

The testers were asked if the interior of the cabin, during the day, was warmer than outdoors (Figure 11). Sixty-nine percent responded that that was the case. One of the main reasons was that they were warmer than in their own homes.

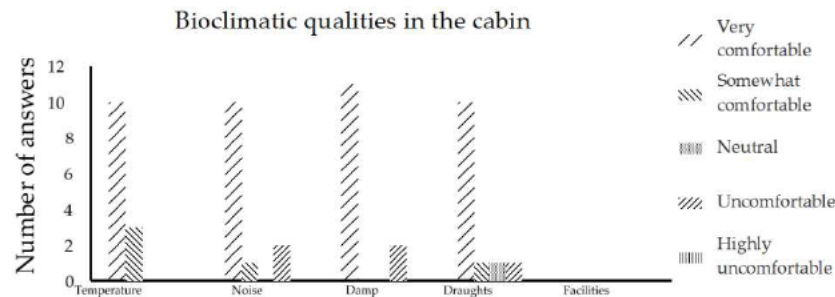


Figure 11. Bioclimatic cabin qualities.

The same question was applied for the night-time case. The majority (92.3%) considered that they felt warmer at night. It should be taken into account that, during the day, doors and windows were opened and the testers did leave the cabin on occasion. This allowed air currents to circulate. This did not happen at night and so the interior temperature was conserved.

A question was applied, in which the testers were asked, “If they could improve the cabin what would that improvement be?”, to which 61.6% responded that they would not have made any changes and 15.4% said that they would make it bigger. The rest of the replies were that they would decorate the place to follow their own tastes (Figure 12).

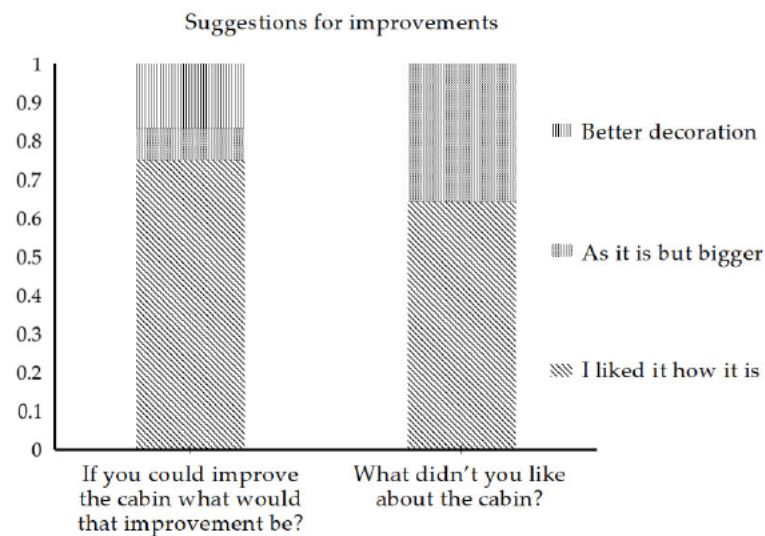


Figure 12. Replies to “What did and didn't you like about the cabin?”.

A similar question but with a negative connotation was also asked in order to counter the effect of the interviewees trying to please the researcher. This question was “What didn't you like about the cabin?”. Even so, 61.6% replied that they did not dislike anything, 15.4% replied that they would like it to be bigger and 23.1% said that the aesthetics were not to their personal liking. These results are consistent with the previous question.

The replies were influenced by the familial situation of the testers. Thus, members of smaller families identified with the prototype, whereas it could be supposed that others need bigger homes.

#### 4. Discussion

The results of the study on the potential for social assimilation of the proposed technology were unexpected.

It was understood that the members of the community where the study took place generally had a low level of formal education and low incomes. Also, they tended to copy what for them was meant to be “better”. That implies that the authors, as researchers, were not the ideal subjects to judge the acceptability of the proposed technology. It was apparent that the collateral benefits, such as energy saving and forest conservation, were of little relevance to the interviewees. Their main interest was in direct material benefits in financial terms [23].

When they talked of a new implementation, they saw it as a way of showing their individuality in a way that was well-received amongst their peers and that could be admired.

Smelser [22] wrote of the need for leaders and this study bears this out. On trying to find these leaders in the community, it was noted that there were none related to everyday activities. Leaders of opinion for the community were those related to the media, especially the television. Most of those interviewed preferred to copy lifestyles such as those seen in soap operas instead of innovative ideas. This would improve their status in the eyes of the rest of the community.

The acceptance of new construction materials comes about from following or conserving status within the community. This status is related to the cost or opulence of the construction style. There was no reflection on the status obtained from thermal comfort, low energy expenditure or a better life for their grandchildren.

Although in the second survey the residents reported that the interior environment was more agreeable than their own home, they remained sceptical that the prototype’s innovative technology was the cause of the improvement in the thermal comfort.

On the question of technological innovation, the respondents were open to it if it allowed them to scale the social hierarchy, even if it clashed with practical matters. It was observed that the acceptance of the prototype was attributable to aesthetic consideration more than thermal comfort. It is important to note that those persons who were invited to consider applying the technique to their own homes were unenthusiastic and justified their replies with “What use would it be to me?”. This was with the objective of wanting to hear in what way this technology would provide a level of admiration from their peers, leaving aside the benefits in terms of physical health (due to better thermal comfort), better quality of life or conservation of the habitat from a more sustainable development point of view.

In this case, it has been shown that the appropriation of the technique to improve a home is possible only if the objective is mainly social and not only technical [24]. That is, that it meant something in the social terms of reference of the community.

The perception of comfort inside the prototype was related to the temperature perception of those surveyed. The interviewees knew empirically that during the coldest months of the year they had to take care of their health. Their solution is to cover themselves with more blankets and, in extreme cases, leave the wood fire lit overnight. They had a notable tolerance to cold [19].

However, in the case of humidity, this was not something that they were concerned about, even though the months of the rainy and dry seasons are not inter-related, neither for temperature nor comfort.

Other observations were made by the interviewer during the research, which were not directly the object of the project.

A lack of engagement and knowledge about treatment and technology of environmental conservation, the surroundings and the landscape were observed. What is usually considered to be rubbish is not so for the residents. They have neither rubbish collection nor a landfill site [23]. The housing plots have soft drink bottles and household cleaning product containers, disposable nappies and plastic bags in them. Although some items are reused, the residents habitually leave them where they are or bury them in their own yards.

The village is growing in a haphazard and mostly horizontal manner. Plots are arbitrarily subdivided for children to build their own houses, which are ever smaller and more cramped. This will have a deleterious impact on the health and extension of the forest if adequate policies are not put in place.

There is a custom to use two kitchens, where firewood is burnt to cook dishes in one and tortillas are cooked in the other. The exploitation of the forest to provide firewood is unregulated.

There is a clear tendency to generate income from weekend tourism, pony trekking, quadbike hire, etc., all of which are largely unregulated and improvised [24].

Water sources, such as springs and wells, are considered private property and even so they are not conserved. The majority of the residents are commoners and entitled to free electricity, so only about 10% of the community have to pay electricity bills.

The commoners do not consider that the forest and other natural resources are theirs and so take them for granted as not their responsibility. They consider them to be eternal and appear not to be aware that they are disappearing.

## 5. Conclusions

One of the most important results from the study is the clear indication of the overriding impact of social perceptions of the proposed technology to improve thermal comfort. That is to say that, more than improved physical conditions, the perceived impact on social standing in the community had much more influence on the likely uptake of the proposed and demonstrated technology. This was despite the clear opinions that the modification of the test cabin evidently provided perceivable improvements in thermal comfort.

This study is a representative sample of how the inhabitants can assimilate environmental proposals in the western and southern part of the Mexico City hinterlands where forest exists. However, it cannot shed light upon how this assimilation would be in the northern part, where the tendency is industrial, or towards the east, which is essentially service-oriented, both with different climatic and ecological conditions, which would be worth considering in further studies.

**Author Contributions:** Methodology, E.G.L.; Writing—original draft, C.H. All authors have read and agreed to the published version of the manuscript.

**Funding:** Funding for this research and the APC was provided by the Universidad Autónoma Metropolitana, Department of Design Theory and Practice, Unidad Cuajimalpa, Mexico City. Project, “El diseño ante el cambio climático: Divulgación, normatividad e información climatológico” 48401022.

**Institutional Review Board Statement:** The Research Committee of the Division of Communication Sciences and Design endorses that the research project entitled “Design for climate change, Dissemination of regulations and climatological information” was registered and approved at session 14.21 of the Divisional Council at DCCD, Universidad Autónoma Metropolitana, Unidad Cuajimalpa, Mexico City.

**Informed Consent Statement:** Informed consent was obtained from all subjects involved in the study.

**Data Availability Statement:** The data presented in this study are available on request from the corresponding author.

**Acknowledgments:** This work was carried out at the Universidad Autónoma Metropolitana, Department of Design Theory and Practice, Unidad Cuajimalpa, Mexico City, project “El diseño ante el cambio climático: Divulgación, normatividad e información climatológico”.

**Conflicts of Interest:** The authors declare no conflict of interest. The funders had no role in the design of the study; in the collection, analyses, or interpretation of data; in the writing of the manuscript; or in the decision to publish the results.

## Appendix A.

### Survey 1

Experimental construction based on alternative technology.

This survey had as a fundamental objective, to find out the acceptability of alternative technology in construction of habitational spaces. It has been designed for the purpose of the present research.

Name: \_\_\_\_\_ Gender: \_\_\_\_\_ Age: \_\_\_\_\_

#### Appendix A.1. Materials

##### 1. What materials is your house made of?

Wall	Adobe	Brick	Wood	Other
Floor	Ceramic tiles	concrete	Compact earth	Other
Ceiling	Reinforced concrete	Galvanized corrugated iron	Traditional wood	Straw or other
Window frame	Wood	Aluminium	Steel	Other

##### 2. Of the rooms in your house, how many of each type are there?

	1	2	3	More than 3
Floors				
Bedrooms				
Bathrooms				
Kitchen				

##### 3. Do you think that your own house has any problems?

Yes	What are they?	No	I don't know	Unanswered

#### Appendix A.2. Appreciation

##### 4. What materials would you like your house to be built with?

Wall	Adobe	Brick	Wood	Other
Floor	Ceramic tiles	Concrete	Compact earth	Other
Ceiling	Reinforced concrete	Galvanized corrugated	Traditional wood	Straw or other
Window frame	Wood	Aluminium	Steel	Other

##### 5. How many rooms would you like your house to have?

	1	2	3	More than 3
Floors				
Bedrooms				
Bathrooms				
Kitchens				

##### 6. On a scale of 1 to 5: where 1 is very cold and 5 very warm, where would you place your house?

Very cold	Cold	Neutral	Warm	Very warm
1	2	3	4	5

7. When you are inside your house, do you sometimes feel cold?

Yes	No	I don't know	Unanswered
-----	----	--------------	------------

7.1. How often you feel cold inside your house?

Frequently		Occasionally	
All the year	All the year	Some weeks	Some days

7.2. How you manage feeling cold?

Chimney \_\_\_\_\_ Blankets \_\_\_\_\_ Firewood \_\_\_\_\_  
 Heaters \_\_\_\_\_ Kitchen stove \_\_\_\_\_ Not solved \_\_\_\_\_  
 Others (explain) \_\_\_\_\_

8. Inside your house do you sometimes feel warm?

Yes	No	I don't know	Unanswered
-----	----	--------------	------------

8.1. How often you feel warm?

Frequently		Occasionally	
All the year	All the year	Some weeks	Some days

8.2. How you manage feeling warm?

Fan \_\_\_\_\_ Opening windows \_\_\_\_\_  
 Evaporative cooler \_\_\_\_\_ Nothing \_\_\_\_\_ Other \_\_\_\_\_

9. On a scale of 1 to 5: where 1 is very humid and 5 very dry, where would you place your house?

Very humid	Humid	Neither humid	Dry	Very dry
1	2	nor dry 3	4	5

9.1. If your answer is between 1 to 3, why?

It lacks waterproofing in the roof \_\_\_\_\_ Moisture rises through the floor \_\_\_\_\_  
 It lacks waterproofing of the walls \_\_\_\_\_ Internal leaks \_\_\_\_\_  
 I don't know \_\_\_\_\_ Unanswered \_\_\_\_\_

9.2. On a scale of 1 to 5 how wet/dry is your bedroom?

Very humid	Humid	Neither humid	Dry	Very dry
1	2	nor dry 3	4	5

What is the reason?

It lacks waterproofing in the roof \_\_\_\_\_ Moisture rises through the floor \_\_\_\_\_  
 It lacks waterproofing of the walls \_\_\_\_\_ Internal leaks \_\_\_\_\_  
 I don't know \_\_\_\_\_ Unanswered \_\_\_\_\_

9.3. On a scale of 1 to 5 how humid/dry is your bathroom?

Very humid	Humid	Neither humid	Dry	Very dry
1	2	nor dry 3	4	5

What is the reason?

It lacks waterproofing in the roof \_\_\_\_\_ Moisture rises through the floor \_\_\_\_\_  
 It lacks waterproofing of the walls \_\_\_\_\_ Internal leaks \_\_\_\_\_  
 I don't know \_\_\_\_\_ Unanswered \_\_\_\_\_

9.4. On a scale of 1 to 5 how wet/dry is your kitchen?

Very humid 1	Humid 2	Neither humid nor dry 3	Dry 4	Very dry 5
-----------------	------------	----------------------------	----------	---------------

Which is the reason?

It lacks waterproofing in the roof \_\_\_ Moisture rises through the floor \_\_\_

It lacks waterproofing of the walls \_\_\_ Internal leaks \_\_\_

I don't know \_\_\_\_\_ Unanswered \_\_\_\_\_

10. Have you heard of the following words?

	Yes	No	Where Did You Hear Them?
Environmental Education			
Ecology			
Environment			
Sustainable Building			
Sustainability			
Energy			
Alternative Technologies			
Global warming			

11. Can you describe what they mean?

	Yes	No	Short description
Environmental Education			
Ecology			
Environment			
Sustainable Building			
Sustainability			
Energy			
Alternative Technologies			
Global warming			

12. Has this knowledge helped you in your daily life?

Yes	No	Why?

13. Do you consider that environmental education is essential for you?

Yes	No	Why?

14. Were you or someone in your family a farmer or farm worker?

Yes	Some great grandparents	Grand parents	Parents	Your children	I don't know	Unanswered

15. Do you know where the water you drink comes from?

Yes	No	Where?
-----	----	--------

16. Do you know where your waste water goes?

Yes	No	Where?
-----	----	--------

17. When you eat something, where do you dispose of the garbage?\_\_\_\_\_

18. Do you know where your garbage goes? Where?\_\_\_\_\_

19. Do you know of another electricity source other than that in your house?

Yes	No	Which?	I don't know	Unanswered
-----	----	--------	--------------	------------

### Survey 2

Experimental construction based on alternative technology.

This survey has a main objective of finding the acceptance of alternative technology in the construction of habitable spaces. It has been designed to directly follow the purpose of this research and data will serve just as a statistical sample.

Name:\_\_\_\_\_ Gender:\_\_\_\_\_ Age:\_\_\_\_\_

1. Inside the house, did you feel?

	Yes	No
Cold		
Hot		
Damp		
Draughts		

2. Did you sleep well?

Yes\_\_\_\_\_ No\_\_\_\_\_

3. On a scale of 1 to 5: where 1 means strongly disagreeable and 5 means strongly agreeable, where do you classify the following items?

	1	2	3	4	5
	Strongly Disagreeable	Disagreeable	Neither Agreeable nor Disagreeable	Agreeable	Strongly Agreeable
House					
Ceiling					
Wall					
Floor					
Temperature					
Noise					
Damp					
Wind					
Facilities					

4. Would you reproduce the ceiling in your own house?

Yes\_\_\_\_\_ No\_\_\_\_\_ Why?\_\_\_\_\_

5. If you could make some improvements to this house, what would you do?\_\_\_\_\_



6. Do you consider that inside this house is warmer or colder than the exterior during the day?  
Yes \_\_\_\_\_ No \_\_\_\_\_ Why? \_\_\_\_\_
7. Do you consider that inside the house is warmer or colder than the exterior during the night? \_\_\_\_\_
8. What didn't you like about the house or your experience living here? \_\_\_\_\_

## References

- García-López, E.; Heard, C. A study of the social acceptability of a proposal to improve the thermal comfort of a traditional dwelling. *Appl. Therm. Eng.* **2015**, *75*, 1287–1295. [CrossRef]
- Herrero, S.T.; Nicholls, L.; Strengers, Y. Smart home technologies in everyday life: Do they address key energy challenges in households? *Curr. Opin. Environ. Sustain.* **2018**, *31*, 65–70. [CrossRef]
- Balest, J.; Vettorato, D. Social acceptance of energy retrofit in social housing: Beyond the technological viewpoint. In *Smart and Sustainable Planning for Cities and Regions: Results of SSPCR 2017 2*; Springer: Cham, Switzerland, 2017; pp. 167–177.
- Cong, G. Sustaining the Traditional Stilt House of Tujia Ethnicity in Southeast Chongqing, China. Ph.D Thesis, University of Queensland, Brisbane, Australia, 2015. Available online: [https://espace.library.uq.edu.au/view/UQ:387779/s4271195\\_phd\\_submission.pdf](https://espace.library.uq.edu.au/view/UQ:387779/s4271195_phd_submission.pdf) (accessed on 5 October 2022).
- Valderrama-Ulloa, C.; Silva-Castillo, L.; Sandoval-Grandi, C.; Robles-Calderon, C.; Rouault, F. Indoor Environmental Quality in Latin American Buildings: A Systematic Literature Review. *Sustainability* **2020**, *12*, 643. [CrossRef]
- Araya, R.; Guillaumet, A.; Valle, D.; Duque, M.D.P.; Gonzalez, G.; Cabrero, J.M.; De León, E.; Castro, F.; Gutierrez, C.; Negrão, J.; et al. Development of Sustainable Timber Construction in Ibero-America: State of the Art in the Region and Identification of Current International Gaps in the Construction Industry. *Sustainability* **2022**, *14*, 1170. [CrossRef]
- Censo de Población y Vivienda 2020, INEGI. Available online: <https://www.inegi.org.mx/programas/ccpv/2020/default.html#Tabulados> (accessed on 11 November 2022).
- Montoya, B.C. La “educación burguesa”: Realidad y ficción sociológicas de un concepto. *Témpora. 1ª Época Pasado Presente Educ.* **1986**, *7*, 47–62.
- Freire, P. *Cartas a Quien Pretende Enseñar*; Siglo XXI Editors: Mexico City, Mexico, 1997.
- García, E. *Modificaciones al Sistema de Clasificación Climática de Köppen*, 5th ed.; Instituto de Geografía, Universidad Nacional Autónoma de México: Mexico City, Mexico, 2004.
- Nivon Bolan, E. *Políticas Culturales en México: 2006–2020: Hacia un Plan Estratégico de Desarrollo Cultural*; Miguel Angel Porrúa: Mexico City, México, 2006.
- AMAIM. Perfiles Socioeconómicos, Asociación Mexicana de Agencias de Investigación de Mercado, México. 2007. Available online: [www.amaim.gob.mx](http://www.amaim.gob.mx) (accessed on 5 October 2009).
- Niveles Socioeconómicos en México, Nivel Socioeconómico D (Clase Pobre). 2022. Available online: [https://www.economia.com.mx/nivel\\_socioeconomico\\_d\\_clase\\_pobre.htm](https://www.economia.com.mx/nivel_socioeconomico_d_clase_pobre.htm) (accessed on 11 November 2022).
- Cruz Rodríguez, M.S. *Espacios Metropolitanos 2: Población, Planeación y Políticas de Gobierno*; Universidad Autónoma Metropolitana, Unidad Azcapotzalco: Mexico City, Mexico, 2007.
- Mormont, M. *La Sociologie de L'environnement*; Université de Lovaine: Leuven, Belgium, 1987.
- Hyman, H. *Diseño y Analisis de las Encuestas Sociales*; Amorrortu Editores Sa: Buenos Aires, Argentina, 1988.
- Pardinas, F. *Metodología y Técnicas de Investigación en Ciencias*; Siglo XXI Editores: México City, Mexico, 1999.
- Hyman, H. *Taking Society's Measure: A Personal History of Survey Research*; Russell Sage Foundation: New York City, NY, USA, 1991.
- Auliciems, A.; Dear, R. Thermal Adaptation and Variable Indoor Climate Control. *Hum. Bioclimatol.* **1998**, *5*, 61–86.
- Bonnet, M. Education for Sustainable Development: A Coherent Philosophy for Environmental Education? *Camb. J. Educ.* **1999**, *29*, 313–324. [CrossRef]
- González Gaudiano, E. *Elementos Estratégicos para el Desarrollo de la Educación Ambiental en México*; en el Instituto Nacional de Ecología, Universidad de Guadalajara: México City, Mexico, 1993.
- Smelser, N. *Teoría de la Conducta Colectiva*; Alianza: México City, Mexico, 1997.
- Tilbury, D.; Stevenson, R.B. (Eds.) *Education and Sustainability: Responding to the Global Challenge*; Commission on Education and Communication: Gland, Switzerland; Cambridge, UK, 2002.
- Hong, S.-K. Cause and consequence of landscape fragmentation and changing disturbance by socio-economic development. *J. Environ. Sci.* **1999**, *11*, 181–188.

**Disclaimer/Publisher's Note:** The statements, opinions and data contained in all publications are solely those of the individual author(s) and contributor(s) and not of MDPI and/or the editor(s). MDPI and/or the editor(s) disclaim responsibility for any injury to people or property resulting from any ideas, methods, instructions or products referred to in the content.



# Orthodox or Sustainable Economic Recovery

Sazcha M. Olivera-Villarroel, Ivan Egido-Zurita, and Alethea G. Candia-Calderón

## Contents

Introduction .....	2
Theoretical Framework .....	3
From the Urgency of Economics to the Importance of Sustainability .....	3
The Symbiosis of Humanity with the Environment: The Economy .....	4
Economic Policy for Recovery Considering Climate Action .....	7
Methodological Framework .....	8
Observation Unit .....	8
Unit of Analysis .....	10
Applied Method .....	10
Results: Where and How Are We? .....	12
Discussion .....	24
Conclusions and Recommendations .....	27
References .....	28

## Abstract

The COVID-19 pandemic has caused a sui generis worldwide crisis, where the economic recession was one of the earliest and direct health impacts. In addition to being an unprecedented situation globally, the recovery form is uncertain. As mentioned by António Guterres, Secretary-General of the UN, the usual responses will not work, and creative responses are needed aiming at a more sustainable and inclusive recovery. In this context, the present research aims to analyze public policies in Latin American and Caribbean countries to implement a “green” recovery that aims not only to get out of the current economic crisis but also to reduce the effects of climate change and avoid falling back into an

S. M. Olivera-Villarroel (✉) · A. G. Candia-Calderón  
Autonomous Metropolitan University – Cuajimalpa (UAM), Mexico City, Mexico  
e-mail: [solivera@cua.uam.mx](mailto:solivera@cua.uam.mx)

I. Egido-Zurita  
Inter Alia SRL, Bolivia Lateinamerika-Gruppe e.V., Frankfurt am Main, Germany

economy based on fossil fuels and environmental degradation, i.e., a recovery oriented towards the decarbonization of the economy. For this purpose, five sectors were considered – management of water resources, renewable energy, management and treatment of waste, sustainable construction and management, and recovery of oceans and basins – that have in common the intensive use of labor and moderate investments. These sectors can contribute to the generation of green jobs and development focused on fulfilling the sustainable development goals (SDGs) and the agreed-upon planned national determined contributions (NDCs). Macroeconomic analysis of investment estimation was used as the primary study method. This analysis made it possible to estimate the investments needed to recoup the jobs lost due to the pandemic and the possibility of greening these jobs with the support of hindcasting techniques (or projections for the future). The various scenarios and necessary actions were drawn up to cause the Latin American economy to recover without neglecting sustainability in its development.

---

**Keywords**

COVID-19 · Economic recovery · Sustainable Development Goals · Latin America · Decarbonization

---

**Introduction**

The pandemic caused by the SARS-COV-2 virus has caused a sui generis worldwide crisis and great uncertainty around the recovery (FMI 2020a, b). Of course, the economic recession was one of the earliest and most direct health impacts. Indeed, history shows us the social and political conflict processes caused by other pandemics. The epidemics of the beginning of the last millennium in Europe, for example, brought with them the stigma of minority groups, the increase in anti-Semitism, the limitation of freedom, and even the expropriation of property.

This health crisis found countries of the entire world highly connected and, to a greater or lesser degree, economically interdependent, in what has been called globalization. At the same time, also an unusual environmental crisis was caused by climate change. For this reason, the problems generated by COVID-19 do not fall into a single field, such as public health, nor to a sum of crises in several areas, such as economy, climate change, or social conflict; instead, COVID-19 has caused a systemic concern combining all these fields. This health crisis is especially true because the data show that 60% of infectious diseases come from animals, and about three-quarters come from wildlife. Furthermore, to show a solution tailored to the problem, this study estimates the investment necessary to recover jobs lost due to the pandemic and strategies to green these sources of employment. This recovery will help generate an economic recovery, but it will also strengthen the sectors necessary to mitigate the effects of climate change.

For this purpose, this document is divided into six parts; on the one hand, an analysis of the available literature was carried out on the importance of moving towards a sustainable economy, the identification of the relationship between the economy and the environment, and succinct analysis of the main actions developed by world organizations to guide the development of mitigation strategies for the effects of climate change. On the other, the macroeconomic approach was used to estimate the investment necessary to recover the jobs lost by the sector of interest. The Shapley method was used to generate the prioritization of economic activities. Subsequently, a brief analysis of the investigation results was carried out. Finally, the main conclusions and recommendations are described.

---

## Theoretical Framework

### From the Urgency of Economics to the Importance of Sustainability

The effects of the economic crisis resulting from COVID-19 in the social sphere will aggravate current problems such as the increase in child labor, malnutrition and nutrition-related mortality, food insecurity, unemployment; and it is expected that it will cause a setback in the advances that were achieved to end poverty (CEPAL 2020; FMI 2020a).

The world's governments implemented emergency measures both to reduce the slope of the epidemiological curve and reduce the slope of the recession and economic crisis (Gourinchas et al. 2021). Since March 2020, more than a thousand measures have been implemented worldwide to expand social aid and protection in 200 countries (Molina et al. 2020). Direct transfer as basic temporary income (TBI) is estimated to have helped 15% of the world's population, with the difference that in low- and middle-income countries, the per person distribution was between US\$ 7 and US \$ 9, while it is between US\$ 121 and US\$ 123 per person in high-income countries.

On the other hand, it should be noted that the economic recovery after each economic crisis increased greenhouse gas emissions (GHG), one of the leading causes of climate change (Hanna et al. 2020). The economic recovery caused by the COVID-19 pandemic does not appear to be the exception. For this reason, with the economic recovery initiatives, it is possible to fear the worsening of the situation caused by climate change. Even more worrying is the link this climate crisis could have with the health crisis.

Indeed, the link between the outbreak of this pandemic and the development model, based on mineral extraction and fossil fuel resources, which is in force in most countries of the world, has not been ruled out. For example, some evidence shows a link between epidemics of animal transmission and extractive activities. Even though there is no direct link between climate change and the emergence of diseases, it has been proven that the effects of climate change worsen their spread (Martins 2020). Indeed, the data mentioned above that 60% of emerging infectious diseases (EID) originate from animals, most of which are wild. Such transmission

makes sense when the disproportionate way these animals interact with people and groups of people is considered – in agriculture expansion, deforestation, hunting, and animal trafficking, among others.

In this scenario, it is sensible to orient any economic policy of recovery, of any scale, if not to stop, to reduce the effects of climate change. Otherwise, the counter-productive effects could be much more severe for the population's well-being. This dilemma is not new and is like what Ralf Dahrendorf characterized as “perverse alternatives” when he argued that three main development aims (creation of wealth, social cohesion, and political freedom) were not necessarily compatible; instead, they conflicted with each other (Dahrendorf 1995; Baldwin and Weder 2020). To a considerable extent, economic recovery should be aimed at strengthening the conditions so that the production of goods and services can guarantee decent employment, economic stability, and the generation of wealth and environmental and social sustainability.

## **The Symbiosis of Humanity with the Environment: The Economy**

Economic activities have a strong connection with the environment – agriculture and electricity supply, among others – that begin to green up through recognizing their relationships with the environment. Such is the case with construction or transportation. In this sense, actions in public policy focused on a “green” recovery, aimed not only at getting out of the current economic crisis but also at reducing the effects of climate change, are more than necessary. Furthermore, they require recognizing the importance of economic, societal, and environmental interaction. Following the ILO proposal (2016, p. 17), these interactions can be identified as:

1. Environment as an input: activities where natural resources are the primary raw material of economic activity. The environment is prevalent in economic activities such as agriculture, forestry, livestock, fishing, manufacturing, and mining.
2. Environmental management: Activities that focus on managing natural resources and reducing negative impacts on the environment. It is seen in pollution control, natural resource management, and the greening of products and services.
3. Reaction to environmental changes: Activities that adapt to climate change and other environmental risks. The reaction includes protection through insurance against natural disasters, reforestation and soil restoration, and constructions that help resist environmental changes.
4. Environmental quality as a necessity: Some activities are susceptible to environmental quality, such as ecotourism, which would cease to exist if the proper functioning of the ecosystems is not maintained. (ILO 2016, p. 17)

From the functionalist approach, the environment fulfills specific functions, such as:

1. The environment is part of the production function of many economic goods.
2. The environment acts, in effect, as a recipient of residues and wastes of all kinds, resulting from productive activity as a consumptive of society.

3. Supplies natural assets (landscapes, parks, and others) whose services are demanded by society,
4. Finally, it makes up an integrated system that supplies the means to sustain all kinds of life. (Pearce in Olivera and Ferro, 2015, p. 38)

In an earlier analysis, Olivera and Ferro-Azcona (2015, p.12) establish the following classifications concerning the value of environment:

1. Use value refers to an asset's value for its current or future use, direct or indirect. The value is provided by the awareness of its existence and potential use.
2. Non-use value is the most controversial aspect since the person has a positive utility without using the good. We can value a protected area in Africa, not because we plan to use it or visit it, but because others could do it, which makes us feel good (it generates a utility).

The four basic types of non-use value are:

- (i) Existence value – the consumer obtains utility in knowing that something exists (elephants in Africa).
- (ii) Altruistic value – not derived from their consumption but from the fact of knowing that someone else enjoys it; in other words, someone else's utility is within my utility function.
- (iii) Legacy value – similar to the previous one but associated with the well-being of the descendants. Legacy value has a remarkably close relationship with the discount rate that society perceives.
- (iv) Ethical or moral values – those made from an ethical, moral, and even religious parameter or principle.

When these concepts are considered in the sectors studied, their usefulness for the analysis is confirmed. For example, in the renewable energy sector, the supply of electricity (production) has a relationship with the environment as an input, with use value given that it uses components of this as raw material for energy generation and with the non-use value in consumption (legacy value, due to the positive effects on climate change that guarantees better options for future generations). The same happens in the gas and water supply. However, the construction sector is the most diverse. Different activities are derived from it that could be more directly oriented to climate action or greening, such as reducing waste and pollutants (altruistic value) and eco-techniques such as collectors, solar panels, water savings, and the efficiency of heating and air-conditioning systems (use value), among others (Olivera and Ferro-Azcona 2015).

Suppose we group each sector according to the type of employment generation. These can be divided into (1) non-specialized green employment, referring to unskilled labor used for agricultural work, forestry, or infrastructure generation; (2) specialized services, referring to the design and implementation of machines,

**Table 1** Link between the economy and the environment

Sector	Some green activities	Link economy environment	Typology of job
Agriculture and Livestock	Forest management, forest management and protected natural areas, watershed and fisheries management	Environment as an input; indirect use-value; intrinsic existence value.	Unskilled green employment
		Legacy and ethical/moral value in consumption	Monitoring and certification
Electricity supply	Renewable energies (wind, solar, bioenergy, geothermal, hydroelectric)	Environment as input and tangible asset.	Unskilled green employment
	Energy efficiency	Legacy and ethical/moral value in consumption	Specialized Services
			Monitoring and certification
Gas and water supply	Sewage treatment. Retaining walls. Watershed arborization	Environment as an input, indirect use value Legacy and ethical/moral value in consumption	Unskilled green employment
			Monitoring and certification
Construction	Eco techniques such as collector and solar panels, saving water, green buildings (double glazing, insulation, building materials, and ventilation), waste reduction, and environmental pollution. Efficiency of heating and air conditioning systems.	Management of the environment and reaction to Changes in the environment.	Unskilled green employment
		Legacy and ethical/moral value in consumption	Specialized services
			Monitoring and certification
Transportation and complementary and auxiliary activities	Public (massive) and non-motorized transport. Electronic transport	Management of the environment and reaction to changes, in the environment. Legacy and ethical/moral value in consumption	Unskilled green employment
			Specialized services
			Monitoring and certification

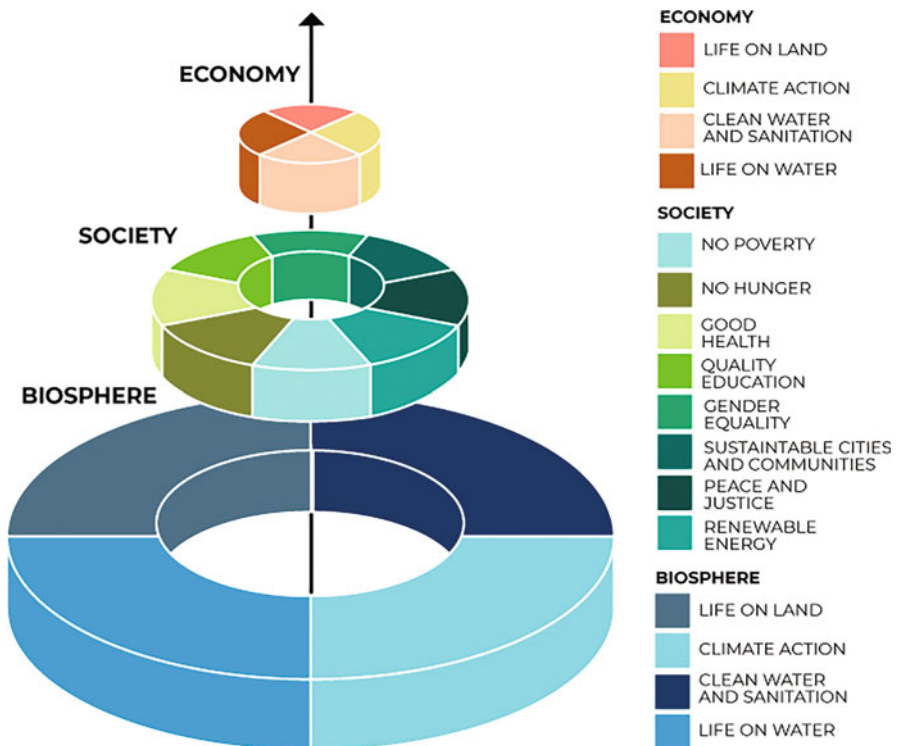
Source: Self-elaboration based on ILO (2016)

computer/virtual/digital systems, and financial, legal, and sociopolitical advice; and (3) monitoring and certification, which deals with specialized employment in climate or energy efficiency issues. It would also generate a specialized certification system – environmental ISO for each sector (see Table 1).

### Economic Policy for Recovery Considering Climate Action

In light of international law and the United Nations conventions, its member states assumed commitments to face the most relevant problems in the world. In this context, the Sustainable Development Goals (SDGs) are a global vision of how the world wants to see itself in 2030, that is, to guide any economic recovery policy of any scale, at least to curb GHG emissions, to decrease the effects of climate change. The SDGs give us a framework so that the economic recovery should be oriented towards strengthening the conditions to produce goods and services while guaranteeing decent employment, economic stability, the generation of wealth, and environmental and social sustainability.

In 2016, Rockström and Sukhdev charted the link between the sustainable development goals in a “Wedding Cake” (Fig. 1). They argued that if the bases (biosphere) are neglected, the negative implications on the “Society and Economy” levels are irreparable. The goals of the level of Society and Economy are not innocuous to the biosphere goals but dependent on these.



**Fig. 1** “Wedding Cake”. (Source: Rockström and Sukhdev (2016) The illustration above is free to use under the Creative Commons license (CC BY 4.0), <https://www.stockholmresilience.org/research/research-news/2016-06-14-the-sdgs-wedding-cake.html>)



The implications of this model for the design and implementation of economic policies to recover from the COVID-19 crisis are decisive. They confirm more than ever that sustainability is not an economic or environmental concept but of the entire planetary system.

Parallel to the SDGs, nationally determined contributions (NDCs) were agreed upon; the NDCs constitute the core of the Paris Agreement, considering compliance with the United Nations Framework Convention on Climate Change (UNFCCC), since it proved the principle of proportional contributions to the economic size and responsibility in the emissions of the countries.

Following this principle, the NDCs in Latin America and the Caribbean (LAC) are different because of their national circumstances and the way they were formulated. Ecuador, for example, to ratify its planned national determined contributions (NDCs) and establish its first NDCs, carried out a very well-structured participatory process, in which 93 institutions and 891 people from the public and private sectors, academia, civil society, and international organizations participated (Comisión Europea/European Commission 2019; Samaniego et al. 2019). These are aligned with their national plans and have varying degrees of depth in the fields of action they have identified. For this reason, economic recovery policies can be deployed in different sectors of each country.

---

## Methodological Framework

Two areas of analysis were selected to achieve a systemic study of economic recovery and climate action: on the one hand the geographical (countries) and on the other the thematic (sectors). In this sense, for the analysis of the research, the following elements are considered.

### Observation Unit

A mixed criterion was considered by analyzing the countries: the GDP per capita and the economically active population (EAP) structure were selected to study the employment sector. It was shown that according to each country's economic and labor characteristics, there is a relationship between the sector's employment generators. However, this relationship is called structural heterogeneity with low production levels and sectors that generate surpluses but with little job creation. In other words, a country is more heterogeneous because its workforce is concentrated in sectors with a low production level. In the region, the persistence of structural heterogeneity is a consequence of the concentration of technical progress in certain strata, which leaves essential segments of the economy on the margins of the modernization process. Since the incorporation of progress in most Latin American economies has not been generalized or homogeneous, it has not spread to all sectors and branches of economic activity in each country (Infante 2011). In this sense, seven regions stand for the different structural heterogeneity levels (Table 2).

**Table 2** GDP per capita and distribution of the EAP according to occupation sector for the selected countries

Country	GDP per cápita	% EAP agriculture	% EAP industry	% EAP services	% contribution to GDP of the agricultural sector	Analysis group
Bolivia (Plurinational State of)	3552	28.2	22.5	49.3	12.25	High
Brazil	8717	9.4	20.7	69.9	8.05	Low
Chile	13,457	9.1	20.7	69.2	9.21	Low
Colombia	6532	16.4	19.3	64.3	11.65	Moderate
Ecuador	6184	26.1	19.1	54.8	4.32	Low
Mexico	9863	12.9	25.3	60.2	7.21	High
Dominican Republic	8282	9.8	19.4	70.8	4.76	Moderate
Latin America (weighted average)	8847	13.8	21.2	65	10.2	–

Source: Self-elaboration based on data from the World Bank and CEPALSTAT. 2019 data

- (i) Countries that produce primary goods with a high structural heterogeneity. This group includes Bolivia and Ecuador. These two countries have more than 25% of their EAP in primary activities and per-capita income below \$6200.
- (ii) Countries that produce primary and secondary goods (industrialized) with a moderate structural heterogeneity. The second group is Colombia and the Dominican Republic, and both countries have middle-income economies and similar EAPs in service and industrial sectors.
- (iii) Countries that produce industrialized goods and services with a low structural heterogeneity. The third group includes Brazil and Mexico, the two most powerful economies in the region and the most populated countries in LAC. Chile joins them as it has the region's highest GDP per capita and an EAP structure like Brazil and Mexico.

It was also found how these countries concentrated their NDCs and contributed to the SDGs to link the economic situation to public policy-oriented climate action. As shown in Tables 2 and 4, the central public policies promoted by the Bolivian government are to eradicate hunger and poverty. It also emphasizes basic sanitation, renewable energy, and caring for the environment. Ecuador, for its part, has as its principle the eradication of poverty and the creation of actions to mitigate the effects of climate change.

Colombia's public policies revolve around creating decent jobs, fostering an alliance to achieve all the SDGs, and specific climate actions. The Dominican Republic also focuses on creating decent jobs, to a lesser extent in the coalition to achieve all the SDGs, but with the same intensity as Colombia in climate action.

Chile directs its policies to aim at joint alliances to achieve the SDGs and emphasizes actions to mitigate the effects of climate change. For its part, Brazil has a system of policies aimed at developing terrestrial ecosystems and non-polluting energy. Finally, Mexico does not present a solid preference for one of the development goals. It is more homogeneous in its choice; it acts in all the SDGs, where the SDG generation of sustainable cities and communities stands out.

## Unit of Analysis

For the study, the critical sectors for reducing greenhouse gases (GHGs) with a significant potential to create jobs are considered the unit of analysis. In addition to being potential generators of positive externalities to the environment with the best management of habitat conservation and ecosystem services, five sectors were selected: agriculture (forest conservation), water, construction, transportation, and electricity.

## Applied Method

To estimate the investment necessary to recover the number of jobs lost due to the pandemic, the number of jobs and the gross value of production by economic sector (agriculture, water, forest conservation, construction, transportation, and electrical energy) were obtained first. Given the disaggregation of the information, it was impossible to access the gross fixed capital formation (GFCF) data by sector and country. Therefore, it is assumed that the GFCF changes according to the return rate, which varies from 0.05 to 0.5. In this sense, the GFCF is estimated by sector and country as follows:

$$\text{GFCF}_i^p = \text{VBP}_i^p * \text{TR}$$

Where:

$\text{GFCF}_i^p$  = gross fixed capital formation of economic sector i and country p

$\text{VBP}_i^p$  = gross value of production of economic sector i and country p

TR = rate of return

Subsequently, the direct employment coefficient was calculated with the sectoral information on total employment and the GFCF, which measures each sector's employment requirement or the employment level per monetary unit of investment. For this effect the following formula was used:

$$\text{CE}_i^d = \frac{N_i^p}{\text{GFCF}_i^p}$$

Where:

$CE_i^d$  = coefficient of direct employment by country and sector.

$N_i^p$  = the level of employment in sector  $i$ .

$GFCF_i^p$  = gross fixed capital formation of economic sector  $i$  and country  $p$ .

The subscript  $d$  is indicative of the mean of direct employment.

This employment coefficient (CE) helps estimate the number of jobs generated by sector  $i$  of the economy according to direct investment from the sector itself. The GFCF is expressed in millions of dollars and the number of jobs generated for every million dollars invested.

Once the employment coefficient has been calculated, the number of jobs lost due to the pandemic is estimated. Since there are no fixed data, the estimated percentage of the ILO was used in its report "COVID-19 and the world of work, 2020." According to an analysis for each economic sector, they estimate, the percentage of jobs lost in the region is as follows: the agricultural sector has a calculated loss of 3% of the labor sources in this area; this percentage rises to 13% in the construction sector; and the sectors most affected are service sectors with a loss of 18.3% of their jobs. Based on these percentages, the job loss was estimated as follows:

$$NEP_i^p = NE_i^p * \%EP_i^p$$

Where:

$NEP_i^p$  = number of jobs lost in sector  $i$  of country  $p$

$NE_i^p$  = total number of jobs in sector  $i$  of country  $p$

$\%EP_i^p$  = estimated percentage of job losses in sector  $i$  of country  $p$

Subsequently, following the formula, the investment needed for the recovery of jobs is estimated according to sector and country:

$$IRE_i^p = \frac{NEP_i^p}{CE_i^d/10}$$

Where:

$IRE_i^p$  = investment needed to create jobs in sector  $i$  of country  $p$

$NEP_i^p$  = number of jobs lost in sector  $i$  of country  $p$

$CE_i^d$  = coefficient of direct employment by country and sector

Finally, to find the priority activities to be implemented by country, the relative weights of each activity were calculated, using the Shapley decomposition – a method that estimates the relative contributions of the various explanatory variables and the contribution to the variance of each part of the index.

Olivera (2007) shows that the steps for estimating the weighting of the sectors, using the Shapley method, are as follows:

1. An index is generated with average or equal weights.

$$\text{Index} = \frac{1}{3} * \text{comp1} + \frac{1}{3} * \text{comp2} + \frac{1}{3} * \text{comp3}$$

2. In a second stage, the percentage of contributions of the variables that make up the index to the total variance of the previously estimated index is calculated.

$$\theta = \beta_1 * x_1 + \beta_2 * x_2 + \dots + \beta_k * x_k$$

where  $\theta$  is the index;  $\beta_i$  represents the relative contribution of each component used to the index, which is a first step that has the same value  $\beta_i = \beta_j$  and must add 1 to maintain identity and consistency in the estimate of the decomposition to be developed (Shorrocks 1999); and  $x_1, x_2, \dots, x_k$  represent the components of the index, and then the partial R square for the variable  $x_j$  can be calculated by the Shapley-Owen decomposition (Zaiontz 2017):

$$R_j^2 = \sum_{TCV - \{x_j\}} \frac{R^2(T \cup \{x_j\}) - R^2(T)}{k * C(k-1, |T|)}$$

where  $V = \{x_1, x_2, \dots, x_k\}$  and  $|T|$  = the number of elements in some subset  $T$  of  $V$ . Also,  $R^2(T)$  = the value of  $R$  squared for the regression of the components in  $T$  on  $\Theta$ , which will tend to value close to 1 in the case of applying the weighting of indices. The method assumes that  $R^2(\emptyset) = 0$ .

This method allowed the development of strategic planning for the future and showed steps that the region should follow to achieve sustainable economic growth considering the SDGs and NDCs.

---

## Results: Where and How Are We?

Before the COVID-19 outbreak in the world, Latin America and the Caribbean (LAC) was in an unfavorable economic situation due to the fall in the international price of commodities, global financial volatility, and tension in international relations generated by international relations between the United States and China. Indeed, the general growth of the region was less than 1% in 2019. Furthermore, 30% of its population was in poverty, had a GDP per capita of 8847, and a Gini index higher than 0.46 (Banco Mundial 2020a).

At the same time, it must be recognized that Latin America is a heterogeneous region with countries that have a GDP per capita below the US \$ 4000, as in the case of Bolivia, Ecuador, or Haiti, where close to 30% of people in employment are in the

agricultural sector, with economies considered mono-producing, and more than 25% of its populations with incomes below the poverty line. Then there are the middle-income countries (Colombia, Dominican Republic), with Gini inequality indices that vary between 0.43 and 0.50. Economies are characterized by the production of primary goods for export and products for consumption in the domestic market. In addition, they are characterized by specialization in certain products and services. Finally, LAC has upper-middle-income countries, such as Mexico, Chile, or Brazil, with the strongest economies in the region with a per capita GDP of over US \$ 8700. Characterized by their manufacturing and raw materials export, they have a vast industrial zone and are below the regional average for the population employed in the agricultural sector (13.71%) (Table 3).

These characteristics of structural heterogeneity in the region mean that for every million dollars invested in the sectors analyzed, the following are generated, on average: 300 jobs in the case of the first group of countries (mono-agricultural producers), 200 jobs in the second group (exporters of primary goods), and 100 hundred jobs in manufacturing exporting countries. Regardless of the amount of labor generated by this sector, a characteristic must be considered: most jobs are low-quality work, low income, and without social protection.

Some specific sectors are labor generators. In effect, the sectors of transport, telecommunications, and complementary activities generate an average of 20 jobs for every million dollars of investment at the LAC level. Indeed, Mexico, Chile, and the Dominican Republic are countries that generate more jobs in these sectors. However, for every million invested in the construction sector, a little less than one job is generated, while countries classified as mono-producers for every million invested only develop one job. However, countries like Mexico and the Dominican Republic generated up to four jobs on average. On the other hand, sectors such as the supply of electricity, gas, and water, due to the type of activities they carry out, are the ones that generate the least number of jobs, given that for every two million invested, less than one job is created. However, these types of activities are known as strategic sectors because of their contribution to GDP.

Based on these characteristics, a green economic boost strategy must be generated, emphasizing investment in both job-generating and surplus-generating sectors. In other words, a system of incentives and disincentives must be installed, which guides the operators of these sectors to move towards productive actions that promote climate action or are at least climate neutral (Table 4). A greening effect of the activities is necessary, be it the change of the energy matrix or sustainable construction. Whatever the case, this change must be controlled to avoid urgent growth without future (BID 2019a, b).

To the above scenario, the effects of climate change must be added, causing fires in the Amazon, floods in Central America, drought in northern Mexico, hurricane threats in the Caribbean, and others. The IADB projects that the impact of climate change will cost approximately US \$ 100 billion per year by 2050 (BID 2020). For this reason, and as mentioned throughout the research, it is necessary to generate a form of green economic recovery that helps flatten the health curve (number of deaths from COVID), the economic angle, and the curve of the impact of climate

**Table 3** General characteristics of the study countries

Country	Population	Territorial extension	GDP per capita	GINI	% Poor population (below the poverty line)	% Agriculture	Contribution to GDP	Degree of structural heterogeneity
Bolivia (Plurinational State of)	11,513,100	1,083,300	3552	42.2	34.6	28.2	22.5	49.3
Brasil	211,049,527	8,358,140	8717	53.9	25.4	9.4	20.7	69.9
Chile	18,729,160	756,108	13,457	44.4	8.6	9.1	20.7	69.2
Colombia	50,339,443	1,109,500	6532	50.4	27	16.4	19.3	64.3
Ecuador	17,373,662	248,360	6184	45.4	25.2	26.1	19.1	54.8
Mexico	127,575,529	1,943,950	9863	45.4	41.9	12.9	25.3	60.2
Dominican Republic	10,738,958	48,310	8282	43.7	22.8	9.8	19.4	70.8
<i>Latin America (weighted average)</i>	<i>646,430,841</i>	<i>20,038,832</i>	<i>8847</i>	<i>46.2</i>	<i>30.2</i>	<i>13.8</i>	<i>21.2</i>	<i>65</i>

Source: Elaboration based on data from the World Bank and CEPALSTAT. 2019 data

change. In this sense, the following section explains the close relationship between the economy and the environment (Table 4).

(i) *Countries that produce primary goods with a high degree of structural heterogeneity*

For the specific cases of Bolivia and Ecuador, the decomposition method found agriculture as the primary sector to invest in, which is reflected in the NDCs of both countries. Bolivia also incorporates forest management into its development agenda. In this sense, and given the sector's importance, it is necessary to make an average investment of 13.6 and 26.3 million dollars for the Bolivian and Ecuadorian cases, respectively. With this, it will be possible to generate large-scale sources of employment, depending on the investment activity. These can help to quickly and precisely reduce GHGs, with tree planting, watershed management, forest fire reduction, and climate-smart agricultural production.

Another priority activity within the NDCs is that of water resources, which ranks second in the prioritization index since recent studies have found that the main effect of climate change in the Andean region will be reflected in the increase in droughts and the melting of the snow-capped mountains of the Andes (DW 2020). Likewise, it is considered that access to water is one of the leading human rights. In that case, the central government will have to generate public policies for the management of this resource, with an investment of between 18 thousand and 26 thousand million dollars in activities such as increasing the coverage of irrigation, basic sanitation, water storage measures, diversification of drinking water sources, and above all ensuring access for all inhabitants of both countries to drinking water to avoid water stress and the lack of this resource in the future.

The diversification of electricity generation appears within the NDC for both countries and is the third-place priority. Considering this sector is linked to the change in the energy matrix, the jump to renewable energies brings many advantages. The main one is the absence of polluting emissions, which makes this type of energy a source that respects the environment, essential for sustainable development in Bolivia and Ecuador. In the same way, by not consuming raw materials, the operating cost of renewable energies is much lower than that of conventional energies, and it is not exposed to variations in the price of oil or other raw materials. In sum, apart from being an activity that generates surpluses and not labor, it must be recognized that, from a social point of view, renewable energies favor local development since they generate economic activity distributed in the place where they are used, being particularly useful in rural electrification and in supplying other economic activities in isolated areas. However, in some parts of the world, it has been found that renewable energy kWh for kWh requires more labor than fossil fuel electric power, particularly in Mexico and Brazil (Elkington 2018).

It should be noted that the construction sector no longer shares the same prioritization between countries since, for the Bolivian case, it appears in a lame fourth place, while for the Ecuadorian case, it is in the fifth place. None of the countries



**Table 4** Employment, the gross value of production, gross capital formation, COVID-19 job loss, direct employment requirement, and investment for job recovery

Country	Heading	Total employment (number of people)	Employment/gross accumulated capital formation	Estimation of the number of jobs lost by COVID-19	Investing to recover jobs (in millions of dollars)	Investment Priority Index
Bolivia (Plurinational State of)	Agriculture, livestock, hunting, forestry, and fishing	1,699,830	374.1	50,994.90	13.63	0.92
	Electricity supply	66,507	0.1	12,037.73	12,112.41	0.7
	Gas and water supply	40,762	0.3	7377.96	2480.85	0.69
	Construction	410,863	0.38	53,412.19	13,931.62	0.68
	Transportation and complementary and auxiliary activities	1,982,889	0.64	358,902.91	56,234.73	0.63
Brazil	Agriculture, livestock, hunting, forestry, and fishing	8,634,279	116.36	259,028.37	222.61	0.78
	Electricity supply	799,431	0.02	144,697.03	685,693.60	0.65
	Gas and water supply	489,974	0.06	88,685.28	140,443.27	0.47
	Construction	6,748,136	0.13	877,257.68	690,327.95	0.44
	Transportation and complementary and auxiliary activities	38,594,277	0.63	6,985,564.14	1,117,376.94	0.06
Chile	Agriculture, livestock, hunting, forestry, and fishing	4,018,274	87.9	23,982.00	272.89	0.71
	Electricity supply	214,204	0.03	35,843.07	116,403.54	0.7

	Gas and water supply	131,286	0.09	21,968.33	23,841.69	0.69
	Construction	1,528,848	0.42	97,175.00	22,981.45	0.69
	Transportation and complementary and auxiliary activities	10,630,821	5.21	141,216.20	2708.25	0.66
Colombia	Agriculture, livestock, hunting, forestry, and fishing	1,699,830	202.6	120,548.22	59.5	0.86
	Electricity supply	66,507	0.03	38,770.89	152,507.61	0.69
	Gas and water supply	40,762	0.08	23,762.80	31,236.50	0.65
	Construction	410,863	0.08	198,750.24	241,074.01	0.61
	Transportation and complementary and auxiliary activities	1,982,889	0.73	1,924,178.60	263,208.52	0.54
Ecuador	Agriculture, livestock, hunting, forestry, and fishing	2,396,431	272.72	71,892.93	26.36	0.92
	Electricity supply	53,337	0.04	9653.95	25,840.98	0.7
	Gas and water supply	32,690	0.11	5916.94	5292.73	0.69
	Construction	530,857	0.05	69,011.41	138,164.40	0.66
	Transportation and complementary and auxiliary activities	543,224	0.08	98,323.54	125,580.76	0.65
México	Agriculture, livestock, hunting, forestry, and fishing	6,958,032	178.4	208,740.96	117.01	0.84
	Electricity supply	364,686	0.02	67,188.58	353,301.82	0.68
	Gas and water supply	223,517	0.06	41,180.10	72,363.02	0.58

(continued)

**Table 4** (continued)

Country	Heading	Total employment (number of people)	Employment/gross accumulated capital formation	Estimation of the number of jobs lost by COVID-19	Investing to recover jobs (in millions of dollars)	Investment Priority Index
	Construction	4,572,025	5.64	603,398.64	10,689.46	0.32
	Transportation and complementary and auxiliary activities	2,950,518	31.64	4,144,248.04	13,097.46	0.25
Dominican Republic	Agriculture, livestock, hunting, forestry, and fishing	424,140	99.34	12,724.20	12.81	0.78
	Electricity supply	50,496	0.05	9238.74	19,151.41	0.7
	Gas and water supply	30,949	0.14	5662.45	3922.58	0.69
	Construction	386,079	4.06	51,506.65	1268.89	0.66
	Transportation and complementary and auxiliary activities	358,790	28.46	348,712.97	1225.20	0.66

Source: Elaboration with data from ILO (2020) and CEPALSTAT. The estimates of the loss of jobs by sector were made from ILO estimates for Latin America. They estimate that for the second half of 2020, there was a loss of 18.1% of jobs in the service sector (tertiary) and 13% in the construction sector

considers this sector within its NDCs, and this occurs because this sector has a low long-term employment generation factor.

However, it should be noted that it is a generator of transversal multiplier effects, especially in cement production, glass, ceramics (both floors and brick), imported steel, and other supplies. If these countries want to boost the sector and recover the jobs lost by the pandemic, an average investment of 13 billion dollars is estimated for the Bolivian case and an investment ten times more (130 billion dollars) for the Ecuadorian case; these countries can invest in short-term projects, such as the construction of retaining walls in the maintenance of bridges, roads, and primary infrastructure, among others. These projects will help support the cities adequately and generate many jobs quickly. In addition, the sector can develop medium-term projects with the construction of works aimed at adapting to climate change, such as the construction of urban waste plants, water treatment plants, and dams, among others.

In the fifth place, for the Bolivian case, and in the fourth place, for the Ecuadorian case, is the transport sector that allows us to face two major problems that afflict the largest cities of both countries; we are talking about air pollution due to GHGs emitted by motor vehicles and traffic congestion caused by the high number of cars and poor road distribution. A fixed transport system must be developed to decrease traffic, with electrical energy that helps reduce atmospheric pollutants and GHGs. An example of the generation of massive and sustainable media is that of Ecuador and the development of its first metro line in Quito or the ten cable car lines implemented in La Paz, Bolivia, which supplies better mobility and reduces the GHGs of these cities.

Finally, the last of the sectors chosen is the urban waste management sector. Apart from the fact that this sector affects all the cities of the country and generates soil and water pollution, it is considered last, since it does not follow the immediate generation of sources of work, one of the conditions imposed on the chosen sectors, given that medium- and long-term studies and construction of recycling plants are needed for their execution. However, this does not mean that the sector is dismissed; it is linked to the quality of life in urban areas, impacts employing the least qualified workforce, and can be associated with medium- or long-term electricity generation (Table 5).

(ii) *Countries that produce primary and secondary goods (industrialized) with a moderate structural heterogeneity*

For Colombia and the Dominican Republic's specific case, the agricultural sector is the primary sector to intervene and be incorporated into the NDC for both countries. This sector proved to be especially important for the Colombian case since this country is the leading exporter of coffee in the region, a result reflected in the contribution of the 4% that this product makes to the Colombian GDP and the cultivation of coffee. In Colombia, it covers 877,144 ha in 600 municipalities and 22 departments, encompassing more than 550,000 coffee-producing families, which implement a mixed agricultural system that combines coffee with livestock, plantain

**Table 5** Sectors that include adaptation elements in the NDC

Country	Energy	Agriculture	Forest	Land-use change and forestry	Biodiversity	Industry	Transport	Fishing	Infrastructure	Hydro resource	Risk management	Housing	Health	Tourism	Coastal zone	Cities
Bolivia (Plurinational State of)																
Brasil																
Chile																
Colombia																
Ecuador																
Mexico																
Dominican Republic																

**Source:** Self-elaboration based on the Samaniego et.al (2019)

crops, or corn, among other agricultural activities (FNCC 2018). In this sense, it is estimated that the investment that must be made to recover the number of jobs lost due to the pandemic is 59 million dollars for the Colombian case. This investment should aim to improve practices related to coffee growing and post-harvest processing that can reduce the environmental footprint of this product, directing its efforts to climate-smart agriculture.

In the case of the Dominican Republic, agricultural activity is centered on two crops, sugar and rice, which in 2012 represented 11% of GDP and about 15% of Dominican jobs. But for some time now, this contribution was decimated due to, on the one hand, natural disasters that, according to the World Bank estimates, in the last 20 years, the Caribbean countries have each annually spent between 1% and 9% of their GDP to deal with the effects of meteorological hazards, and many of these expenses fell on small farmers, and, on the other hand, the change in consumption habits of the European market has caused the region's traditional imports – sugar, bananas, cocoa, and rice – to contract (Banco Mundial 2013). According to estimates, if the number of jobs lost due to COVID is to be recovered, the Dominican government will have to invest 12 million dollars in improving the response to disasters, especially that which helps small farmers increase productivity and reduce vulnerability to boost climate-smart agriculture.

The second priority sector in both countries is water and gas supply. An exciting analytical element is that this sector does not appear marked in their NDC for the Colombian case; however, it is a priority for the rest of the countries. This element can be interpreted considering the geographical characteristics of Colombia, given that it has a per capita availability of water resources of 45,408 cubic meters, well

above the world average of 8209 (Ministry of Environment and Sustainable Development 2020). However, regardless of the relative advantage of this country, it is necessary to remember that one of the main consequences of climate change is the increase in droughts, so investment in this sector should not be neglected.

The case of the Dominican Republic is the opposite of that of Colombia. This country has 2378 cubic meters of water per inhabitant, a figure well below the world average, which means that several cities, such as Santiago and Greater Santo Domingo, have a high degree of water stress. In addition to the above, it is added that the most substantial number of water sources is underground (60%), which does not supply human consumption and the demand of agricultural areas. In addition, apart from the fact that 85% of the homes in the Dominican Republic have access to running water, 79.2% (1,665,009 households) buy water in bottles and 12.3% (258,488 households) from delivery trucks, according to the Third Socioeconomic Study of Households (3ESH 2018). These indicators show the level of vulnerability of the DR, so it is necessary to invest in wastewater treatment plants, fluvial water storage, and desalination plants and the diversification of its water sources (surface sources), to avoid water stress and a lack of coverage in areas of greater vulnerability.

The electric power supply sector, in addition to being in the NDCs of both countries, is the third priority sector for Colombia and the Dominican Republic, given that the change of the energy matrix is a latent need for all the countries in the region. Colombia got a relative advantage by positioning itself as one of the countries with the cleanest electricity generation matrix in the world. As of December 2018, the installed generation capacity in the National Interconnected System was 17,312 megawatts (MW). Of this installed capacity, 68.4% corresponded to hydraulic generation, 30% to thermal generation (13.3% with natural gas, 7.8% with liquid fuels, and 9.5% with coal), and approximately 1% with nonconventional renewable energy sources (FNCER) (wind, solar, and biomass) (BID 2020).

The construction sector varies according to the country; for the Colombian case, it is in the fourth place, while for the Dominican case, it is fifth. In the Colombian NDC, the term “Infrastructure” is inserted as an active sector, in the sense that it is considered a transversal sector that can help in the achievement of many other projects connected with the rest of the sectors without neglecting the development of sustainable housing constructions. In the Dominican case, this sector is not inserted in its NDCs; it should not be forgotten that it is a transversal sector that can help achieve the aims of the other sectors. With an estimated investment of around 1200 million dollars, the Dominican Republic can not only recover the jobs lost to COVID, but it could also invest in a more efficient water storage system or in desalination plants themselves that will help combat the problem of water shortage.

Finally, the transport sector is positioned in the fourth place in the Dominican Republic; it should be noted that its most populated city (Santo Domingo) has an integrated public system, which consists of three metro lines and one cable car; however, the problem does not revolve around the public system, but around the transport system destined for tourism. Furthermore, if it is considered that the tourism sector in the Dominican Republic is currently one of the most substantial

supports in its economy, the contribution of the same in the GDP of the country is more than 16%. For this reason, the Dominican government incorporated this sector into its NDCs. With an average investment of 1225 million dollars, transportation systems for tourists could be improved, switching to cleaner energy.

In the case of Colombia, the transportation sector ranks fifth among its most prominent cities (Bogotá, Cali, and Cartagena) with massive public systems. These continue to use fossil fuels; a clear example of this is the bus system of rapid transit (BRT) “Transmilenio” which is the primary mass transport in Bogotá and uses diesel as fuel, which does not help to reduce the GHGs of the city. So with an average investment of 263,208 million, the bus fleet system could be diversified by changing the fuel type and even taking advantage of many cyclists in the city. It is possible to construct more cycle lanes and thus generate an environmental awareness in its population.

(iii) *Countries producing industrialized goods and services with a low structural heterogeneity*

Given that the fastest recovery with a minor investment is in the agriculture sector, all countries with low levels of structural heterogeneity will have this sector as their priority investment activities. In the case of Mexico, with 117 million dollars, it will recover the more than 208,700 jobs lost. This investment should implement climate-smart agricultural practices to reduce GHGs and generate better production with resilient systems. As for Chile, this country, within the framework of its NDCs, is committed to the sustainable management and recovery of 100,000 hectares of forest, mainly native, which will represent the capture and reduction of greenhouse gases by around 600,000 tons of CO<sub>2</sub> equivalent per year, starting in 2030 (FAO 2018); in this order of ideas, with an average investment of 272 million dollars, Chile should invest in afforestation and care programs for endemic plants.

Brazil, since 2010, through the implementation of the Low-Carbon Agriculture Program (ABC), supplied incentives and resources to rural producers to adopt more sustainable agricultural production techniques. The idea was that agricultural and livestock production should be more efficient, giving more significant benefits to producers and more food to the population while simultaneously protecting the environment – the program aimed to reduce CO<sub>2</sub> emissions by around 38% by 2020 (FAO 2012). This program is uncertain in its NDCs, so with an average investment of 222 million dollars, it should be taken as the primary strategy for the development of sustainable agriculture, including the restoration of another 15 million hectares of degraded grasslands by 2030 and the improvement of 5 million hectares of crops before 2030 (FAO 2018).

The water and gas supply sector is placed second. As mentioned above, these sectors are essential not only because of their capacity to generate surpluses or jobs but primarily because water forms the liquid element for the survival of people. In this sense, all the countries incorporated this sector into their NDCs. In this sense, Mexico, within its NDCs, committed to guaranteeing the integral management of water in its different uses (agricultural, ecological, urban, industrial, and domestic).

These goals can be achieved with an average investment of 72,363 million dollars, which can be invested in specific programs for the relocation of infrastructure that is located in high-risk areas in priority tourist destinations and will implement restoration actions for unoccupied sites, will incorporate criteria adaptation to climate change in public investment projects that consider construction and maintenance of infrastructure, and will guarantee the treatment of urban and industrial wastewater, ensuring the quantity and good quality of water, in human settlements with more than 500,000 inhabitants (FAO 2018).

Concerning Brazil and its NDCs, it takes electricity management as its primary sector. It is committed to promoting new clean technology standards and energy efficiency measures to improve low-carbon infrastructure. For this purpose, with an average investment of 685,693 million dollars, Brazil will be able to recover the number of jobs lost and collaborate with reducing GHG by decarbonizing its energy.

Another sector that appears to be reflected in the NDCs of Brazil is the transport sector. It is estimated that with an average investment of 1,117,376 million dollars, Brazil will be able to promote further efficiency measures and improvement of transport infrastructure, especially public transport in the urban areas, which will cause, on the one hand, the reduction of GHGs and, on the other hand, more efficient road management.

Chile, for its part, has different socioeconomic characteristics from other countries in the region, as it has the highest GDP per capita in LAC. It belongs to the category of high-income countries according to the World Bank; in addition, it has the most favorable external debt rating on the continent. Its economic system is based on services (63.9% of GDP), mining (14.2% of GDP), and exports. This country, having such unique characteristics, focuses its efforts on agriculture, followed by the transport sector, gas and water supply, construction, and finally electricity. Likewise, the country within its NDCs focuses its public policies on achieving green (sustainable) cities, so it is not surprising that the water and transport sectors, in this case, occupy more privileged places than the rest of the countries analyzed.

Concerning the construction sector and considering that this country invested many efforts to develop green cities and sustainable infrastructure (agreements within its NDCs), it made Santiago de Chile the most sustainable city in Latin America (Mercados 2016). Now, due to the pandemic, this sector presented a loss of more than 97 thousand jobs, so it is estimated that with an investment of 22,981 million dollars, Chile can recover these jobs and at the same time continue to advance in the achievements obtained, not only for its largest city but also for the entire country. On the other hand, a factor to consider is that it is not possible to generate sustainable cities without thinking about transport; in this sense, as MMAA (2020) mentions:

Santiago shows significant advances in the use of bicycles and the generation of safe pedestrian spaces. The public bicycle system of several communes, the start of constructing a wide network of bicycle lanes, and the pedestrianization of roads in the city center are significant. After a dreadful start, the Trans-Santiago system has merged itself as the broadest



and best-served integrated system (buses, metro) in Latin America and emerging countries. (MMAA 2020)

Therefore, with an investment of two billion dollars, Chile can quickly recover lost sources, strengthen its public system, generate more and better cycle paths, and change the fleet of public motorized vehicles that use fossil fuel for a new line with renewable power. This same line must be followed by the energy sector, which, with an investment of 116,403 million dollars, will be able to generate the much-desired process of decarbonizing the energy matrix since, currently, electricity stands for only 22%. At the same time, the rest corresponds to biomass (15%) and fossil fuels (63%) (MMAA 2020). However, if this qualitative leap is achieved, it will imply an actual reduction in GHGs.

---

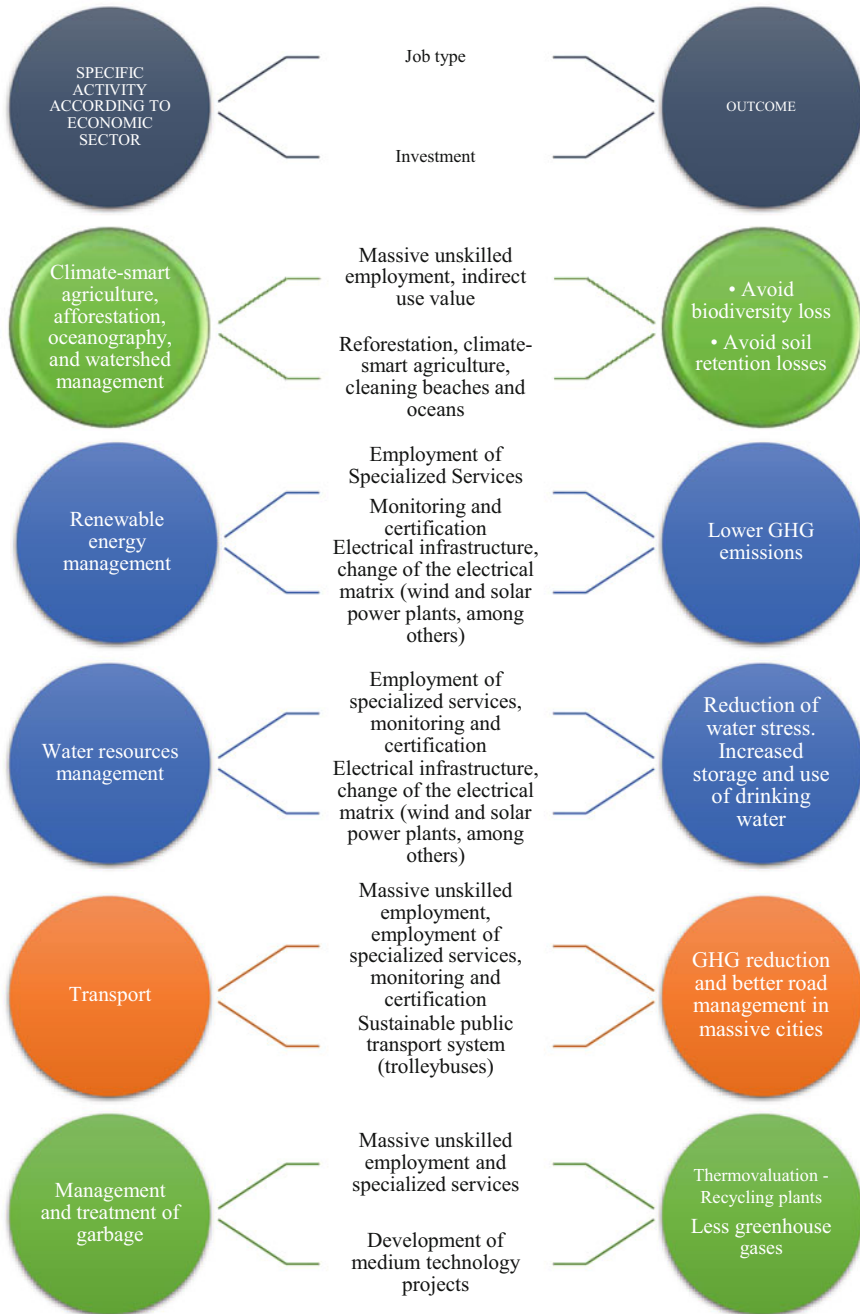
## Discussion

As mentioned above, given the economic and social crisis that the region and the entire world are going through, in general, there is a prevailing need to generate economic recovery mechanisms, but not in extractive sectors, which are destined to disappear in the medium term, but in green sectors which help to flatten the economic and environmental curve. In this sense, and given the little information available, it was decided to take as the leading green activities those whose information is available in all the study countries, and that follows the premise of being green job generators. Figure 2 shows agriculture, energy management, transportation, construction, and garbage management.

The link corresponding to agricultural activities is the most intensive sector in unskilled labor since 200 jobs are generated for every million invested. In addition, according to ILO estimates, on average, this sector accounts for 16% of the green jobs generated in the region (ILO 2016). These jobs range from forestry, control, care of protected areas, and beach cleaning. All these sources of employment and creating unskilled jobs prevent biodiversity loss and improve soil retention.

Activities related to renewable energy management are considered to generate surpluses and not labor. However, within the framework of the change in the energy matrix, employment in renewable energies has had considerable growth in recent years (ILO 2016). By 2019, 51.7% of the energy produced in Latin America was renewable, and more than 65% of their energy is renewable in Brazil and Colombia. However, this sector has a minor job creation for every two million dollars invested. On average, for Latin America in 2019, only one was created. However, if we analyze the total number of green jobs, this sector accounts for 19% of green jobs in LAC, according to ILO estimates.

Even so, the investment analysis must be carried out differentially by country. Indeed, although it seems that electricity coverage is complete in all Latin American countries, there are countries like Bolivia, where, despite the public investment in the energy sector generated in recent years, electricity coverage is not 100%. This country has 86% coverage in rural areas and 95% in urban areas. These data must



**Fig. 2** Selected activities, employment they generate, investment projects, and expected results. (Source: Self-elaboration)

be sorted out and ensure that the entire population has access to electricity. In addition, among the advances made by Bolivia, it is highlighted that, after a substantial investment in changing the energy matrix, it now generates 69 MW with hydroelectric plants, 27 MW through wind energy, 5 MW from solar energy, and 37 MW in a generation of biomass. These advances must be supported and promoted to a green economic recovery (Banco Mundial 2020b).

The water resources management sector is considered one of the most important since water affects all aspects of development and is related to most SDGs. In addition, due to population growth, the intensive use of this resource, the more significant variability of rainfall, and climate change combine in an unfavorable framework for sustainable development and economic growth (Banco Mundial 2020b). Furthermore, given the characteristics of Latin America and the Caribbean, where only 35% of the population has improved sanitation systems, it is necessary to invest in this type of wastewater treatment, river water storage, and desalination plants; diversification of its water sources (underground and surface sources); and socialization campaigns for the rational use of this resource, among others, to avoid water stress and a lack of coverage in areas of greatest vulnerability.

The transport sector can help combat two main problems in the region's medium and large cities, poor air quality and the excessive increase in the region's number of vehicles in use, causing road congestion and poor traffic control. On the one hand, it must be recognized that automobiles are one of the primary sources of air pollution. For example, Mexico City contributes 52% of PM10 particulate emissions, 55% of PM2.5 particulate emissions, and 86% of carbon monoxide and nitrogen oxide emissions. At the regional level, on the other hand, it is estimated that transport contributes to a substantial part of anthropogenic GHG emissions since it is 15% of global GHG emissions and 23% of GHG emissions from fossil fuels in 2009 (BID 2013; page 23).

In addition, the volume of cars bought, their use, and the level of emissions derived from them are greater than expected from the region's population and gross domestic product (GDP) levels. As LAC countries modernize and develop, trends suggest that this will be accompanied by an increase in the acquisition and use of automobiles. If current trends continue, by 2030, LAC countries will approach the level of motorization that existed in Europe in the 1960s but with more urban regions with populations above five million inhabitants than those in that continent then or today (BID 2019a; page 13). In this sense, the need for investing in creating public, massive, integrated, and above all sustainable systems that contribute to the ordering of traffic and the reduction of GHGs stands out.

Finally, waste management is a crucial activity of the green economy because of its capacity to generate jobs and its implications for issues such as health and safety (ILO 2016). In the selected countries, it can be found that the Dominican Republic has the best identification of waste since only 10% of its destruction is not categorized. At the same time, Bolivia has the lowest waste sorting capacity, with 22.7% of unsorted waste. Plastic stands for 10% of destruction, as does paper (this percentage shows a more significant deviation in the cases of Bolivia and the Dominican Republic, given the variation in their waste selection capacities).

Given the population density of each country, it is not surprising that Brazil generates more than 79 billion tons per year, while Bolivia generates 2 billion tons of garbage per year. However, in the trash for Latin America, the garbage that reaches a waste treatment landfill or is recycled fluctuates between 5% and 30%. Therefore, it is necessary to invest in creating more and better recycling and thermo-recovery plants, which will create more jobs due to their capacity to generate large-scale labor requirements and reduce environmental pollution.

All these activities contribute to the economy by creating jobs, generating surpluses, and reducing GHGs. However, a strategic plan must be drawn up by the country, in which economic recovery measures are incorporated according to the specific needs of each one. In this sense, with the help of the Shapley decomposition method, seen in section “[Applied Method](#)”, and with the use of multiple criteria that consider, on the one hand, the number of jobs created, the investment made, and the benefits for growth in the medium term, it was possible to find priority activities. In addition, these results were related to the adaptation sectors of the NDC that each country had adopted before the pandemic to generate a strategy more strongly associated with the region’s demands.

---

## Conclusions and Recommendations

History shows that each economic crisis brought an increase in greenhouse gas emissions. Given that countries were betting on a desperate recovery instead of a sustainable recovery, however, and because of climate change that the world is going through, we cannot fall back into this historical error. Therefore, and considering the nationally determined contributions (NDCs), the Sustainable Development Goals (SDGs), the Paris Agreement, framed in compliance with the United Nations Framework Convention on Climate Change (UNFCCC), should be needed for the governments of the region generates an “environmentally intelligent” recovery that is committed to the conservation of the planet and long-term sustainable development.

The pandemic surprised the region with a socioeconomic crisis: GDP growth of less than 1%, more than 30% of its population living in poverty, a GDP per capita of \$8847, and a Gini index greater than 0.46. It developed a productive infrastructure and managed extreme weather events (keeping walls, watershed management, and forest fires, among others). With the agreements mentioned above, the economic recovery strategy must be prepared with a view to sustainable development with the generation of green jobs that help reduce the effects of the crisis caused by COVID-19. It is considering generating a story that places the economy of the countries analyzed on a path of lower GHG emissions.

Green jobs can be generated with reasonable investments if the ideal activities are chosen, such as tree planting, watershed management, forest fire reduction, climate-smart agricultural production, increased irrigation coverage, basic sanitation, storage measures of water, diversification of drinking water sources, the creation of a public

system based on electric transport such as trolleybuses, and the design of recycling plants, among others.

These actions help generate new sources of employment and mitigate the effects of the economic crisis; they also contribute to the economy's greening and guide the country towards climate resilience by supporting the most vulnerable municipalities.

---

## References

- Baldwin R, Weder B (2020) Mitigating the COVID economic crisis: act fast and do whatever it takes. CEPR Press, UK
- Banco Mundial (2013) Agricultura en la República Dominicana: Muy vulnerable, poco asegurada. Banco Mundial
- Banco Mundial (2020a) Pandemia, recesión: la economía mundial en crisis. The World Bank IBRD – IDA
- Banco Mundial (2020b) Global economic prospects. World Bank Group, Washington, DC
- BID (2019a) Financiando el futuro con el Grupo BID. Retrieved from <https://policycommons.net/artifacts/304749/financiando-el-futuro-con-el-grupo-bid/1221868/>
- BID (2019b) 5 pasos para un financiamiento sostenible y verde. BID. Retrieved from <https://blogs.iadb.org/sostenibilidad/es/5-pasos-para-un-financiamiento-sostenible-y-verde/>
- BID (2020) Compromisos climáticos y presupuestos nacionales: identificación y alineación. Estudios de caso de. BID, Argentina, Colombia, Jamaica, México y Perú
- CEPAL (2020) Enfrentar los efectos cada vez mayores del COVID-19 para una reactivación con igualdad: nuevas proyecciones. Comisión Económica para América Latina y el Caribe (CEPAL), Santiago de Chile
- Comisión Europea (2019) Avances en la Acción Climática de América Latina: Contribuciones Nacionalmente Determinadas al 2019. Programa EUROCLIMA+, Dirección General de Desarrollo y Cooperación – EuropeAid. Comisión Europea, Bruselas
- Dahrendorf R (1995) Economic opportunity, civil society and political liberty. United Nations Research Institute for Social Development (UNRISD, Geneva)
- DW, M. f (2020) La Tierra se calienta, los Andes se derriten. Ciencia y Ecología
- Elkington J (2018) Triple resultado. He aquí por qué es hora de repensarlo. Harvard Business Review
- FAO (2012) Brasil: producción agrícola y recursos naturales. FAO
- FAO (2018) Análisis y Sistematización de documentos de contribución prevista Nacionalmente determinada (CPND) en países de América Latina y el Caribe (LAC), en base a la Convención marco de Naciones Unidas sobre el Cambio Climático. FAO, Santiago
- FNCC, F. N (2018) Huella ambiental del café en Colombia. Documento guía. CNPMLTA, Quantis International, Bogotá
- Fondo Monetario Internacional FMI (2020a) Actualización de las perspectivas de la Economía Mundial – Junio 2020. Retrieved from <https://www.imf.org/es/Publications/WEO/Issues/2020/06/24/WEOUpdateJune2020>
- Fondo Monetario Internacional (FMI) (2020b) Una crisis como ninguna otra, una recuperación incierta. International Monetary Fund
- Gourinchas PO, Kalemli-Özcan Ş, Penciakova V, Sander N (2021) Fiscal policy in the age of COVID: does it 'get in all of the cracks?' vol w29293. National Bureau of Economic Research. [https://www.nber.org/system/files/working\\_papers/w29293/w29293.pdf](https://www.nber.org/system/files/working_papers/w29293/w29293.pdf)
- Hanna R, Xu Y, Victor DG (2020) After COVID-19, green investment must deliver jobs to get political traction. Nature 582(7811):178–180
- ILO (2016) Green jobs for a sustainable development. The Uruguayan case. Organization International Labor, Ginebra

- ILO (2020) Observatorio de la OIT: La COVID-19 y el mundo del trabajo, Quinta edición. Estimaciones actualizadas y análisis. OIT. [https://www.ilo.org/global/topics/green-jobs/publications/WCMS\\_493362/lang-en/index.htm](https://www.ilo.org/global/topics/green-jobs/publications/WCMS_493362/lang-en/index.htm)
- Infante R (2011) Heterogeneidad estructural, empleo y distribución del ingreso. CEPAL, Santiago de Chile
- MADS, M. d (2020) Gestión Integral del Recurso Hídrico. Ministerio de Ambiente y Desarrollo Sostenible, Bogotá
- Martins A (2020, Julio 21) El mundo está tratando los síntomas de la pandemia de covid-19, pero no las causas. BBC
- Mercados (2016) Santiago es la ciudad más sustentable de Latinoamérica y 71 en el mundo. El Mostrador, Santiago de Chile
- Ministerio de Medio Ambiente y Agua (2020) Informe bienal de actualización de Chile sobre Cambio Climático. [https://cambioclimatico.mma.gob.cl/wp-content/uploads/2021/01/Chile\\_4th\\_BUR\\_2020.pdf](https://cambioclimatico.mma.gob.cl/wp-content/uploads/2021/01/Chile_4th_BUR_2020.pdf)
- Molina GG, Ortiz-Juarez E, NETWORK, U. G. P (2020) Temporary basic income: Protecting poor and vulnerable people in developing countries. United Nations Development Programme, New York
- Olivera SM (2007) Explotación de Recursos No Renovables en Áreas protegidas: valoración de las Áreas protegidas en Bolivia. Universidad Nacional Autónoma de México, División de Estudios de Posgrado, Facultad de Economía, Ciudad de México
- Olivera-Villarroel SM, Ferro-Azcona H (2015) Exploitation of non-renewable resources in protected areas: valuation of protected areas in Bolivia. *Int J Bus Soc Sci* 6(11):1
- Planas M, Cárdenas JC (2019) La matriz energética de Colombia se renueva. Banco Iberoamericano de Desarrollo BID
- Rockström J, Sukhdev P (2016) How food connects all the SDGs. Stockholm Resilience Centre. Retrieved from Retrieved from: <https://www.stockholmresilience.org/research/research-news/2016-06-14-the-sdgs-wedding-cake.html>
- Samaniego J, Alatorre JE, Reyes O, Ferrer J, Muñoz L, Arpaia L (2019) Panorama de las contribuciones determinadas a nivel nacional en América Latina y el Caribe, 2019: avances para el cumplimiento del Acuerdo de París
- Shorrocks AF (1999) Decomposition procedures for distributional analysis: a unified framework based on the Shapley value. University of Essex, Mimeo
- Zaiontz (2017) Shapley-Owen decomposition tools and applications. <https://www.real-statistics.com/multiple-regression/shapley-owen-decomposition/>